A global assessment of drought sensitivity of tree species and forest ecosystems using dendrochronology and remote sensing

by

Vinicius Manvailer

A thesis submitted in partial fulfillment of the requirements for the degree of

Doctor of Philosophy

in

Forest Biology and Management

Department of Renewable Resources

University of Alberta

Abstract

Forests in water-limited regions of the world face increasing risks from intensifying drought events under climate change. Yet assessing and comparing drought vulnerability of forests at broad spatial scales remains a difficult problem. Analysis efforts are typically constrained by fragmented data sources and multiple co-varying factors in empirical research. This makes it very difficult to compare species and populations across different regions for the purpose of vulnerability assessments or to find resilient species and genotypes for climate change adaptation in forest management. This thesis addresses these limitations by developing a framework to assess drought sensitivity and resilience in tree species populations using a combination of dendrochronology, remote sensing, and methodological advances in historical biology analysis. The aim is to derive ecologically meaningful, scalable metrics that support both a better understanding of forest responses to drought and the development of practical tools for adaptive forest management.

A foundational step toward this goal was the systematic evaluation and correction of the International Tree Ring Database (ITRDB), the world's largest dendrochronological archive. Metadata inconsistencies, species misidentifications, and formatting errors were corrected for approximately 20% of records. Subsequently, consistently detrended site chronologies were developed using three smoothing approaches to preserve different frequency components of growth variability. This cleaned and harmonized dataset enabled reliable downstream analysis of drought sensitivity across nearly 5,000 sites, focusing on the 20 most widely represented tree species.

To ensure that dendroclimatological analyses are based on appropriate climatic inputs, a comparative evaluation of global precipitation datasets was carried out using two biological indicators: tree-ring growth and satellite-derived vegetation greenness (MODIS-EVI). The study found that multi-source climate datasets such as MSWEP outperformed single-source products, particularly in regions with sparse weather station coverage. However, for long-term historical applications, the climate station based UDEL-TS product showed superior alignment with biological data prior to the 1940s. These results offer guidance for selecting suitable climate datasets in ecological applications, addressing a frequently overlooked source of uncertainty in vulnerability assessments.

Given the sparse and uneven geographic distribution of tree-ring data, the thesis next evaluated whether analytical methods developed for dendroclimatology could be applied to satellite-based vegetation indices. By calculating climate sensitivity metrics from annual EVI time series and comparing them with those derived from tree rings, it was shown that remotely sensed proxies capture similar climatic constraints on growth across major forest biomes. Although EVI-based estimates tend to smooth short-term lag effects and may reflect different aspects of physiological response, the correspondence in limiting climate factors suggests that remote sensing products can be used to extend drought sensitivity assessments to areas without dendrochronological records.

Building on these foundations, the thesis introduces a standardized Resilience to Ecological Drought index (RED50), which quantifies the capacity of trees to recover from a modeled drought event that causes a 50% growth reduction. This approach addresses key limitations of vulnerability assessments by controlling for variation in drought severity and decoupling recovery estimates from specific species, regional populations, site conditions, or sampling

years. Applying RED50 to tree-ring sites globally revealed that species and populations with lower resistance, those that suppress growth during drought, tend to recover more fully afterwards. High RED50 values were often observed in species or populations from historically drier or warmer environments, particularly in trailing-edge regions at the margins of species' ranges.

The RED50-based analysis of drought resilience highlights the role of species- and provenance-level adaptation in shaping recovery capacity, where local populations have evolved traits that support resilience under recurrent water limitation. Importantly, the same ecological signal is observed both among and within species: drought-adapted species tend to dominate drier sites within regions, and drought-adapted populations tend to show higher resilience across regions. Two complementary strategies emerge from this pattern: first, relocating resilient genotypes within species—such as from dry interior or trailing-edge provenances—can inform seed sourcing under climate change; second, short-distance assisted migration at the species level can be used to shift species composition within regions toward those with higher inherent drought resilience.

Preface

Chapter 2 has been submitted as a journal article, entitled: Manvailer, V. and Hamann, A. “A snapshot of the international tree ring database (ITRDB) with improved metadata and error corrections”. VM and AH conceptualized the research and developed the methodology. VM curated the data, carried out the data cleaning, generated the figures and tables, and wrote the first draft of the manuscript. AH provided advice for the analysis and edited the manuscript.

Chapter 3 has been published as Manvailer, V. and Hamann, A. 2024. “Validation of global precipitation time series products against tree ring records and remotely sensed vegetation greenness” PLoS One 19: e0299111 (*https://doi.org/10.1371/journal.pone.0299111*). VM and AH conceptualized the research, developed the methodology, and designed the figures and tables. VM curated the data, carried out the analysis, and wrote the first draft. AH provided advice for the analysis and edited the manuscript.

Chapter 4 has been prepared for submission as a journal article, entitled: Manvailer, V. and Hamann, A., Sang Z. “Climate sensitivity of global seasonal forests inferred from remote sensing versus dendrochronology”. VM, SZ, and AH conceptualized the research and developed the methodology. VM curated the data, carried out the analysis, designed the figures and tables, and wrote the first draft. AH and SZ contributed to the interpretation and edited the manuscript.

Chapter 5 has been submitted as a journal article, entitled: Manvailer, V. and Hamann, A. “A standardized resilience index to ecological droughts (RED50) reveals local adaptation of tree species and their populations”. VM and AH conceptualized the research. VM developed the methodology, carried out the analysis, designed the figures and tables, and wrote the first draft. AH provided advice for the analysis and edited the manuscript.

Dedication

“Success is not final, failure is not fatal: it is the courage to continue that counts.”

Winston Churchill

To my wife and daughter — for walking with me through the uncertain and the unknown, for believing in me even before I believed in myself, and for making this journey to Canada as much a personal triumph as a professional one. This work is as much yours as it is mine.

Acknowledgements

We are the sole leads of our own paths, but no journey is ever walked alone. When choosing to go the distance we commit to overcome what we don't yet know and often count on those whom we have not yet met – an experience that often builds who are. On this journey I have met countless others from whom I collected learning and values that allowed me to continue moving and transformed me in many ways. For those that helped me walk this path, even if a few steps, I leave here my most sincere gratitude.

This work would have never been possible without my supervisor, **Dr. Andreas Hamann**, who took a chance on me and became the tugboat guiding me through nuanced waters. His patience, transparency, and remarkable sense of humor made this journey not only more enjoyable, but more hopeful during its toughest stretches. Thank you for the long hours, the steady guidance, and the many opportunities you've provided along the way.

I am indebted to those who invested in me long before I could return the favor — when I had only my will and my time to offer. **Dr. Thales Henrique Dias Leandro**, your belief in me has been a cornerstone of my career, taking me further than I could have imagined at the beginning.

Dante, thank you for your ingenious solutions to impossible problems (in the time before LLMs) and for the inclusive, lighthearted atmosphere you create so naturally.

To my fellow SIS lab members — whether our time together was long or brief — your contributions, conversations, and even coffee breaks were invaluable. Special thanks to **Mariah, Sophia, Lars**, and all others who shared their time with me on this journey.

I gratefully acknowledge my sponsor, **CAPES**, whose funding supported my tuition and living expenses for this research. I also would like to thank supervisory committee members who have taken their time to dive into my work, contribute perspectives and serve on my examining committee.

To my family — my mother **Christina** for her kindness, **Irani** for the foundational strength and values you instilled, my sister **Karina** for your examples of grit and excellence, and my sister

Cybelle for being a reference of inner strength, and to my nephew **Gabriel** and niece **Hadassa** for bringing joy from afar.

Along this path I've met people who may not have directly shaped this thesis, but who nonetheless recharged me and with whom I was able to renew my dreams: **Catarina and Cesar**, and **James** — thank you for your light and energy every time we meet.

To my daughter, whose love has nourished me through her cooking, care, and shared joy in my milestones — thank you for believing in me and cherishing each win along the way with countless dinner, cakes, your funny jokes and stories from your everyday life.

And to my wife — the one who has walked closest to me through every emotion this work has stirred. You have shown patience, support, and positivity beyond measure, with a lightness no one else could have brought. Your unwavering belief in me carried me through the hardest moments. This thesis — and every step that led here — stands on the foundation of your love.

Table of Contents

List of Tables

List of Figures

Chapter 1. General introduction

1.1. Drought impacts to forested ecosystems

In many forested regions, especially those experiencing seasonal water deficits, climate change has altered disturbance regimes and increased physiological stress. Among the most commonly reported changes are shifts in the frequency, intensity, and duration of drought events (Cook et al. 2016; Greenwood et al. 2017; Hammond et al. 2022), which have been shown to reduce growth, increase mortality, and alter competitive dynamics in affected forest ecosystems (Ciais et al. 2005; Clark et al. 2016; Gazol et al. 2018). Drought can impair water transport and photosynthesis in trees, disrupting carbon uptake and leading to hydraulic failure in xylem tissues (Hartmann et al. 2013; Choat et al. 2018). These processes are associated with two commonly observed mortality mechanisms: embolism-induced hydraulic failure and carbon starvation following sustained stomatal closure (Hartmann et al. 2013; Kono et al. 2019; Prats et al. 2023). While the relative importance of these mechanisms varies by species and drought characteristics, both have been implicated in dieback events in moisture-limited environments.

In addition to direct physiological stress, drought can increase forest vulnerability to biotic disturbances and compound effects from other stressors. Prolonged dry periods may weaken tree defenses, increasing susceptibility to pests and pathogens and contributing to delayed mortality over multiple years (Marini et al. 2017; Pirtskhalava-Karpova et al. 2024). Drought also interacts with other disturbance agents, such as fire, which may occur more frequently or with greater severity when fuel moisture is low (Seidl et al. 2017; Luo et al. 2024). These interactions have been linked to cascading effects on forest structure, composition, and the delivery of ecosystem functions such as carbon storage and water regulation (Kannenberg et al. 2019; Knutzen et al. 2023).

The severity and persistence of drought impacts depend on the ability of trees and forest communities to resist, survive, and recover from water deficits. These capacities vary widely among species, populations, and site conditions, and are expected to shape future forest dynamics under continued climate change. Understanding these response mechanisms remains a

prerequisite for identifying where and for whom drought poses the greatest risk, and for developing informed strategies to manage that risk.

1.2. Forest management responses and the need for scalable assessments

Observed drought-related impacts on forest growth and survival have motivated the adoption of silvicultural practices aimed at reducing water stress and improving recovery potential. Among these, selective thinning has been shown to lower competition for soil moisture, enhance physiological function such as photosynthetic rates, and reduce drought-induced mortality in several species and regions (Sohn et al. 2016b; Zald et al. 2022). By decreasing stand density, thinning may support carbon balance and hydraulic safety during drought, as demonstrated by lower mortality rates and improved post-drought recovery (Klockow et al. 2018).

Another applied response to climate change is assisted migration, where tree species or populations with traits suited to drier conditions are introduced to regions expected to become more arid (Montwé et al. 2016; Sang et al. 2019; Sebastian-Azcona et al. 2020; D'Orangeville et al. 2025). This approach leverages our understanding of species' adaptive traits, such as rooting depth (Bachofen et al. 2024) or efficient hydraulic architecture (Carlquist 2012; Anderegg and Meinzer 2015), to guide the movement of seed sources or species. While promising in concept, its implementation hinges on robust information about which species and populations are most likely to succeed under changing climatic conditions.

Additionally, technological advances in climate modeling and remote sensing now offer new opportunities to evaluate forest vulnerability over large areas (Xue and Su 2017; Correa-Díaz et al. 2019; Eliades et al. 2024). However, the integration of such tools into forest management remains limited, in part because of methodological challenges in translating climate signals into biological response across diverse ecosystems. Process-based models, while powerful, often require detailed parameterization and are sensitive to uncertainty in species-specific physiological inputs. At the same time, empirical studies, though often grounded in rich ecological data and context, are difficult to compare across regions due to variation in site conditions, study designs, and measurement approaches.

As a result, current vulnerability assessments often lack consistency and scalability. Regional studies may identify drought-sensitive species or management interventions that are effective under local conditions, but they are not easily generalizable. Efforts to support reforestation or adaptation planning at larger scales require methods that can compare responses across species and regions in a consistent, interpretable way. This gap forms the basis for the present study, which seeks to develop standardized, biologically meaningful metrics for drought sensitivity and recovery, using tree-ring data and remotely sensed observations to inform management decisions under climate change.

1.3. Tree-ring research and vulnerability assessments

Over the last several decades, tree-ring data have been widely used to reconstruct past climate variability and to investigate ecological responses to climate extremes beyond the period covered by instrumental records (e.g., Folland et al., 2001). Pearl et al. (2020) noted that studies in the fields of dendroclimatology and dendroecology have more than quadrupled in the past two decades, providing a valuable basis for assessing how climate variability influences tree growth over long timescales. Applications now extend beyond climate reconstruction to tracking forest productivity, detecting growth declines, and evaluating forest health under changing environmental conditions (Hogg et al. 2005; Williams et al. 2013; Schöngart et al. 2015; Vasconcellos et al. 2019). Tree-ring records have also been used to examine the impacts of extreme events (Villalba and Veblen 1998; Bond-Lamberty et al. 2014; Dorman et al. 2015), to link changes in fire frequency to climate (Brandes et al. 2019; Sáenz-Ceja and Pérez-Salicrup 2019; Spînu et al. 2020; Brown et al. 2020) and to quantify drought sensitivity (Herweijer et al. 2007; Huang et al. 2018; DeSoto et al. 2020a; Bose et al. 2021).

The International Tree Ring Database (ITRDB) serves as the primary repository for such data, enabling large-scale reanalyzes that go beyond the scope of individual studies. Examples include global estimates of annual CO_2 sequestration trends (Brienen et al. 2020a), which suggest that carbon uptake has increased in recent decades but may be accompanied by reduced tree longevity, potentially offsetting long-term carbon storage. Other analyses have applied common statistical frameworks to evaluate tree-growth sensitivity to drought in North America (Cook et al. 2007), Europe (Cook et al. 2015, 2020) and South America (Morales et al. (2020). Tree-ring

derived parameters have also been incorporated into models predicting future growth under climate change (Charney et al. 2016).

Despite these advances, ITRDB data have been less fully utilized for comparative studies aimed at supporting forest management. For example, coordinated assessments of drought resilience, resistance, and recovery across multiple species in the same region are rare. Such comparisons could help identify species with advantageous drought-response traits for specific sites. Likewise, evaluating climate limiting factors to growth could inform species selection in reforestation programs under changing climate conditions. For a single species occurring across diverse environments, comparisons among populations could reveal differences in vulnerability related to local adaptation, guiding the selection of seed sources suited to future climates.

These opportunities point to the potential of dendrochronology for informing large-scale, management-relevant vulnerability assessments. However, the lack of standardized analytical approaches and the uneven global distribution of dendrochronology sampling sites remain major barriers to making such comparisons across species, populations, and regions.

1.4. Current challenges in drought vulnerability assessments

Tree-ring data offer a useful approach for understanding how forests have responded to past climate variability and climate trends, with implications for their likely response under future climate change. However, their broader use in drought vulnerability assessments is complicated by methodological and data limitations. Chronologies are often produced for site-specific questions, using different sampling strategies and detrending methods depending on the ecological context or research aim (Nehrbass-Ahles et al. 2014a; Büntgen et al. 2021). For example, researchers studying snowpack or runoff reconstruction may intentionally sample trees in topographic positions that accumulate water (Martin et al. 2018) , while ecological studies may prioritize a representative cross-section of stand conditions (Pederson et al. 2014; Krusic et al. 2015). Although these decisions are justified for individual studies, they reduce comparability across datasets and hinder synthesis at larger spatial scales.

Efforts to standardize tree-ring data have improved the coherence of large-scale reanalyzes, though often at the cost of accuracy at the tree or stand level (Coulthard et al. 2020). Site-level standardization and more flexible detrending methods can help mitigate this trade-off, but may also remove long-term growth trends important for detecting decadal shifts in moisture availability. Still, these approaches remain effective for identifying acute drought responses over one to two-year periods. Comparisons among species are particularly challenging in heterogeneous environments, where topography and microsite conditions strongly influence growth. Even within a species, response differences may reflect a combination of climate exposure and local adaptation. While such variation limits the transferability of findings, it also offers a valuable opportunity to examine provenance-level differences in drought response, which may be used to inform reforestation strategies under future climates.

Reliable climate data are equally essential for evaluating growth sensitivity and attributing responses to drought. Multiple gridded datasets exist, varying in spatial resolution, time span, and underlying data sources (Sun et al. 2018). Traditional interpolations based on weather stations (New et al. 2002; Harris et al. 2020) coexist with satellite-derived or reanalysis products that offer global coverage but start later and may vary in accuracy depending on region (Nguyen et al. 2019). Errors in precipitation, in particular, can be high in regions with sparse station networks or complex terrain (e.g., Zandler et al. (2019). While cross-validation against stations is commonly used (Kluver et al. 2016; Cui et al. 2017), such methods often suffer from spatial autocorrelation and do not fully capture uncertainties in poorly monitored areas (Dinku et al. 2008).

One possible solution is to validate climate datasets against independent biological responses. Tree growth, as reflected in ring width or remotely sensed greenness indices, is a biologically meaningful integrator of temperature and precipitation variability. All else being equal, data products that best correlate with growth responses are likely to more accurately reflect ecologically relevant climate variation, especially in moisture-limited environments. This approach allows for both practical data selection and provides a potential contribution to broadening independent validation methods for climate data.

Studying response to drought requires employing a definition of drought, which presents its own set of challenges. Indices such as the SPEI provide a consistent climatic basis for detecting anomalies (Gavin et al. 2007; Vicente-Serrano et al. 2013; Spangenberg et al. 2024), but they often fail to capture species-specific physiological thresholds or site-level buffering effects. For example, drought tolerance can differ dramatically between species with deep or shallow rooting systems, as seen in northeastern Italy where *Prunus mahaleb* maintained function during extreme drought while co-occurring *Quercus pubescens* suffered high mortality (Nardini et al. 2013, 2016). Local topography can similarly mediate drought impacts, with trees in valleys experiencing less stress due to runoff accumulation (Galiano et al. 2010). These dynamics highlight the limitations of climate-based definitions of drought and point to the need for biologically anchored metrics.

Beyond species-level differences, substantial variation in drought response exists among populations of the same species, reflecting both local adaptation and phenotypic plasticity in response to environmental heterogeneity. Some populations may exhibit trait variation due to plastic responses to soil conditions, microclimate, or stand structure, while others show genetically based differences that have evolved under divergent climate regimes (Sniderhan et al. 2018; Vizcaíno-Palomar et al. 2019; Silvestro et al. 2023). Distinguishing between these sources of variation is notoriously difficult in observational studies, yet both mechanisms contribute to observed drought resilience across landscapes. For example, trees from drier or more variable climates often show greater capacity to maintain growth under water stress, whether due to inherited traits such as narrower vessels and deeper roots, or through plasticity in morphology or physiology. These factors interact with environmental modifiers such as soil water-holding capacity, topographic position, or stand competition (Galiano et al. 2010; Cavin et al. 2013; Paz-Kagan et al. 2017; Gutierrez Lopez et al. 2021), making it challenging to generalize vulnerability at the species level. Given local adaptations (plastic and evolutionary), climate change may expose even mesic populations to moisture stress that exceeds their evolved tolerances, leading to drought impacts well beyond historically water-limited ecosystems.

To advance comparative vulnerability assessments, analytical approaches that recognize and accommodate this biological complexity are needed. One promising direction involves the development of standardized metrics that evaluate drought response relative to each population's

baseline climate conditions, thereby decoupling drought severity from absolute climate values and improving comparability across regions and taxa. This perspective aligns with the concept of ecological drought, which defines drought not simply by climatic anomalies, but by their impact on specific species, populations, or ecosystems. For example, a moderate climate anomaly may constitute a severe drought for populations with narrow hydraulic safety margins or shallow rooting systems, while the same event may have little effect elsewhere. Standardizing drought impact based on relative growth decline—such as estimating a population's capacity to recover from a hypothetical event that causes a fixed percentage of growth reduction—can help isolate intrinsic resilience from differences in climate exposure. This approach of identifying regions, species or populations most vulnerable (or resilient to climate change) could help to set priorities for where management interventions may be most needed due to heightened vulnerability, while also identifying candidate species and populations that show greater resilience and may be suitable for reforestation and restoration activities under drought-prone conditions.

1.5. Objectives and thesis structure

This thesis addresses the challenge of quantifying drought vulnerability in forests at scales relevant to global change research and forest management. While it is well understood that drought impacts forest growth and survival, the capacity to compare species and populations across regions, or to evaluate droughts defined by climate data in an ecological contexts, remains difficult to implement across large geographic scales. This limitation stems not only from ecological complexity but also from fragmented data, variable quality of both ecological and climate data, and methodological limitations to evaluate drought impacts across diverse ecosystems and climate conditions. The overarching objective of this thesis is to develop and test a coherent framework for assessing drought sensitivity and resilience across tree species, populations, and regions using both dendrochronological and remote sensing approaches.

Chapter 2 begins by resolving the issue of inconsistent and incomplete dendrochronological data, which can compromise robust, large-scale conclusions. It contributes a harmonized and quality-checked dataset based on the International Tree Ring Database (ITRDB), correcting metadata and standardizing chronology formats across thousands of sites. By assembling a

consistent empirical foundation, this chapter establishes a reliable baseline for analyzing interspecific and regional patterns in growth sensitivity and recovery under drought.

Chapter 3 turns to the question of climate inputs, recognizing that the accuracy of available climate data products are often assumed rather than tested for a specific purpose. Here, we focus on comparing monthly historical precipitation products, which can substantially vary in their estimates (historical temperature datasets mostly conform). Multiple global precipitation products are independently validated against biological response variables of interest in this research, tree-ring width and remotely sensed vegetation greenness, to determine how well these datasets represent the moisture variability that drives tree growth. This evaluation helps clarify which datasets are suitable for ecological modeling and which may misrepresent drought dynamics in regions with sparse station coverage or complex topography.

With the input datasets established, we turn to applications that explore climatic growth limitations at scale. Tree-ring analysis remains one of the most powerful tools for assessing how climate constrains forest productivity, including drought, because of its long temporal reach. These biological records often extend well before the availability of instrumental climate data and offer insights into past response to interannual climate variability. However, the spatial distribution of tree-ring sampling is limited and uneven, with large gaps in key regions of the world. In **Chapter 4**, we test whether the same analytical approaches commonly used in dendrochronology can be applied to satellite-derived vegetation indices. Although remotely sensed records only extend back a few decades and with high-quality data mostly available since the early 2000s, they offer near-global coverage with consistent, empirical observations. This chapter investigates how well remote sensing metrics replicate patterns of climatic sensitivity inferred from tree-ring data, evaluating their potential to scale drought vulnerability assessments to areas where dendrochronological records are lacking or sparse.

Chapter 5 represents the core methodological contribution of this thesis by developing and applying a new standardized Resilience to Ecological Drought index (RED50), which quantifies the capacity of trees to recover from a hypothetical drought event that causes a 50% reduction in growth. Building on the harmonized dendrochronological dataset and climate validation work of the preceding chapters, this analysis addresses a key limitation in previous research: the

difficulty of comparing drought vulnerability across species and regions due to variation in drought severity, species composition, local population adaptation, and site conditions. By standardizing the drought impact to a fixed growth reduction and modeling recovery independent of the climatic event severity, this chapter disentangles these confounding influences and enables ecologically meaningful comparisons across diverse environments. The resulting RED50 metric reveals both general patterns of species resilience and differences among regional provenances within the same species. This approach not only enhances our understanding of drought adaptation but provides a practical tool to inform climate-resilient reforestation and assisted migration. By linking growth responses to climate through a standardized analytical framework, this chapter delivers a scalable and actionable contribution to genotype selection and species choice in forest management where drought is a potential concern under climate change.

Taken together, the chapters in this thesis offer a structured approach to assessing forest drought vulnerability, with the aim of improving our ability to compare species and population responses to historical droughts and support informed decisions in forest management under changing climate.

1.6. References

Anderegg WRL, Klein T, Bartlett M, et al (2016) Meta-analysis reveals that hydraulic traits explain cross-species patterns of drought-induced tree mortality across the globe. Proc Natl Acad Sci U S A 113:5024–5029. https://doi.org/10.1073/pnas.1525678113

Anderegg WRL, Meinzer FC (2015) Wood anatomy and plant hydraulics in a changing climate. In: Hacke UG (ed) Functional and ecological xylem anatomy. Springer International Publishing, Cham, pp 235–253

Bachofen C, Tumber-Dávila SJ, Mackay DS, et al (2024) Tree water uptake patterns across the globe. New Phytol 242:1891–1910. https://doi.org/10.1111/nph.19762

Bond-Lamberty B, Rocha A V., Calvin K, et al (2014) Disturbance legacies and climate jointly drive tree growth and mortality in an intensively studied boreal forest. Glob Chang Biol 20:216–227. https://doi.org/10.1111/gcb.12404

Bose AK, Scherrer D, Camarero JJ, et al (2021) Climate sensitivity and drought seasonality

determine post-drought growth recovery of Quercus petraea and Quercus robur in Europe. Sci Total Environ 784:147222. https://doi.org/10.1016/j.scitotenv.2021.147222

Brandes AF das N, Sánchez-Tapia A, Sansevero JBB, et al (2019) Fire records in tree rings of moquiniastrum polymorphum: Potential for reconstructing fire history in the Brazilian atlantic forest. Acta Bot Brasilica 33:61–66. https://doi.org/10.1590/0102-33062018abb0282

Brienen RJW, Caldwell L, Duchesne L, et al (2020) Forest carbon sink neutralized by pervasive growth-lifespan trade-offs. Nat Commun 11:1–10. https://doi.org/10.1038/s41467-020-17966-z

Brown SR, Baysinger A, Brown PM, et al (2020) Fire history across forest types in the Southern Beartooth mountains, Wyoming. Tree-Ring Res 76:27. https://doi.org/10.3959/TRR2018-11

Büntgen U, Allen K, Anchukaitis KJ, et al (2021) The influence of decision-making in tree ring-based climate reconstructions. Nat Commun 12:. https://doi.org/10.1038/s41467-021-23627-6

Carlquist S (2012) How wood evolves: a new synthesis. Botany 90:901–940. https://doi.org/10.1139/b2012-048

Carlquist S (1977) Ecological factors in wood evolution: a floristic approach. Am J Bot 64:887–896. https://doi.org/10.2307/2442382

Castellanos-Acuña D, Hamann A (2020) A cross-checked global monthly weather station database for precipitation covering the period 1901 to 2010. Geosci Data J in press:1–11. https://doi.org/10.1002/gdj3.88

Charney ND, Babst F, Poulter B, et al (2016) Observed forest sensitivity to climate implies large changes in 21st century North American forest growth. Ecol Lett 19:1119–1128. https://doi.org/10.1111/ele.12650

Choat B, Brodribb TJ, Brodersen CR, et al (2018) Triggers of tree mortality under drought. Nature 558:531–539. https://doi.org/10.1038/s41586-018-0240-x

Choat B, Jansen S, Brodribb TJ, et al (2012) Global convergence in the vulnerability of forests to drought. Nature 491:752–755. https://doi.org/10.1038/nature11688

Ciais P, Reichstein M, Viovy N, et al (2005) Europe-wide reduction in primary productivity caused by the heat and drought in 2003. Nature 437:529–533.

https://doi.org/10.1038/nature03972

Clark JS, Iverson L, Woodall CW, et al (2016) The impacts of increasing drought on forest dynamics, structure, and biodiversity in the United States. Glob Chang Biol 22:2329–2352. https://doi.org/10.1111/gcb.13160

Cook BI, Cook ER, Smerdon JE, et al (2016) North American megadroughts in the Common Era: Reconstructions and simulations. Wiley Interdiscip Rev Clim Chang 7:411–432. https://doi.org/10.1002/wcc.394

Cook ER, Seager R, Cane MA, Stahle DW (2007) North American drought: Reconstructions, causes, and consequences. Earth-Science Rev 81:93–134. https://doi.org/10.1016/j.earscirev.2006.12.002

Cook ER, Seager R, Kushnir Y, et al (2015) Old World megadroughts and pluvials during the Common Era. Sci Adv 1:1–10. https://doi.org/10.1126/sciadv.1500561

Cook ER, Solomina O, Matskovsky V, et al (2020) The European Russia Drought Atlas (1400–2016 CE). Clim Dyn 54:2317–2335. https://doi.org/10.1007/s00382-019-05115-2

Correa-Díaz A, Silva LCR, Horwath WR, et al (2019) Linking remote sensing and dendrochronology to quantify climate-induced shifts in high-elevation forests over space and time. J Geophys Res Biogeosciences 124:166–183. https://doi.org/10.1029/2018JG004687

Coulthard BL, St. George S, Meko DM (2020) The limits of freely-available tree-ring chronologies. Quat Sci Rev 234:106264. https://doi.org/10.1016/j.quascirev.2020.106264

Cui W, Dong X, Xi B, Kennedy A (2017) Evaluation of Reanalyzed Precipitation Variability and Trends Using the Gridded Gauge-Based Analysis over the CONUS. J Hydrometeorol 18:2227–2248. https://doi.org/10.1175/JHM-D-17-0029.1

D'Orangeville L, Itter MS, Dos Santos JM, Taylor AR (2025) Can tree-rings inform assisted migration? Revisiting provenance trials across Atlantic Canada to compare local adaptation between red spruce populations. For Ecol Manage 578:122482. https://doi.org/10.1016/j.foreco.2024.122482

DeSoto L, Cailleret M, Sterck F, et al (2020) Low growth resilience to drought is related to future mortality risk in trees. Nat Commun 11:1–9. https://doi.org/10.1038/s41467-020-14300-5

Dinku T, Connor SJ, Ceccato P, Ropelewski CF (2008) Comparison of global gridded

precipitation products over a mountainous region of Africa. Int J Climatol 28:1627–1638. https://doi.org/10.1002/JOC.1669

Domec JC, Gartner BL (2001) Cavitation and water storage capacity in bole xylem segments of mature and young Douglas-fir trees. Trees - Struct Funct 15:204–214. https://doi.org/10.1007/s004680100095

Dorman M, Svoray T, Perevolotsky A, et al (2015) What determines tree mortality in dry environments? A multi-perspective approach. Ecol Appl 25:1054–1071. https://doi.org/10.1890/14-0698.1

Düthorn E, Holzkämper S, Timonen M, Esper J (2013) Influence of micro-site conditions on tree-ring climate signals and trends in central and northern Sweden. Trees - Struct Funct 27:1395–1404. https://doi.org/10.1007/s00468-013-0887-8

Eliades F, Sarris D, Bachofer F, et al (2024) Understanding tree mortality patterns: A comprehensive review of remote sensing and ground-based studies

Evans MEK, Falk DA, Arizpe A, et al (2017) Fusing tree-ring and forest inventory data to infer influences on tree growth. Ecosphere 8:. https://doi.org/10.1002/ecs2.1889

Evans MEK, Justin Derose R, Klesse S, et al (2022) Adding tree rings to North America's National Forest Inventories: An essential tool to guide drawdown of atmospheric CO2. Bioscience 72:233–246. https://doi.org/10.1093/BIOSCI/BIAB119

Folland CK, Karl TR, Christy JR, et al (2001) Observed climate variability and change. In: T HJ, Ding Y, Griggs DJ, et al. (eds) Climate change 2001: The scientific basis. contribution of working group I to the third assessment report of the Intergovernmental Panel on Climate Change. Cambridge University Press, Cambridge, United Kingdom and New York, NY, USA, p 881

Fritts HC (1976) Tree Rings and Climate. Academic Press Inc, London

Galiano L, Martínez-Vilalta J, Lloret F (2010) Drought-induced multifactor decline of Scots Pine in the Pyrenees and potential vegetation change by the expansion of co-occurring Oak species. Ecosystems 13:978–991. https://doi.org/10.1007/s10021-010-9368-8

Gao S, Liu R, Zhou T, et al (2018) Dynamic responses of tree-ring growth to multiple dimensions of drought. Glob Chang Biol 24:5380–5390. https://doi.org/10.1111/gcb.14367

Gao Y, Chen Z, Chen J, et al (2024) A bibliometric analysis of the mechanisms underlying

drought-induced tree mortality. Forests 15:. https://doi.org/10.3390/f15061037

Gavin DG, Gunning C, Veblen TT (2007) Drought Induces Lagged Tree Mortality in a Subalpine Forest in the Rocky Mountains. Oikos 116:1983–1994

Gazol A, Camarero JJ, Vicente-Serrano SM, et al (2018) Forest resilience to drought varies across biomes. Glob Chang Biol 24:2143–2158. https://doi.org/10.1111/gcb.14082

Girardin MP, Guo XJ, Metsaranta J, et al (2021) A national tree-ring data repository for canadian forests (Cfs-trend): Structure, synthesis, and applications. Environ Rev 29:225–241. https://doi.org/10.1139/er-2020-0099

Golian S, Javadian M, Behrangi A (2019) On the use of satellite, gauge, and reanalysis precipitation products for drought studies. Environ Res Lett 14:075005. https://doi.org/10.1088/1748-9326/AB2203

Greenwood S, Ruiz-Benito P, Martínez-Vilalta J, et al (2017) Tree mortality across biomes is promoted by drought intensity, lower wood density and higher specific leaf area. Ecol Lett 20:539–553. https://doi.org/10.1111/ele.12748

Hammond WM, Williams AP, Abatzoglou JT, et al (2022) Global field observations of tree die-off reveal hotter-drought fingerprint for Earth's forests. Nat Commun 13:. https://doi.org/10.1038/s41467-022-29289-2

Harris I, Osborn TJ, Jones P, Lister D (2020) Version 4 of the CRU TS monthly high-resolution gridded multivariate climate dataset. Sci Data 7:109. https://doi.org/10.1038/s41597-020-0453-3

Hartmann H, Moura CF, Anderegg WRL, et al (2018) Research frontiers for improving our understanding of drought-induced tree and forest mortality. New Phytol 218:15–28. https://doi.org/10.1111/nph.15048

Hartmann H, Ziegler W, Trumbore S (2013) Lethal drought leads to reduction in nonstructural carbohydrates in Norway spruce tree roots but not in the canopy. Funct Ecol 27:413–427. https://doi.org/10.1111/1365-2435.12046

Heilman KA, Dietze MC, Arizpe AA, et al (2022) Ecological forecasting of tree growth: Regional fusion of tree-ring and forest inventory data to quantify drivers and characterize uncertainty. Glob Chang Biol 28:2442–2460. https://doi.org/10.1111/gcb.16038

Hellmann L, Hülsmann L, Reinig F, et al (2016) Diverse growth trends and climate responses across Eurasia's boreal forest. Environ Res Lett 11:. https://doi.org/10.1088/1748-

9326/11/7/074021

Herweijer C, Seager R, Cook ER, Emile-Greay J (2007) North American droughts of the last millennium from a gridded network of tree-ring data. J Clim 20:1353–1376. https://doi.org/10.1175/JCLI4042.1

Hogg EH, Brandt JP, Kochtubajda B (2005) Factors affecting interannual variation in growth of western Canadian aspen forests during 1951-2000. Can J For Res 35:610–622. https://doi.org/10.1139/x04-211

Huang M, Wang X, Keenan TF, Piao S (2018) Drought timing influences the legacy of tree growth recovery. Glob Chang Biol 24:3546–3559. https://doi.org/10.1111/gcb.14294

Jansen S, Baas P, Gasson P, et al (2004) Variation in xylem structure from tropics to tundra: Evidence from vestured pits. Proc Natl Acad Sci 101:8833–8837. https://doi.org/10.1073/pnas.0402621101

Kannenberg SA, Novick KA, Alexander MR, et al (2019) Linking drought legacy effects across scales: From leaves to tree rings to ecosystems. Glob Chang Biol 25:2978–2992. https://doi.org/10.1111/GCB.14710

Klockow PA, Vogel JG, Edgar CB, Moore GW (2018) Lagged mortality among tree species four years after an exceptional drought in east Texas. Ecosphere 9:. https://doi.org/10.1002/ecs2.2455

Kluver D, Mote T, Leathers D, et al (2016) Creation and validation of a comprehensive 1° by 1° daily gridded North American dataset for 1900–2009: Snowfall. J Atmos Ocean Technol 33:857–871. https://doi.org/10.1175/JTECH-D-15-0027.1

Knutzen F, Averbeck P, Barrasso C, et al (2023) Impacts and damages of the European multi-year drought and heat event 2018 - 2022 on forests, a review. Egusph Prepr 1–56

Kono Y, Ishida A, Saiki S-T, et al (2019) Initial hydraulic failure followed by late-stage carbon starvation leads to drought-induced death in the tree Trema orientalis. Commun Biol 2:8. https://doi.org/10.1038/s42003-018-0256-7

Krusic PJ, Cook ER, Dukpa D, et al (2015) Six hundred thirty-eight years of summer temperature variability over the Bhutanese Himalaya. Geophys Res Lett 42:2988–2994. https://doi.org/10.1002/2015GL063566

Levionnois S, Jansen S, Wandji RT, et al (2020) Linking drought-induced xylem embolism resistance to wood anatomical traits in Neotropical trees. New Phytol nph.16942.

https://doi.org/10.1111/nph.16942

Li J, Chen D, Yang X, et al (2024) Effects of Stand Density, Age, and Drought on the Size–Growth Relationship in Larix principis-rupprechtii Forests. Forests 15:413. https://doi.org/10.3390/f15030413

Li X, Piao S, Wang K, et al (2020) Temporal trade-off between gymnosperm resistance and resilience increases forest sensitivity to extreme drought. Nat Ecol Evol 4:1075–1083. https://doi.org/10.1038/s41559-020-1217-3

Linderholm HW (2001) Climatic influence on scots pine growth on dry and wet soils in the central Scandinavian mountains, interpreted from tree-ring widths. Silva Fenn 35:415–424. https://doi.org/10.14214/sf.574

Lotfiomran N, Köhl M (2017) Retrospective analysis of growth: A contribution to sustainable forest management in the tropics

Luo K, Wang X, de Jong M, Flannigan M (2024) Drought triggers and sustains overnight fires in North America. Nature 627:321–327. https://doi.org/10.1038/s41586-024-07028-5

Ma X, Huete A, Moran S, et al (2015) Abrupt shifts in phenology and vegetation productivity under climate extremes. J Geophys Res Biogeosciences 120:2036–2052. https://doi.org/10.1002/2015JG003144

Marini L, Økland B, Jönsson AM, et al (2017) Climate drivers of bark beetle outbreak dynamics in Norway spruce forests. Ecography (Cop) 40:1426–1435. https://doi.org/10.1111/ecog.02769

Martin J, Looker N, Hoylman Z, et al (2018) Differential use of winter precipitation by upper and lower elevation Douglas fir in the Northern Rockies. Glob Chang Biol 24:5607–5621. https://doi.org/10.1111/gcb.14435

Martínez-Vilalta J, Lloret F (2016) Drought-induced vegetation shifts in terrestrial ecosystems: The key role of regeneration dynamics. Glob Planet Change 144:94–108. https://doi.org/10.1016/j.gloplacha.2016.07.009

McDowell NG, Beerling DJ, Breshears DD, et al (2011) The interdependence of mechanisms underlying climate-driven vegetation mortality. Trends Ecol Evol 26:523–532. https://doi.org/10.1016/j.tree.2011.06.003

Montwé D, Isaac-Renton M, Hamann A, Spiecker H (2016) Drought tolerance and growth in populations of a wide-ranging tree species indicate climate change risks for the boreal

north. Glob Chang Biol 22:806–815. https://doi.org/10.1111/gcb.13123

Morales MS, Cook ER, Barichivich J, et al (2020) Six hundred years of South American tree rings reveal an increase in severe hydroclimatic events since mid-20th century. Proc Natl Acad Sci U S A 117:16816–16823. https://doi.org/10.1073/pnas.2002411117

Moreau G, Achim A, Pothier D (2020) An accumulation of climatic stress events has led to years of reduced growth for sugar maple in southern Quebec, Canada. Ecosphere 11:. https://doi.org/10.1002/ecs2.3183

Nardini A, Battistuzzo M, Savi T (2013) Shoot desiccation and hydraulic failure in temperate woody angiosperms during an extreme summer drought. New Phytol 200:322–329. https://doi.org/10.1111/nph.12288

Nardini A, Casolo V, Dal Borgo A, et al (2016) Rooting depth, water relations and non-structural carbohydrate dynamics in three woody angiosperms differentially affected by an extreme summer drought. Plant Cell Environ 39:618–627. https://doi.org/10.1111/pce.12646

Nehrbass-Ahles C, Babst F, Klesse S, et al (2014) The influence of sampling design on tree-ring-based quantification of forest growth. Glob Chang Biol 20:2867–2885. https://doi.org/10.1111/GCB.12599

New M, Lister D, Hulme M, Makin I (2002) A high-resolution data set of surface climate over global land areas. Clim Res 21:1–25. https://doi.org/10.3354/CR021001

Nguyen P, Shearer EJ, Tran H, et al (2019) The CHRS Data Portal, an easily accessible public repository for PERSIANN global satellite precipitation data. Sci Data 6:180296. https://doi.org/10.1038/sdata.2018.296

Pearl JK, Keck JR, Tintor W, et al (2020) New frontiers in tree-ring research. Holocene 30:923–941. https://doi.org/10.1177/0959683620902230

Pederson N, Hessl AE, Baatarbileg N, et al (2014) Pluvials, droughts, the Mongol Empire, and modern Mongolia. Proc Natl Acad Sci U S A 111:4375–4379. https://doi.org/10.1073/pnas.1318677111

Pirtskhalava-Karpova N, Trubin A, Karpov A, Jakuš R (2024) Drought initialised bark beetle outbreak in Central Europe: Meteorological factors and infestation dynamic. For Ecol Manage 554:. https://doi.org/10.1016/j.foreco.2023.121666

Powers JS, Vargas G. G, Brodribb TJ, et al (2020) A catastrophic tropical drought kills

hydraulically vulnerable tree species. Glob Chang Biol 26:3122–3133. https://doi.org/10.1111/gcb.15037

Prats KA, Fanton AC, Brodersen CR, Furze ME (2023) Starch depletion in the xylem and phloem ray parenchyma of grapevine stems under drought. AoB Plants 15:1–12. https://doi.org/10.1093/aobpla/plad062

Rodriguez-Zaccaro FD, Groover A (2019) Wood and water: How trees modify wood development to cope with drought. Plants People Planet 1:346–355. https://doi.org/10.1002/ppp3.29

Rosner S, Světlík J, Andreassen K, et al (2016) Novel hydraulic vulnerability proxies for a boreal conifer species reveal that opportunists may have lower survival prospects under extreme climatic events. Front Plant Sci 7:1–14. https://doi.org/10.3389/fpls.2016.00831

Rozendaal DMA, Zuidema PA (2011) Dendroecology in the tropics: A review. Trees - Struct. Funct. 25:3–16

Sáenz-Ceja JE, Pérez-Salicrup DR (2019) Dendrochronological reconstruction of fire history in coniferous forests in the Monarch Butterfly Biosphere Reserve, Mexico. Fire Ecol 15:. https://doi.org/10.1186/s42408-019-0034-z

Sang Z, Sebastian-Azcona J, Hamann A, et al (2019) Adaptive limitations of white spruce populations to drought imply vulnerability to climate change in its western range. Evol Appl 12:1850–1860. https://doi.org/10.1111/eva.12845

Schöngart J, Gribel R, Ferreira da Fonseca-Junior S, Haugaasen T (2015) Age and growth patterns of Brazil nut trees (*Bertholletia excelsa* Bonpl.) in Amazonia, Brazil. Biotropica 47:550–558. https://doi.org/10.1111/btp.12243

Sebastian-Azcona J, Hacke U, Hamann A (2020) Xylem anomalies as indicators of maladaptation to climate in forest trees: Implications for assisted migration. Front Plant Sci 11:1–8. https://doi.org/10.3389/fpls.2020.00208

Seidl R, Thom D, Kautz M, et al (2017) Forest disturbances under climate change. Nat Clim Chang 7:395–402. https://doi.org/10.1038/nclimate3303

Simmons A, Hersbach H, Muñoz-Sabater J, et al (2021) Low frequency variability and trends in surface air temperature and humidity from ERA5 and other datasets. ECMWF Tech Memo 811:. https://doi.org/10.21957/ly5vbtbfd

Smith-Martin CM, Muscarella R, Ankori-Karlinsky R, et al (2023) Hydraulic traits are not

robust predictors of tree species stem growth during a severe drought in a wet tropical forest. Funct Ecol 37:447–460. https://doi.org/10.1111/1365-2435.14235

Sohn JA, Saha S, Bauhus J (2016) Potential of forest thinning to mitigate drought stress: A meta-analysis. For Ecol Manage 380:261–273. https://doi.org/10.1016/j.foreco.2016.07.046

Spangenberg G, Zimmermann R, Küppers M, et al (2024) Interannual radial growth response of Douglas-fir (Pseudotsuga menziesii (Mirb.) Franco) to severe droughts: an analysis along a gradient of soil properties and rooting characteristics. Ann For Sci 81:. https://doi.org/10.1186/s13595-024-01240-z

Speer JH (2010) Fundamentals of tree-ring research. The University of Arizona Press, Tucson, Arizona

Sperry JS, Love DM (2015) What plant hydraulics can tell us about responses to climate-change droughts. New Phytol 207:14–27. https://doi.org/10.1111/nph.13354

Spînu AP, Niklasson M, Zin E (2020) Mesophication in temperate Europe: A dendrochronological reconstruction of tree succession and fires in a mixed deciduous stand in Białowieża Forest. Ecol Evol 10:1029–1041. https://doi.org/10.1002/ece3.5966

Sun Q, Miao C, Duan Q, et al (2018) A Review of global precipitation data sets: Data sources, estimation, and intercomparisons. Rev Geophys 56:79–107. https://doi.org/10.1002/2017RG000574

Tonelli E, Vitali A, Malandra F, et al (2023) Tree-ring and remote sensing analyses uncover the role played by elevation on European beech sensitivity to late spring frost. Sci Total Environ 857:. https://doi.org/10.1016/j.scitotenv.2022.159239

Trugman AT, Anderegg LDL, Anderegg WRL, et al (2021) Why is tree drought mortality so hard to predict? Trends Ecol Evol 36:520–532. https://doi.org/10.1016/j.tree.2021.02.001

Trugman AT, Detto M, Bartlett MK, et al (2018) Tree carbon allocation explains forest drought-kill and recovery patterns. Ecol Lett 21:1552–1560. https://doi.org/10.1111/ele.13136

van Loo M, Ufimov R, Grabner M, et al (2023) *Quercus petraea* (Matt.) Liebl. from the Thayatal National Park in Austria: Selection of potentially drought-tolerant phenotypes. Forests 14:. https://doi.org/10.3390/f14112225

Vasconcellos TJ de, Tomazello-Filho M, Callado CH (2019) Dendrochronology and

dendroclimatology of *Ceiba speciosa* (A. St.-Hil.) Ravenna (Malvaceae) exposed to urban pollution in Rio de Janeiro city, Brazil. Dendrochronologia 53:104–113. https://doi.org/10.1016/j.dendro.2018.12.004

Venturas MD, Sperry JS, Hacke UG (2017) Plant xylem hydraulics: What we understand, current research, and future challenges. J Integr Plant Biol 59:356–389. https://doi.org/10.1111/jipb.12534

Vicente-Serrano SM, Gouveia C, Camarero JJ, et al (2013) Response of vegetation to drought time-scales across global land biomes. Proc Natl Acad Sci U S A 110:52–57. https://doi.org/10.1073/pnas.1207068110

Villalba R, Veblen TT (1998) Influences of large-scale climatic variability on episodic tree mortality in northern Patagonia. Ecology 79:2624–2640. https://doi.org/10.1890/0012-9658(1998)079[2624:IOLSCV]2.0.CO;2

Williams AP, Allen CD, Macalady AK, et al (2013) Temperature as a potent driver of regional forest drought stress and tree mortality. Nat Clim Chang 3:292–297. https://doi.org/10.1038/nclimate1693

Wilmking M, Maaten-Theunissen M, Maaten E, et al (2020) Global assessment of relationships between climate and tree growth. Glob Chang Biol 26:3212–3220. https://doi.org/10.1111/gcb.15057

Xue J, Su B (2017a) Significant remote sensing vegetation indices: A review of developments and applications. J Sensors 2017:. https://doi.org/10.1155/2017/1353691

Xue J, Su B (2017b) Significant remote sensing Vegetation Indices: A review of developments and Applications. J Sensors 2017:1–17. https://doi.org/10.1155/2017/1353691

Zald HSJ, Callahan CC, Hurteau MD, et al (2022) Tree growth responses to extreme drought after mechanical thinning and prescribed fire in a Sierra Nevada mixed-conifer forest, USA. For Ecol Manage 510:120107. https://doi.org/10.1016/j.foreco.2022.120107

Zandler H, Haag I, Samimi C (2019) Evaluation needs and temporal performance differences of gridded precipitation products in peripheral mountain regions. Sci Reports 2019 91 9:1–15. https://doi.org/10.1038/s41598-019-51666-z

Zargar A, Sadiq R, Naser B, Khan FI (2011) A review of drought indices. Environ Rev 19:333–349. https://doi.org/10.1139/a11-013

Zhang QW, Zhu SD, Jansen S, Cao KF (2021) Topography strongly affects drought stress and

xylem embolism resistance in woody plants from a karst forest in Southwest China. Funct Ecol 35:566–577. https://doi.org/10.1111/1365-2435.13731

Chapter 2. A snapshot of the international tree ring database (ITRDB) with improved metadata and error corrections

2.1. Summary

The international tree ring database (ITRDB) is an important resource to document climate change impacts, reconstruct long-term climate trends, and investigate historical trends in forest health and growth. Founded in 1974, it has been the primary global dendrochronology database, and today contains data representing more than 5,000 sites, 160,000 cores and 250,000 core measurements. Since data formats and metadata requirements have occasionally changed since the inception of the ITRDB, considerable data checking and cleaning efforts are required by investigators who want to use large portions of the database for continental or global research. Here, we contribute a snapshot of the ITRDB (as of October 2021), that contains cross-checked and corrected metadata (~20% of records corrected), consistently formatted raw ring width files (~15% corrected) that can be read by open-source software without issue, as well as consistent site chronologies, developed with three detrending methods (preserving low- medium- and high-frequency variability) for different research objectives. We further report chronology statistics and quality flags that help users exclude portions of the database as desired.

2.2. Background & Summary

Over the last several decades, dendrochronology has become an important research approach to document climate change impacts, reconstruct long-term climate trends, and investigate historical forest health and growth characteristics (Folland et al. 2001). Pearl et al. (2020) estimate that studies in the fields of dendroclimatology and dendroecology have more than quadrupled in the past two decades. Dendrochronology-based research approaches have also gained a variety of management applications in the context of tracking forest productivity and forest health under changing climates (Hogg et al. 2005; Williams et al. 2013; Schöngart et al. 2015; Vasconcellos et al. 2019), to evaluate drought vulnerability of species and forest ecosystems (Herweijer et al. 2007; Huang et al. 2018; DeSoto et al. 2020a; Bose et al. 2021), to study the long-term impacts of extreme climate events (Villalba and Veblen 1998; Bond-Lamberty et al. 2014; Dorman et al. 2015), and to track historical trends in fire frequencies (Brandes et al. 2019; Sáenz-Ceja and Pérez-Salicrup 2019; Spînu et al. 2020; Brown et al. 2020).

The primary data repository for researchers engaged in tree ring research for various objectives is the international tree ring databank (ITRDB). The ITRDB was founded in 1974 by Harold C Fritts through the Tree-Ring Research Laboratory in Tucson, Arizona when its operation was largely dependent on volunteers (Grissino-Mayer and Fritts 1997). However, in 1990, with the establishment of the World Data Center – A for paleoclimatology, the National Atmospheric Administration Oceanic (NOAA) commenced the operation of the ITRDB, providing permanent storage of tree-ring data from around the world (Grissino-Mayer and Fritts 1997). Since then, an advisory committee consisting of international researchers has served as the custodian of the ITRDB. As of 2021, the database contains over 5,000 sites, 160,000 cores and 250,000 data files of core measurements.

The spatial and temporal coverage of the ITRDB has enabled important global and continental-scale re-analyses efforts to yield more general insights than local studies can provide. Examples for larger scale analyses based on the ITRDB include improving estimates of annual CO_2 sequestration (Brienen et al. 2020b), which has shown that carbon sequestration has increased with climate change, but also reduced average tree longevity, potentially compromising overall carbon sequestration. Other important insights derived from ITRDB-based research include forest resilience to drought events in large-scale studies for the US (Cook et al. 2007), Europe

(Cook et al. 2015, 2020) and South America (Morales et al. 2020). ITRDB data has also supported forecasting forest growth in the context of climate change (Charney et al. 2016) and identification of legacy effects from climate extremes (Anderegg et al. 2015).

Working with ITRDB data does, however, present some technical challenges for researchers, because the database relies on author contributions over a period of more than 50 years, and best practices for metadata provision and file formats have changed over this period. Users may find inconsistencies, omissions and data format idiosyncrasies that make batch processing of downloaded ITRDB data difficult. There are multiple versions of Tucson format (*.rwl*) data files, making bulk importing of data challenging. In a major quality control effort, Zhao et al.(2018) has identified and corrected many problematic data files, although some data import issues remain, and metadata issues were not addressed in this study. Metadata submitted by contributing authors is available in the header of original *.rwl* data files, but they often contain omissions, unit errors, or errors in start and end dates of chronologies. The NOAA team has addressed many of these issues, providing corrected metadata in additional hierarchical file formats (*.xlm* and *.json*), but not all problems have been resolved.

Here we contribute a recent snapshot (October 3, 2021) of the ITRDB, which provides data files in a consistent format, readable without issues by the widely used R package dplR (Bunn et al. 2022) for the R programming environment (R Core Team 2021). Header information in these data files has undergone multiple cross-checks for consistency, and we have improved metadata, where unambiguous corrections could be made. The ITRDB further contains author-contributed chronologies that use a wide variety of detrending methods and are therefore not suitable for reanalysis projects. We therefore provide three sets of consistently detrended chronologies that preserve low, medium, or high frequency variability. Lastly, we built a metadata flat file with curated information that allows users to select relevant records for various research purposes, with links to data files, and original publications. The purpose of this contribution is to provide a snapshot of a clean, consistently formatted version of the ITRDB with cross-checked metadata, suitable for large-scale re-analysis projects. We further provide scripts used for some automated error detection tasks that could be applied to future submissions to the ITRDB.

2.3. Methods

2.3.1. Metadata compilation and inclusion of data types

In order to identify inconsistencies and potential errors in the existing ITRDB metadata, we compiled metadata information from different sources into a single flat file, merging information from (1) the header of the individual tree ring (*.rwl*) data files that were contributed by researchers, (2) metadata compiled by Zhao et al. (2018), last updated on Oct 12, 2017, and available as Appendix S1 at https://www.ncdc.noaa.gov/paleo-search/study/25570, (3) the metadata text file on the ITRDB Server last updated on Oct 3rd, 2021, available at https://www1.ncdc.noaa.gov/pub/data/paleo/treering/, and (4) additional NOAA metadata fields available at https://www1.ncdc.noaa.gov/pub/data/metadata/published/paleo/json/ last updated on Nov 5th, 2021.

This metadata information from multiple sources was imported and merged with the appropriate ID field (variously referred to as "studyCode", "fileCode", "CODE", "ID" and "file"). Subsequently, we searched for inconsistencies of any metadata field provided by different sources, accepted the most plausible version, and made additional corrections as described below. After corrections, the corrected metadata was assembled as a flat file and expanded with useful additional fields sourced from NOAA's *.json* file types. We included URLs to each data file, the study name and author notes, the NOAA study page URL, location information, species common and updated scientific names, citations and DOIs or URLs to publications (where available). In addition, we include quality and error flags that we generated as part of this cross-checking effort and currently accepted species names that allows for merging of synonyms. An R script to bulk-import individual *.json* metadata and assemble the flat file is provided as Appendix 1.

A chronology may include multiple types of measurements, some of the measurement types being quite rare. Since the objective of this contribution is to provide a database for large-scale re-analysis efforts, we only included the most common measurements: (1) ring width (indicated in the *.rwl* file name as w, rw, original, or simply left blank without a letter), latewood width (coded as l or lw), earlywood width (e or ew), maximum density (x), minimum density (n), latewood density (t), earlywood density (i) and latewood percent (p). Together, these data types

comprised 99.5% of the data in the ITRDB. The remaining 0.5% of data types, *e.g.*, basal area (ba), basal area mass (bm), blue intensity (b), cell wall thickness (c), tracheid diameter (w), were not included in this compilation and cross-checking effort. We recoded the *.rwl* file names indicating measurement types for consistency according to the conversion matrix provided as Appendix **2**. Our final collection of raw data files comprises chronology data from 5014 sites, with 5008 data files of ring width measurements (containing multiple trees and multiple cores per tree), 625 measurements of latewood width, 621 earlywood width, 576 maximum density, 519 minimum density, 311 latewood density, 311, earlywood density and 49 latewood percent measurements.

2.3.2. Manual location and elevation corrections

We investigated all location discrepancies that exceeded 5 km among any pair of meta-data sources described above (computed with the geosphere package (Hijmans 2021) for the R programming environment (R Core Team 2021). In addition, we checked for inconsistencies among reported country, province or state with a point extraction from a GIS layer with the same information (USGS 1997). To resolve conflicting information, we consulted the author's original publication where available, used Google Earth satellite imagery to judge the plausibility of different candidate locations based on reported location names, and lastly compared reported elevation versus elevation from a digital elevation model as an additional criterion to decide on the most plausible location record. For location records that matched between NOAA metadata and author reported, we re-calculated a decimal degree location from the original degree-minute record with 4-decimal precision to avoid the introduction of additional (albeit very small) rounding errors. For unresolvable location discrepancies, we accepted NOAA's .json files due to its superior quality control procedure and documentation (details available at https://www1.ncdc.noaa.gov/pub/data/paleo/data_management/ITRDBworkflow.txt).

Inconsistencies in reported elevation values were mapped by pairwise comparisons among the different sources of metadata as well as checked against a 30 arcsecond (approximately 1km) Digital Elevation Model (DEM) (USGS 1997). Reported elevation values of zero or missing values were replaced with the DEM value. For mountainous areas, mismatches between a reported elevation and DEM values are common, and typically arise from location coordinate

inaccuracies rather than a mis-reported elevation values. We therefore only investigated discrepancies if no matching elevation values could be found within a 10 km radius, a query implemented with the ArcGIS focal statistics tool (ESRI 2011). As a secondary criterion to focal-point based elevation corrections, we evaluated the percentile value of the reported elevation in species' elevation range. All focal-point DEM discrepancies were corrected if they also corresponded to a position above the 95th or below the 5th percentile of a species' elevation range. With this dual criterion, errors could be corrected with high confidence. Note that elevation corrections are valuable if climate values are estimated directly for sample locations through interpolation techniques that use elevation as a covariate for climate estimates (e.g., for users of climate databases that allow for lapse-rate based temperature corrections (Wang et al. 2016; Marchi et al. 2020)).

2.3.3. Chronology start and end dates

The start and end dates of chronologies are available in metadata, but they are also encoded at the end of the second line of *.rwl* data files and can further be retrieved from row names after import with the *read.rwl()* function of the dplR package (Bunn et al. 2022). The latter reflects years for which ring width data is available. Mismatches were classified into three types. The most common errors were due to how the year is encoded on *.rwl* files: (1) When elevation information is missing, latitude is read as start year and subsequent start and end date reads failed; (2) floating chronologies do not have exact calendar year assigned to them and sometimes are encoded with future years or random starting years *e.g.* 1001 or 101 or 0, (3) some files included a hyphen between start and end year instead of a space which was read into metadata source as negative years. All problems could be unambiguously resolved, and corrected start and end dates of chronologies were included in the final metadata flat file, as well as written into a new set of *.rwl* data files.

2.3.4. Species nomenclature

Species information is available on the first line of the header of *.rwl* files and it is encoded by four letters – generally the first two encode the genus and last two the specific epithet. In order to include the full species name, codes were first converted to NOAA's list of species names (https://www.ncei.noaa.gov/pub/data/paleo/templates/tree-species-code.csv). Subsequently, we

cross-checked the nomenclature against The Plant List database (2013) using the function *TPL()* from the *Taxonstand* package (Cayuela et al. 2021). This database is based on the World Flora Online Dataset of 2013 curated by the Kew Royal Botanical Garden, and then manually updated through the Plants of the World Online (POWO) website, also curated by the Kew Royal Botanical Garden but more frequently updated. Name matching was implemented with a fuzzy match algorithm implemented using the *stringdist_join()* function of the *fuzzyjoin* package (David Robinson 2020). Current accepted names were added to the metadata to allow consolidating synonyms by users of this database, but original ITRDB names and codes were not altered.

2.3.5. Corrections to tree ring data files

To check for formatting issues in Tucson format (*.rwl*) data files, we used the *read.rwl()* function from the dplR package for the R programming software to import all files checked or corrected by Zhao et al. (2018) and any new files added to the database since the cut-off date reported in Zhao et al.'s (2018) publication. For all files that failed to import we programmed a modified version of the *read.tucson()* function (available as Appendix 3 which returns a list of errors encountered in each file. Issues that prevent files from being read included the presence of diacritics and commas in file headers, partially or fully duplicated cores, and mistakes in labels identifying cores or years. For duplicated cores, we followed the same rationale used by Zhao et al. (2018), that is, identical values were deleted, cores with only a partial overlap that had similar values were considered segments of the same core and had their labels adjusted, and in case of fully duplicated cores (complete overlap) the first core in the file was kept and any subsequent duplicates were discarded.

2.4. Data records

2.4.1. Species and geographic coverage

The final database snapshot comprised 5,014 sampled forest stands (sites) with a total sampling effort of 163,236 tree cores representing 228 species. For each forest stand of a given species, multiple trees are usually sampled with 1-2 cores per tree. Dated measurements from all cores collected at a forest stand (site) are then recorded into a single *.rwl* file. After detrending to

remove unwanted age effects and other low frequency variance, cores are then combined to form a single chronology containing the average signal of that stand in *.crn* files, resulting in one chronology per site and measurement type.

The five most commonly sampled genera are *Pinus* (57 species), *Picea* (12), *Quercus* (26), *Pseudotsuga* (2) and *Larix* (8) summing to 3,593 sites and representing 70% of the chronologies of the ITRDB (Figure 2.1). The 50 most sampled species represent 85% of all chronologies of the ITRDB. Gymnosperms comprise most of the chronologies (83% vs 17% angiosperms), but the percentage Angiosperm species is somewhat higher than its raw data representation (32% of species).

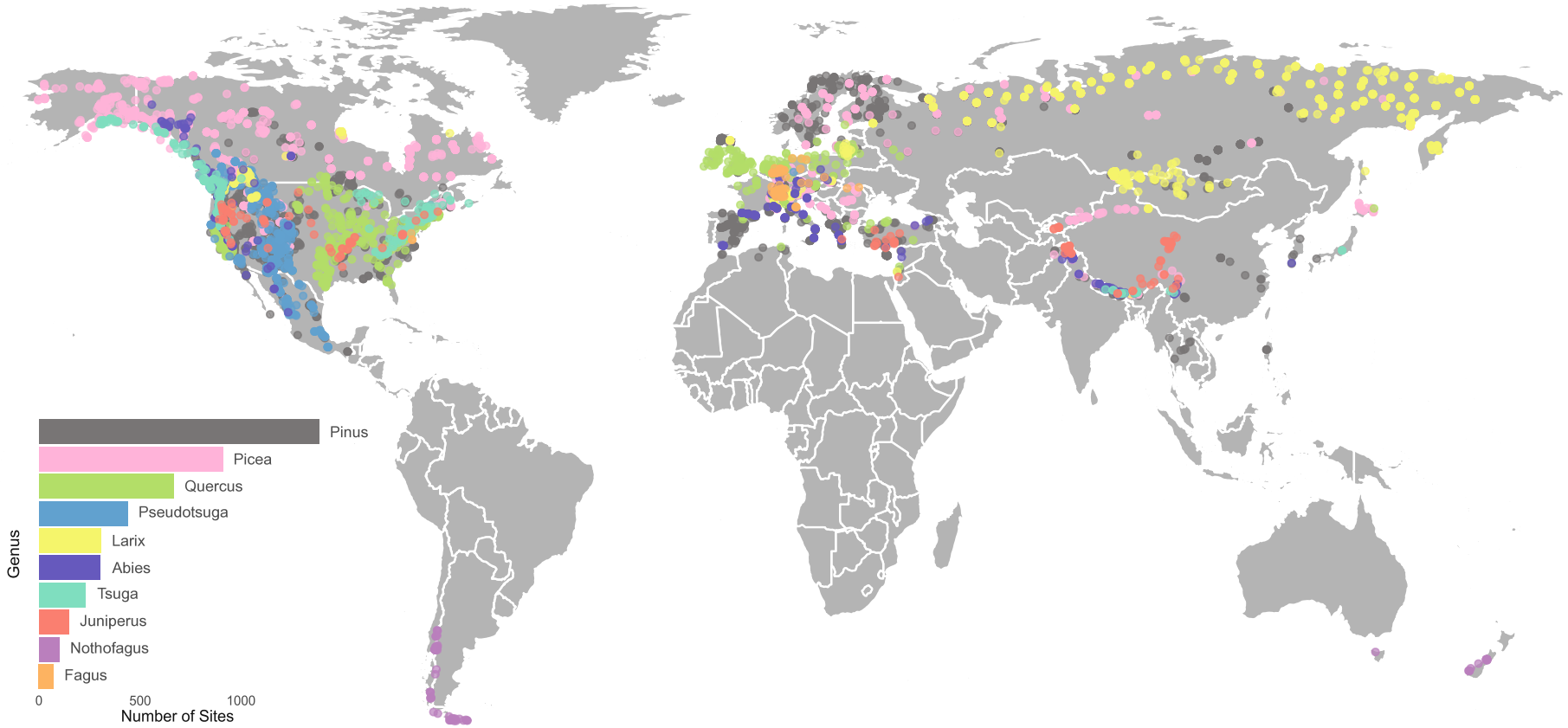

Figure 2.1. Frequency (inset) and distribution of the ten most common genera contributed to the ITRDB representing approximately three quarters of all entries.

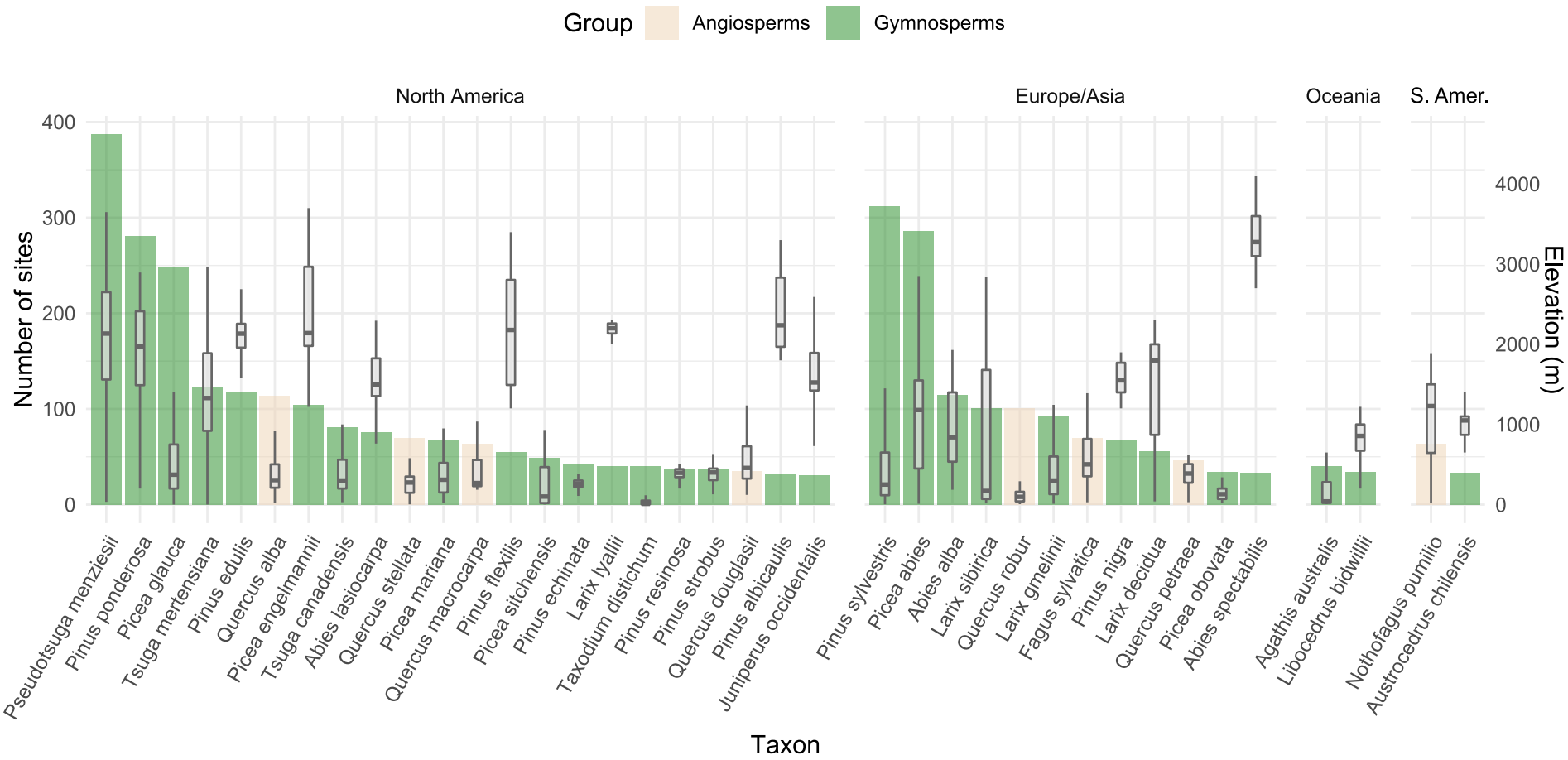

Figure 2.2. Species representation in the ITRDB for the 35 most common species, grouped by continent, and with their elevation distribution overlaid as box plots (right scale).

The majority of chronologies (2768) and species (161) have been contributed from North America, followed by Europe with 1460 and Asia with 393 chronologies (Figure 2.2). Asia is represented with 59 species and Europe with 51 species. Chronologies from other continents amount to 394 chronologies (8% of the ITRDB), mostly located in Oceania (186) and South America (176), and only a small number of chronologies originate in Africa (32).

Both, low and high-elevation species are represented in the database (Figure 2.2), but generally the number of chronologies decreases with increasing elevation. Only 21% of the database contains sites above 2000 m, and sites in the 3000–4000 m range are mostly restricted to North America, representing 295 sites or 4% of the database. A few other high-elevation species with low numbers of chronologies can be found in the Himalayas, including *Abies spectabilis*, *A. pindrow*, *A. forrestii*, *Betula utilis*, *Juniperus przewalskii*, *J. tibetica*, *Picea likiangensis* and *P. smithiana*, which together account for 0.6% of the database.

2.4.2. Temporal coverage

The database records span from 6000 BC to 2019, covering 8019 years of data, with records representing the period from 1700 to 2000 most common (Figure 2.3). Millenia-long chronologies are available from 236 sites (4.7% of the ITRDB), not including floating chronologies from undated fossil samples. The longest chronologies developed comprise 7979 years for *Pinus longaeva* sampled in the White Mountains in California and 7417 years for *P. sylvestris*. *P. longaeva* from Lapland. The median time span of chronologies in the database is 284 years.

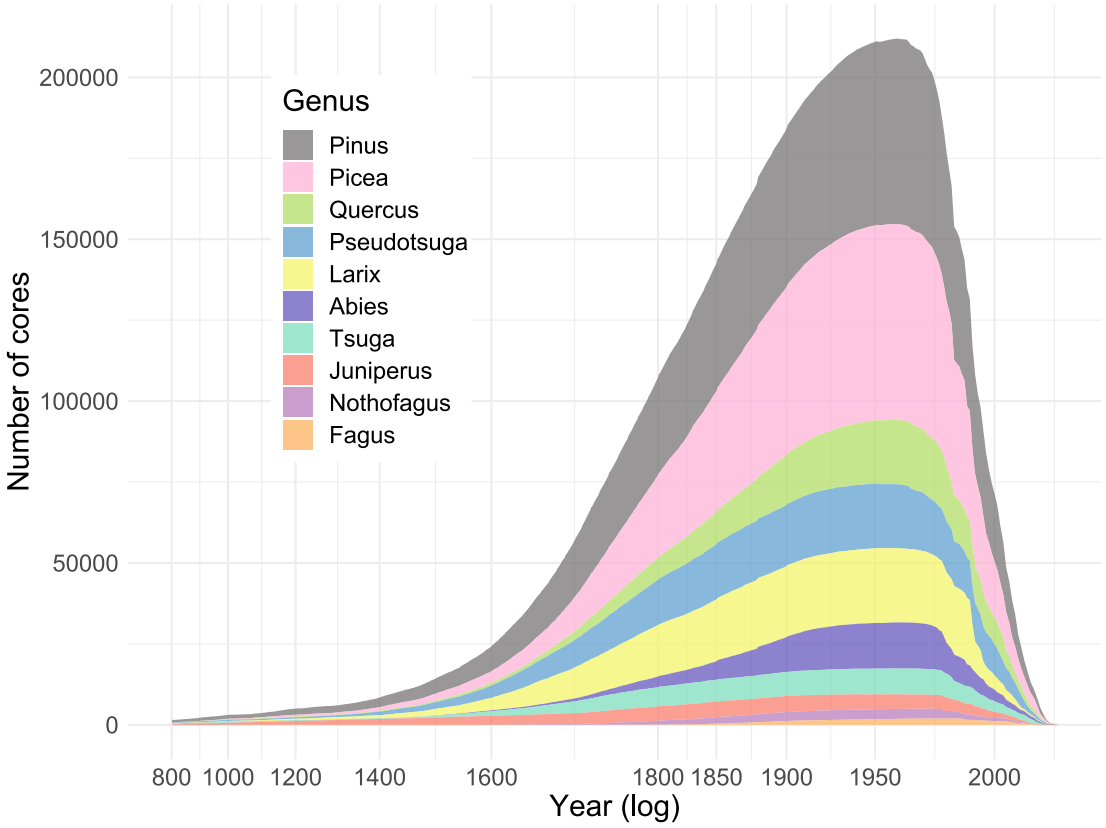

Figure 2.3. Number and proportion of cores for the 10 most common genera found in the database.

2.4.3. Detrended chronology files

We selected three widely used methods that preserve low-medium, medium, or high frequency variability, and that did not require information unavailable in the ITRDB records, (such as cambial age). The chosen detrending methods were: (1) a modified negative exponential curve, which preserves medium to low frequency signals (multidecadal to centennial); (2) the default option of the COFECHA software, which is a smoothing spline with a 32-year interval and cut-off frequency of 50% (Bunn et al. 2022), representing a detrending method commonly used to analyze medium-high variability (interannual to multi-decadal); and (3) the Friedman super smoother (Friedman 1984), which operates more locally than cubic splines and only preserves high frequency variation (interannual to single-decade). While better methods exist for preserving low-frequency variability, e.g., Regional Curve Standardization (Melvin and Briffa 2008), they require additional data on cambial age of samples, and also cannot sensibly be

applied to many shorter chronologies that are contained in the ITRDB. Subsequent to detrending individual cores, chronology data files were generated by averaging detrended and cross-dated cores of a single stand using the function *chron()* of the dplR package for the R programming environment. Scripts used for detrending are available as Appendix 4 and can be modified for different purposes by users of this database.

2.5. Technical Validation

2.5.1. Estimated population signal (EPS) statistics

Generally, chronologies measured more recently show higher concordance among tree cores, as evaluated by the Estimated Population Signal (EPS) statistic (Figure 2.4). EPS is a measure of how much the average chronology reflects the theoretical common signal of an infinitely large population (Wigley et al. 1984). The statistic is strongly driven by number of samples (cores), estimating how much variance can be attributed to the common signal throughout the sample depth. Lower EPS values generally indicate lower predictive power for dendroclimatological analysis (Buras 2017). A commonly used threshold to measure the quality of the chronology is 0.85 meaning a 15% loss in explained variance due to sampling (Figure 2.4, blue vs red). This value can vary depending on the detrending method due to different levels of variance removal associated with the spline or function flexibility. Based on a common detrending method with a 32-year spline and 50% cut-off frequency, 92% of chronologies attain an average EPS statistic above 0.75 across their entire length, and 74% of chronologies have average EPS values above 0.85 across their entire length.

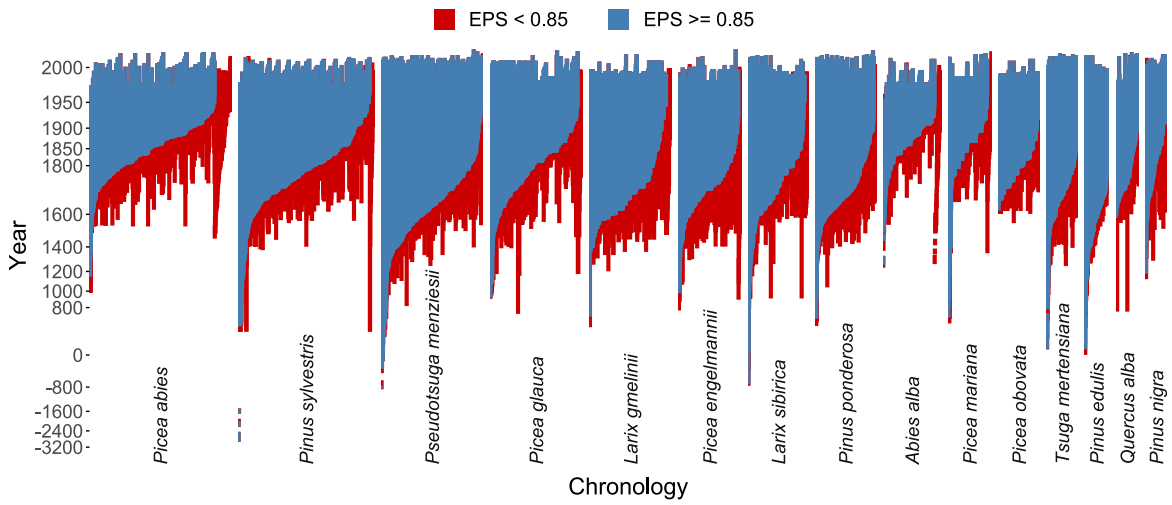

Figure 2.4. Estimated population signal (EPS) statistics for the most common species. The length of individual chronologies is represented by a vertical line. EPS was calculated for a moving window of 50 years and colors represent an EPS quality threshold of 0.85.

2.5.2. Corrections to metadata

Corrections of various types were made to about 35% of ITRDB submissions (Table 2.1). This included 41 major location errors that could be unambiguously corrected with publication information, Google earth imagery, geopolitical boundaries, and elevation information. Further we identified and corrected 162 elevation values that were reported in the imperial measurement system instead of the metric system, 113 implausible elevation values and 354 files that had missing elevation values. For the remaining elevation discrepancies in mountainous areas we accepted the reported elevation values as correct, but we flagged discrepancies to the DEM in the metadata file (Figure 2.5 and Figure 2.6, red).

Errors in the starting and end year of the chronology were detected for 596 chronologies, 62 of these originated from read errors by import algorithms (*e.g.*, when elevation is missing, an algorithm that uses spaces for boundaries may read coordinates as years). For 49 files, years were mistakenly coded with hyphens to indicate the time span between start and end year but those were read as negative years. 19 error were related to floating chronologies which may not have defined calendar years and were arbitrarily given random dates in order to create *.rwl* files. Those were reset to start date of -9999.

Original ITRDB species names were not changed (251 different species), but we added additional metadata fields containing the current accepted names of 243 species, and this field can now be used to aggregate synonyms.

Table 2.1. Summary of corrections to metadata and raw data files (*.rwl* files).

Type of error	Total	% files
File read errors	1309	16.3%
• Diacritic corrections	1278	15.9%
• Duplicated cores	31	0.38%
Location errors	302	3.76%
• Deviation > 100 km	14	0.17%
• Deviation > 10 km	36	0.44%
• Deviation > 1 km	106	1.32%
• Country mismatch	146	1.82%
Elevation errors	632	7.88%
• High deviation in flat areas	113	1.41%
• Conversion errors	163	2.03%
• Missing values filled with DEM	356	4.44%
• Focal point corrections	205	2.55%
Chronology start or end date errors	730	9.10%
• Lat, lon, elev as date	62	0.77%
• Negative end years	49	0.61%
• Multiple	8	0.01%
• Other	611	7.62%
Species corrections	1151	14.34%
• Author name change	498	6.20%
• Epithet change	633	7.89%
• Genus change	20	0.25%
• Conflicting names	12	0.15%
Total files manually corrected	2870*	35.79%*

* Total number of unique files corrected and corresponding percentage of the database.

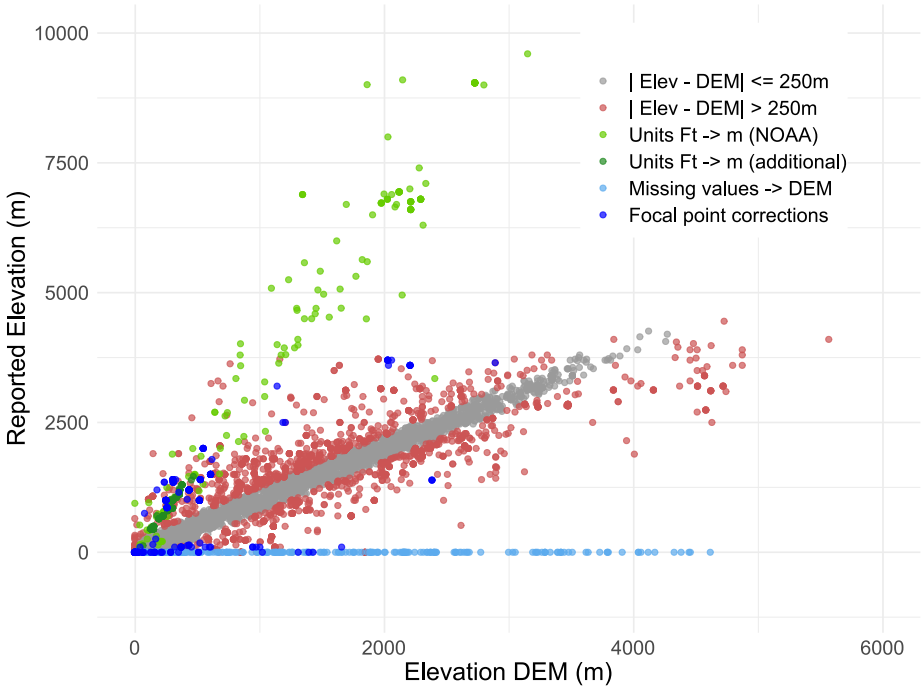

Figure 2.5. Comparison between reported values in *.rwl* files and values extracted from a digital elevation model (DEM). Different colors represent different types of discrepancies identified and corrected.

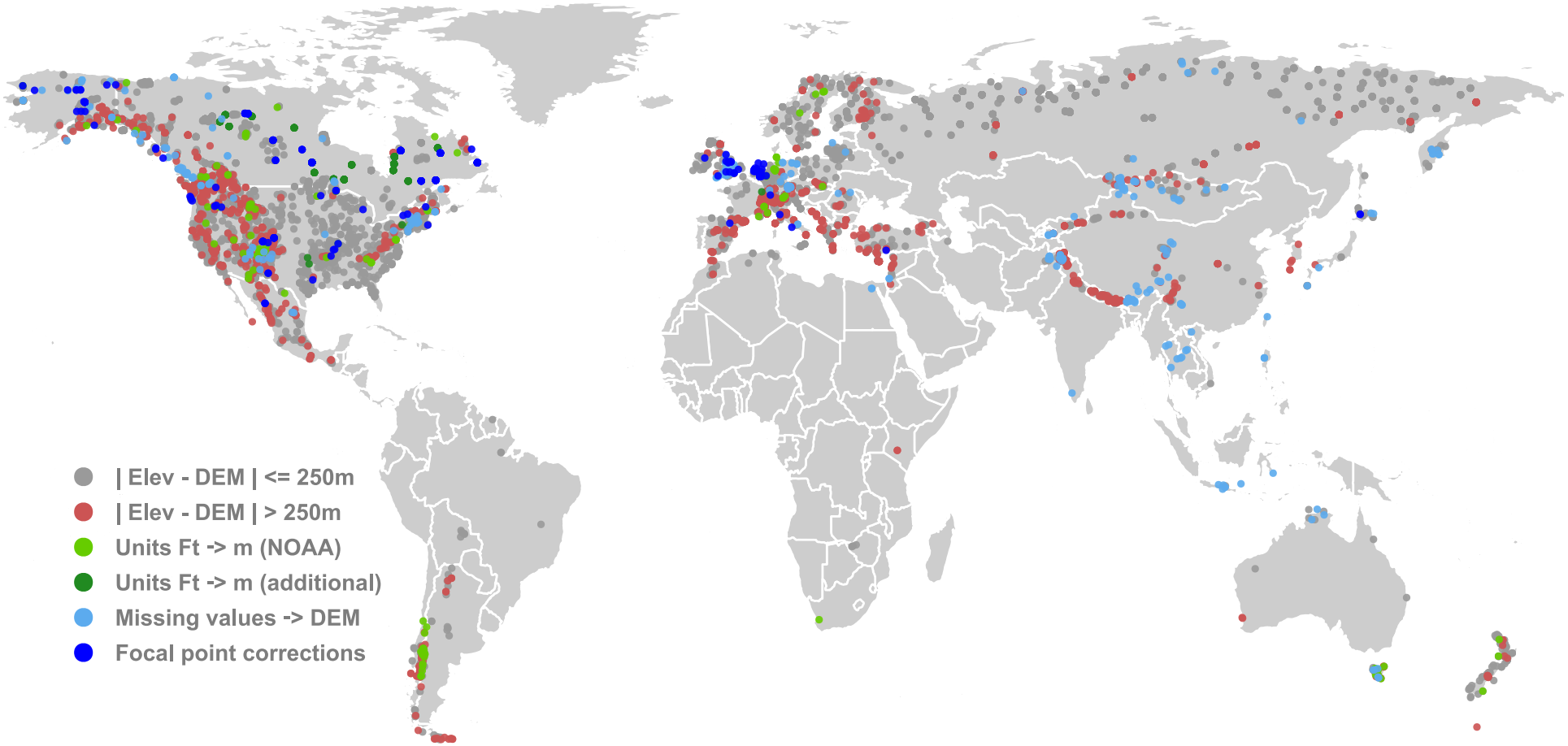

Figure 2.6. Distribution of elevation and other types of discrepancies flagged and corrected in the database.

2.6. Corrections to data files

About one sixth of all files failed to read properly during import with the *dplR* package for the R programming environment (Table 1). Issues that prevent files from being read could be classified generally in six types that were, (1) the presence of diacritics (*e.g.*, “á”, “â”, “ü”) or commas in file headers, (2) duplicated cores, (3) mistakes in decade or core labels, and (4) files with years in the future, and non-standard use of trailing zeros instead of missing values. Except for duplicated cores, the required corrections were straight forward and were carried out in the original *.rwl* files. For duplicated cores we followed a procedure similar to Mina (Mina et al. 2016) who also identified this issue. The first core in the file was kept and any subsequent duplicates were discarded for 36 out of 63 instances of duplication issues, including identical duplications. For the remaining 27 partial duplications, we retained the longest entry and included additional segments of the same core from subsequent entries.

Using the corrected metadata as previously described and corrected data files, we created a new set of *.rwl* files in decadal Tucson format using the function *write.tucson()* of the dplR package (Bunn et al. 2022). The corrections were implemented by setting the corrected metadata as source for the header information in the function parameter options. This final set of .rwl files was tested for compatibility for a variety of software packages, allowing users to bulk-import ITRDB data for analysis without additional efforts or without the need to troubleshoot import errors, incorrect location information or other issues.

2.7. Usage Notes

The database contains (1) a compressed archive of all raw ring width data, (2) chronology files using three different detrending methods, (3) a flat file of meta data for each raw data file and chronology, (4) detailed variable explanations for the meta data flat file, and (5) various appendices with scripts, and records of changes used in this database cleaning and compilation effort. As data format for raw measurements and chronologies, we chose the Tucson decadal format, which has been the standard in dendrochronology community since long before the creation of the ITRDB. While it reflects file size limitations that no longer exist today (Grissino-

Mayer and Fritts 1997), it is the most widely supported by software applications, and is a familiar format in the dendrochronology community.

Wherever possible, we provide flags or variables that allows users to use their own criteria for inclusion or exclusion of records according to their analysis objectives. Data can be filtered by start and end dates of the chronology, number of sampled trees, number of cores per tree, or expressed population signal. For research in mountainous regions, the plausibility of recorded elevations can be checked against a value from a digital elevation model (DEM) or the range of DEM values within a radius of 10 km of the reported location. Furthermore, the data can be easily subset by continent, subcontinental regions, countries and state of province information where applicable, which is now complete for all ITRDB records.

We have further included URLs and DOIs to additional information about original contributors and their publications to facilitate attribution through citation of the original publications. References to URLs and DOIs of each dataset and study page by NOAA is also contained in the meta data flat file for citation and for additional meta data information.

We provide three detrending options that preserve low-medium, medium, or high frequency variability. One of the most common detrending methods, cubic smoothing splines preserves medium frequency variation (although this can be modified by parameter settings). This set of chronologies would be suitable for studies that assess impacts of disturbances and other natural phenomena that can last several years to decades (e.g., impact of logging, forest extraction, insect outbreaks, or severe climatic extreme events). In contrast, the Friedman super smoother method, which operates more locally than cubic splines and only preserves high frequency variation (interannual to single-decade) would be best suited for ecological research that quantifies the influence of interannual variation of environmental variables on tree growth (e.g., identification of limiting climatic factors). Lastly, the modified negative exponential method, which preserves medium to low frequency signals (multidecadal to centennial) would be best suited to study long-term climate shifts and reconstruct past climate variables. We should note, however, that usability of chronology files using this method is also strongly restricted by chronology length (Cook et al. 1995), and additional filtering by chronology length should be applied.

Lastly, we note a limitation, in that this effort to improve the quality and usability of ITRDB data did not include detection of errors in crossdating, which could lead to lower EPS statistics, or errors in start and end dates of whole chronologies that may be revealed through correlation analysis with climate records. A reanalysis by St. George and Ault (St. George and Ault 2014) revealed that for northern hemisphere tree cores, crossdating errors due to missing rings are common, and they could be coded as zeros or as small non-zero values. However, evaluation of raw core data on this aspect was beyond the scope of this study.

2.8. Code Availability

Code used to track errors, update them, and generate new *.rwl* and *.crn* files were created in the R software programming environment version 4.1.2 (Bird Hippie). All codes used here are publicly available on Appendices Appendix **1**, Appendix 3 and Appendix 4.

2.9. References

Anderegg, W.R.L., Schwalm, C., Biondi, F., Camarero, J.J., Koch, G., Litvak, M., Ogle, K., Shaw, J.D., Shevliakova, E., Williams, A.P., Wolf, A., Ziaco, E., Pacala, S., 2015. Pervasive drought legacies in forest ecosystems and their implications for carbon cycle models. Science (80-.). 349, 528–532. https://doi.org/10.1126/science.aab1833

Bond-Lamberty, B., Rocha, A. V., Calvin, K., Holmes, B., Wang, C., Goulden, M.L., 2014. Disturbance legacies and climate jointly drive tree growth and mortality in an intensively studied boreal forest. Glob. Chang. Biol. 20, 216–227. https://doi.org/10.1111/gcb.12404

Bose, A.K., Scherrer, D., Camarero, J.J., Ziche, D., Babst, F., Bigler, C., Bolte, A., Dorado-Liñán, I., Etzold, S., Fonti, P., Forrester, D.I., Gavinet, J., Gazol, A., de Andrés, E.G., Karger, D.N., Lebourgeois, F., Lévesque, M., Martínez-Sancho, E., Menzel, A., Neuwirth, B., Nicolas, M., Sanders, T.G.M., Scharnweber, T., Schröder, J., Zweifel, R., Gessler, A., Rigling, A., 2021. Climate sensitivity and drought seasonality determine post-drought growth recovery of Quercus petraea and Quercus robur in Europe. Sci. Total Environ. 784, 147222. https://doi.org/10.1016/j.scitotenv.2021.147222

Brandes, A.F. das N., Sánchez-Tapia, A., Sansevero, J.B.B., Albuquerque, R.P., Barros, C.F., 2019. Fire records in tree rings of moquiniastrum polymorphum: Potential for reconstructing fire history in the Brazilian atlantic forest. Acta Bot. Brasilica 33, 61–66.

https://doi.org/10.1590/0102-33062018abb0282

Brienen, R.J.W., Caldwell, L., Duchesne, L., Voelker, S., Barichivich, J., Baliva, M., Ceccantini, G., Di Filippo, A., Helama, S., Locosselli, G.M., Lopez, L., Piovesan, G., Schöngart, J., Villalba, R., Gloor, E., 2020. Forest carbon sink neutralized by pervasive growth-lifespan trade-offs. Nat. Commun. 11, 1–10. https://doi.org/10.1038/s41467-020-17966-z

Brown, S.R., Baysinger, A., Brown, P.M., Cheek, J.L., Diez, J.M., Gentry, C.M., Grant, T.A., St. Jacques, J.-M., Jordan, D.A., Leef, M.L., Rourke, M.K., Speer, J.H., Spradlin, C.E., Stevens, J.T., Stone, J.R., Van Winkle, B., Zeibig-Kichas, N.E., 2020. Fire history across forest types in the Southern Beartooth mountains, Wyoming. Tree-Ring Res. 76, 27. https://doi.org/10.3959/TRR2018-11

Bunn, A., Korpela, M., Biondi, F., Campelo, F., Mérian, P., Qeadan, F., Zang, C., 2022. dplR: Dendrochronology Program Library in R.

Buras, A., 2017. A comment on the expressed population signal. Dendrochronologia 44, 130–132. https://doi.org/10.1016/j.dendro.2017.03.005

Cayuela, L., Macarro, I., Stein, A., Oksanen, J., 2021. Taxonstand: Taxonomic standardization of plant species names.

Charney, N.D., Babst, F., Poulter, B., Record, S., Trouet, V.M., Frank, D., Enquist, B.J., Evans, M.E.K., 2016. Observed forest sensitivity to climate implies large changes in 21st century North American forest growth. Ecol. Lett. 19, 1119–1128. https://doi.org/10.1111/ele.12650

Cook, E.R., Briffa, K.R., Meko, D.M., Graybill, D.A., Funkhouser, G., 1995. The ’segment length curse’ in long tree-ring chronology development for palaeoclimatic studies. The Holocene 5, 229–237.

Cook, E.R., Seager, R., Cane, M.A., Stahle, D.W., 2007. North American drought: Reconstructions, causes, and consequences. Earth-Science Rev. 81, 93–134. https://doi.org/10.1016/j.earscirev.2006.12.002

Cook, E.R., Seager, R., Kushnir, Y., Briffa, K.R., Büntgen, U., Frank, D., Krusic, P.J., Tegel, W., Schrier, G. Vander, Andreu-Hayles, L., Baillie, M., Baittinger, C., Bleicher, N., Bonde, N., Brown, D., Carrer, M., Cooper, R., Eùfar, K., DIttmar, C., Esper, J., Griggs, C., Gunnarson, B., Günther, B., Gutierrez, E., Haneca, K., Helama, S., Herzig, F.,

Heussner, K.U., Hofmann, J., Janda, P., Kontic, R., Köse, N., Kyncl, T., Levaniè, T., Linderholm, H., Manning, S., Melvin, T.M., Miles, D., Neuwirth, B., Nicolussi, K., Nola, P., Panayotov, M., Popa, I., Rothe, A., Seftigen, K., Seim, A., Svarva, H., Svoboda, M., Thun, T., Timonen, M., Touchan, R., Trotsiuk, V., Trouet, V., Walder, F., Wany, T., Wilson, R., Zang, C., 2015. Old World megadroughts and pluvials during the Common Era. Sci. Adv. 1, 1–10. https://doi.org/10.1126/sciadv.1500561

Cook, E.R., Solomina, O., Matskovsky, V., Cook, B.I., Agafonov, L., Berdnikova, A., Dolgova, E., Karpukhin, A., Knysh, N., Kulakova, M., Kuznetsova, V., Kyncl, T., Kyncl, J., Maximova, O., Panyushkina, I., Seim, A., Tishin, D., Ważny, T., Yermokhin, M., 2020. The european Russia drought atlas (1400–2016 CE). Clim. Dyn. 54, 2317–2335. https://doi.org/10.1007/s00382-019-05115-2

David Robinson, 2020. fuzzyjoin: Join Tables Together on Inexact Matching.

DeSoto, L., Cailleret, M., Sterck, F., Jansen, S., Kramer, K., Robert, E.M.R., Aakala, T., Amoroso, M.M., Bigler, C., Camarero, J.J., Čufar, K., Gea-Izquierdo, G., Gillner, S., Haavik, L.J., Hereş, A.M., Kane, J.M., Kharuk, V.I., Kitzberger, T., Klein, T., Levanič, T., Linares, J.C., Mäkinen, H., Oberhuber, W., Papadopoulos, A., Rohner, B., Sangüesa-Barreda, G., Stojanovic, D.B., Suárez, M.L., Villalba, R., Martínez-Vilalta, J., 2020. Low growth resilience to drought is related to future mortality risk in trees. Nat. Commun. 11, 1–9. https://doi.org/10.1038/s41467-020-14300-5

Dorman, M., Svoray, T., Perevolotsky, A., Moshe, Y., Sarris, D., 2015. What determines tree mortality in dry environments? A multi-perspective approach. Ecol. Appl. 25, 1054–1071. https://doi.org/10.1890/14-0698.1

ESRI, 2011. ArcGIS Desktop: Release 10.

Folland, C.K., Karl, T.R., Christy, J.R., Clarke, R.A., Gruza, G. V, Jouzel, J., Mann, M.E., Oerlemans, J., Wang, M.J., S-W, S. and, 2001. Observed Climate Variability and Change, in: T, H.J., Ding, Y., Griggs, D.J., Noguer, M., Linden, P.J. van der, Dai, X., Maskel, K., Johnson, C.A. (Eds.), Climate Change 2001: The scientific basis. Contribution of working group I to the third assessment report of the Intergovernmental Panel on Climate Change. Cambridge University Press, Cambridge, United Kingdom and New York, NY, USA, p. 881.

Friedman, J.H., 1984. A variable span Smoother, Journal of American Statistical Association.

https://doi.org/10.21236/ADA148241

Grissino-Mayer, H.D., Fritts, H.C., 1997. The International Tree-Ring Data Bank: an enhanced global database serving the global scientific community. The Holocene 7, 235–238. https://doi.org/10.1177/095968369700700212

Herweijer, C., Seager, R., Cook, E.R., Emile-Greay, J., 2007. North American droughts of the last millennium from a gridded network of tree-ring data. J. Clim. 20, 1353–1376. https://doi.org/10.1175/JCLI4042.1

Hijmans, R.J., 2021. geosphere: Spherical Trigonometry.

Hogg, E.H., Brandt, J.P., Kochtubajda, B., 2005. Factors affecting interannual variation in growth of western Canadian aspen forests during 1951-2000. Can. J. For. Res. 35, 610–622. https://doi.org/10.1139/x04-211

Huang, M., Wang, X., Keenan, T.F., Piao, S., 2018. Drought timing influences the legacy of tree growth recovery. Glob. Chang. Biol. 24, 3546–3559. https://doi.org/10.1111/gcb.14294

Marchi, M., Castellanos-Acuña, D., Hamann, A., Wang, T., Ray, D., Menzel, A., 2020. ClimateEU: Scale-free climate normals, historical time series, and future projections for Europe. figshare.

Melvin, T.M., Briffa, K.R., 2008. A “signal-free” approach to dendroclimatic standardisation. Dendrochronologia 26, 71–86. https://doi.org/10.1016/j.dendro.2007.12.001

Mina, M., Martin-Benito, D., Bugmann, H., Cailleret, M., 2016. Forward modeling of tree-ring width improves simulation of forest growth responses to drought. Agric. For. Meteorol. 221, 13–33. https://doi.org/10.1016/j.agrformet.2016.02.005

Morales, M.S., Cook, E.R., Barichivich, J., Christie, D.A., Villalba, R., LeQuesne, C., Srur, A.M., Eugenia Ferrero, M., González-Reyes, Á., Couvreux, F., Matskovsky, V., Aravena, J.C., Lara, A., Mundo, I.A., Rojas, F., Prieto, M.R., Smerdon, J.E., Bianchi, L.O., Masiokas, M.H., Urrutia-Jalabert, R., Rodriguez-Catón, M., Muñoz, A.A., Rojas-Badilla, M., Alvarez, C., Lopez, L., Luckman, B.H., Lister, D., Harris, I., Jones, P.D., Park Williams, A., Velazquez, G., Aliste, D., Aguilera-Betti, I., Marcotti, E., Flores, F., Muñoz, T., Cuq, E., Boninsegna, J.A., 2020. Six hundred years of South American tree rings reveal an increase in severe hydroclimatic events since mid-20th century. Proc. Natl. Acad. Sci. U. S. A. 117, 16816–16823. https://doi.org/10.1073/pnas.2002411117

Pearl, J.K., Keck, J.R., Tintor, W., Siekacz, L., Herrick, H.M., Meko, M.D., Pearson, C.L., 2020. New frontiers in tree-ring research. Holocene 30, 923–941. https://doi.org/10.1177/0959683620902230

R Core Team, 2021. R: A language and environment for statistical computing. Vienna, Austria.

Sáenz-Ceja, J.E., Pérez-Salicrup, D.R., 2019. Dendrochronological reconstruction of fire history in coniferous forests in the Monarch Butterfly Biosphere Reserve, Mexico. Fire Ecol. 15. https://doi.org/10.1186/s42408-019-0034-z

Schöngart, J., Gribel, R., Ferreira da Fonseca-Junior, S., Haugaasen, T., 2015. Age and growth patterns of Brazil nut trees (*Bertholletia excelsa* Bonpl.) in Amazonia, Brazil. Biotropica 47, 550–558. https://doi.org/10.1111/btp.12243

Spînu, A.P., Niklasson, M., Zin, E., 2020. Mesophication in temperate Europe: A dendrochronological reconstruction of tree succession and fires in a mixed deciduous stand in Białowieża Forest. Ecol. Evol. 10, 1029–1041. https://doi.org/10.1002/ece3.5966

St. George, S., Ault, T.R., 2014. The imprint of climate within Northern Hemisphere trees. Quat. Sci. Rev. 89, 1–4. https://doi.org/10.1016/j.quascirev.2014.01.007

The Plant List, 2013. . Version 1.1.

USGS, 1997. USGS 30 ARC-second Global Elevation Data, GTOPO30. Research Data Archive at the National Center for Atmospheric Research, Computational and Information Systems Laboratory. https://doi.org/https://doi.org/10.5065/A1Z4-EE71.

Vasconcellos, T.J. de, Tomazello-Filho, M., Callado, C.H., 2019. Dendrochronology and dendroclimatology of Ceiba speciosa (A. St.-Hil.) Ravenna (Malvaceae) exposed to urban pollution in Rio de Janeiro city, Brazil. Dendrochronologia 53, 104–113. https://doi.org/10.1016/j.dendro.2018.12.004

Villalba, R., Veblen, T.T., 1998. Influences of large-scale climatic variability on episodic tree mortality in northern Patagonia. Ecology 79, 2624–2640. https://doi.org/10.1890/0012-9658(1998)079[2624:IOLSCV]2.0.CO;2

Wang, T., Hamann, A., Spittlehouse, D., Carroll, C., 2016. Locally downscaled and spatially customizable climate data for historical and future periods for North America. PLoS One 11. https://doi.org/10.1371/journal.pone.0156720

Wigley, T.M.L., Briffa, K.R., Jones, P.D., 1984. On the average value of correlated time series, with applications in dendroclimatology and hydrometeorology. Am. Meteorol. Soc. 201–

213.

Williams, A.P., Allen, C.D., Macalady, A.K., Griffin, D., Woodhouse, C.A., Meko, D.M., Swetnam, T.W., Rauscher, S.A., Seager, R., Grissino-Mayer, H.D., Dean, J.S., Cook, E.R., Gangodagamage, C., Cai, M., Mcdowell, N.G., 2013. Temperature as a potent driver of regional forest drought stress and tree mortality. Nat. Clim. Chang. 3, 292–297. https://doi.org/10.1038/nclimate1693

Zhao, S., Pederson, N., Orangeville, L.D., Hillerislambers, J., Boose, E., Penone, C., Bauer, B., Jiang, Y., Manzanedo, R.D., 2018. The International Tree-Ring Data Bank (ITRDB) revisited: Data availability and global ecological representativity. J. Biogeogr. 46, 355–368. https://doi.org/https://doi.org/10.1111/jbi.13488

Chapter 3. Validation of global precipitation time series products against tree ring records and remotely sensed vegetation greenness

3.1. Summary

Global interpolated climate products are widely used in ecological research to investigate biosphere-climate interactions and to track ecological response to climate variability and climate change. In turn, biological data could also be used for an independent validation of one aspect of climate data quality. All else being equal, more variance explained in biological data identifies the better climate data product. Here, we compare seven global precipitation time series products, including gauge-based datasets (CRU-TS, UDEL-TS, GPCC), re-analysis products (ERA5, CHELSA), a satellite-based dataset (PERSIANN) and a multi-source product that draws on gauge, re-analysis, and satellite data (MSWEP). We focus on precipitation variables, because they are more difficult to interpolate than temperature, and show larger divergence among gridded data products. Our validation is based on 20 years of remotely sensed vegetation greenness (MODIS-EVI) and 120 years of tree ring records from the International Tree Ring Data Bank (ITRDB). The results for the 20-year EVI based validation shows that all gauge and re-analysis data products performed similarly, but were outperformed by the multi-source MSWEP product, especially in regions with low weather station coverage, such as Africa. For analyzing long 120-year time-series, UDEL-TS showed superior performance prior to the 1940s, with especially large margins for northern Asia and the Himalayas region. For other regions, CRU-TS and GPCC could be recommended. We provide maps that can guide the best regional choice of climate product for research involving time series of biological response to historic climate variability and climate change.

3.2. Introduction

Researching biological response to interannual climate variability, long-term climate trends or climate extreme events requires reliable historical climate data. Such data are usually provided as gridded data products that have been interpolated from weather stations, allowing for estimates of climate variables for any study site or sample location (Speer 2010; Golian et al. 2019; Serrano-Notivoli et al. 2021). However, depending on the climate variables required, the topographic complexity of the landscape, and the distance between the study site of interest and the nearest weather station, climate estimates from different data products may be very variable in quality (García-Suárez et al. 2009; Sun and Liu 2016; Fontana et al. 2018). Generally, temperature variables are easier to interpolate and even in mountainous areas they follow predictable patterns according to adiabatic or environmental lapse rates. This is not the case for precipitation variables that are driven by more difficult to model processes, such as orographic lift and rain shadows that do not scale in straight-forward ways with elevation. Furthermore, the shorter the historical time period to be predicted (annual, monthly or daily), the more precipitation estimates are driven by spatially distinctly bounded, and randomly occurring weather events, making interpolations especially challenging (Augustine 2010).

Nevertheless, at monthly spatial resolution, global and regional gridded climate data products are available from many sources, and these products are based on two general types of data sources. Traditionally, gridded climate data is produced from interpolating weather station data (gauge-base) using a variety of interpolation methods (New et al. 2002; Harris et al. 2020). Since approximately the year 2000, time series climate data products based on remotely sensed temperature and precipitation have become available from high-quality satellite-based sensors (Nguyen et al. 2019). However, both approaches have their own limitations. Gauge-base data provides long-term climate datasets (100+ years) but is often severely limited by regional and temporal gaps in weather station coverage (Castellanos-Acuña and Hamann 2020). Remote sensing-based datasets, on the other hand, have homogeneous coverage of the earth's surface that are covered by the orbital path of the satellites (between 60° latitude north and south), but the earliest datasets only start around the 1980s with high quality data only available since around the year 2000. Some gridded climate data products make use of both data sources, where

remotely sensed climate estimates are used where available, and adjusted with weather station information (Simmons et al. 2021).

Making selections among different climate data products could therefore potentially be an important choice for researchers studying climate-biosphere interactions. For gauge-based precipitation products, there are two main reasons why estimates may differ in precision and accuracy. First, authors of different interpolated climate data products may have different levels of access to weather station data from specific countries or regions (Sun et al. 2018), and second, different interpolation algorithms used may result in varying regional quality of climate variable estimates (Sun et al. 2018; Serrano-Notivoli et al. 2021). The choice of interpolation algorithms is not particularly important for regions with dense weather station coverage, where most methods yield very similar estimates and validation statistics. However, for remote regions with sparse or no weather station coverage, such as high montane, high latitude, or other undeveloped regions of the world, interpolation methods can substantially diverge in their climate estimates (Sun et al. 2018; Zandler et al. 2019). This divergence among different interpolation approaches often goes undetected because areas without training data also have no weather stations available for validation.

While validation of the accuracy of climate data is usually performed against weather station data by the authors of climate data products, these validations are generally meaningless for cross-product comparisons. First, there are many valid approaches to validation including various statistical methods, different options to subset training and validation data, and different approaches to deal with autocorrelations among nearby weather station records that may inflate validation statistics (Dinku et al. 2008; Kluver et al. 2016; Fung et al. 2022; Xu et al. 2023). As such, validation statistics from different studies are not directly comparable. Second, after validation statistics have been computed, the withheld validation data will be re-joined with the training data to create the final climate data product to take advantage of all available information. For valid product comparisons, all authors would need to use the same validation data, withheld from the training data, and as such *post hoc* product comparisons with weather station records are not possible.

Biological data, on the other hand, offers an independent data source for validating one aspect of the quality of climate data products. In this study we use 20 years of global historical remote sensing records of vegetation greenness (MODIS-EVI) and 120 years of tree ring records from the International Tree Ring Data Bank (ITRDB). This independent validation is based on the strength of plant-climate associations, with the expectation that variance explained in biological data should be higher for better quality climate data sets. We note that this is only a *partial* validation, because the accuracy of absolute climate values cannot be assessed with biological data sources. However, we can assess the precision of plant-climate interactions in time series. To describe this limitation in other words, we cannot assess systematic bias of climate estimates for any location with biological data, but statistical precision of climate data tracking inter-annual variation of historical biological records can be quantified. For this comparison, we can hold all model parameters and top-level attributes (such as missing values and length of data coverage) constant, with only the climate data source varying in the validation analysis.

This study contributes such an independent validation effort for seven widely used global historical climate products CRU v4, UDEL-TS, GPCC, ERA5, CHELSA, MSWEP and PERSIANN, described in more detail below. Our objective is to carry out two types of comparisons: one long-term evaluation against 120 years of tree ring records for three weather station-derived products with the same long time series coverage (CRU v4, UDEL-TS, GPCC). In a second comparison, we use 20 years of recent global historical remote sensing records of vegetation greenness for validation. For more recent time periods, remote sensing-based products (PERSIANN), re-analysis products that combine observational data with general circulation models (ERA5, CHELSA), and multi-source models that combine gauge, satellite, and re-analysis data (MSWEP) could yield better precipitation estimates, especially for regions with sparse weather station coverage. Our objective is to provide region-specific guidance to researchers, who investigate time series of biological responses to historic climate variability and climate change, as to which climate product is most suitable for their research.

3.3. Methods

3.3.1. Climate data products

We selected seven widely used global, monthly climate data products with a historical coverage dating to the beginning of the 21st century for gridded products derived from weather station records, and dating back to the 1980s for remote-sensing or reanalysis based climate products. This includes the CRU TS 4.05 dataset from the Climatic Research Unit of the University of East Anglia (Harris et al. 2020), the Terrestrial Precipitation product from the University of Delaware (UDEL) (Matsuura and Willmott 2018), the Full Data Monthly Product v2018 from the Global Precipitation Climatology Centre (GPCC) (Schneider et al. 2018), the 5th generation reanalysis product (ERA5) of the European Centre for Medium-Range Weather Forecasts (Simmons et al. 2021), the climatologies at high resolution for the earth's land surface areas v2.1 (CHELSA) from the Swiss Federal Institute for Forest, Snow and Landscape Research (Karger et al. 2021), the Precipitation Estimation from Remotely Sensed Information using Artificial Neural Networks - Climate Data Record (PERSIANN-CDR) from the Center for Hydrometeorology and Remote Sensing at the University of California (Nguyen et al. 2019), and the Multi-Source Weighted-Ensemble Precipitation (MSWEP) product from Department of Civil and Environmental Engineering at the Princeton University (Beck et al. 2019). Attributes of these climate data products are summarized in Table 3**.1**. A general map of weather stations with at least 30 years of precipitation data is shown in Figure 3.1, based on Castellanos and Hamann (Castellanos-Acuña and Hamann 2020), to represent general regional climate data coverage. However, not all of the above gauge-based climate products would have utilized all of these stations for interpolation, depending on different exclusion criteria.

Table 3.1. Global interpolated precipitation products evaluated in this study. Datasets were generated by the University of East Anglia Climatic Research Unit (CRU), the University of Delaware Terrestrial Precipitation (UDEL), the Global Precipitation Climatology Centre (GPCC), the European Centre for Medium-Range Weather Forecasts Reanalysis v5 (ERA5), the Swiss Federal Institute for Forest, Snow and Landscape Research (CHELSA), the Center for Hydrometeorology and Remote Sensing at the University of California (PERSIANN), and the Department of Civil and Environmental Engineering at Princeton University (MSWEP).

Dataset	Type	Resolution	Start	End[1]
CRU4	Gauge	0.5°	1901	2022
UDEL	Gauge	0.5°	1901	2017
GPCC	Gauge	0.25°	1890	2022
ERA5	Reanalysis	0.25°	1950	2022
CHELSA	Reanalysis	30"	1979	2022
PERSIANN	Satellite	0.25°	1983	2022
MSWEP	Multi-source	0.01°	1979	2022

[1] at the time of data access, 2022 implies ongoing updates.

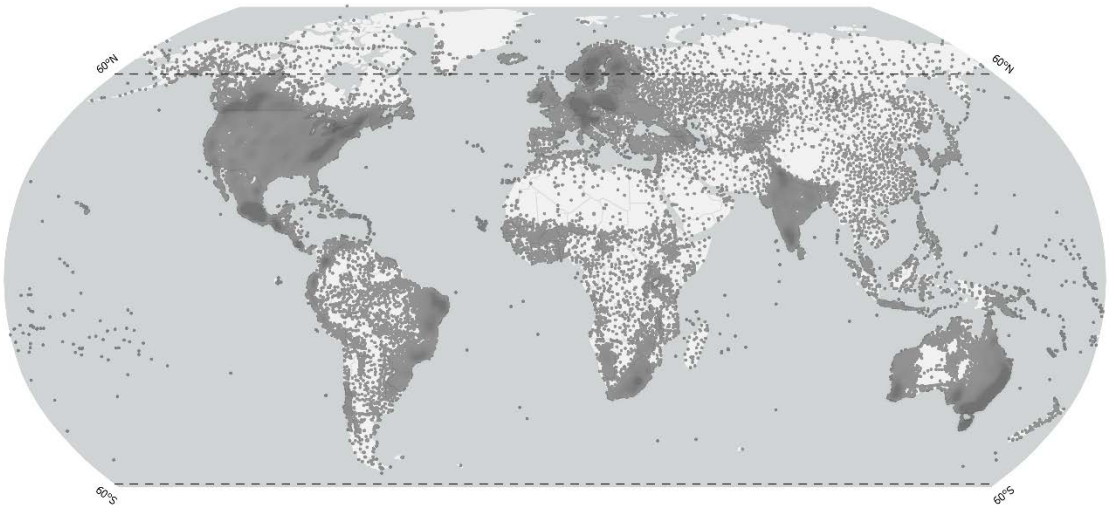

Figure 3.1. Spatial coverage of weather stations with precipitation records. Remotely sensed precipitation estimates are not available above 60° latitude, indicated by the dashed line. The figure uses public domain spatial data from Natural Earth (http://www.naturalearthdata.com/) and public domain location data from the International Tree Ring Databank (https://www.ncei.noaa.gov/products/paleoclimatology/tree-ring).

3.3.2. Tree ring records

A global dataset of tree ring records was obtained from the International Tree Ring Data Bank (ITRDB) (Grissino-Mayer and Fritts 1997; Zhao et al. 2018). Raw tree ring measurements from approximately 150,000 cores collected at 4422 sites were used to develop site- and species-specific chronologies. Chronologies were detrended using the Friedman Super-Smoother method to remove both long- and medium-frequency variability and maintain short-frequency (year-to-year) variability. This removes age-related trends in tree ring data that may be confounded with long-term climate trends or decadal climate oscillations. Our analysis therefore evaluates how well tree ring data tracks inter-annual climate variability. The Friedman Super-Smoother method was implemented with the package dplR (Bunn 2008, 2010; Bunn et al. 2022) for the R programming environment (R Core Team 2022). We used the default parameters of the function *detrend()*, which were equal case weights (*wt* parameter), automatic span detection using cross-validation (*span* = "cv") and default bass (*bass* = 0). After detrending, each series of cross-dated ring width measurements from the same site and of the same species were averaged using a robust biweighted mean to reduce the effect of outliers in the final chronology, implemented with the function *chron()*, of the package dplR (Bunn 2008, 2010; Bunn et al. 2022) for the R programming environment (R Core Team 2022). The function *chron()*, was also used to fit an autoregressive model to remove temporal autocorrelation (pre-whitening), which maximized correlations with precipitation data (determined empirically, post hoc). The spatial coverage of tree ring records is shown in Figure 3.2, and the overlap of chronology records with climate data products is shown in Figure 3.3 The validation was restricted to complete pairwise comparisons across all data products. In other words, all data products were evaluated based on an identical number of chronologies and years per chronology.

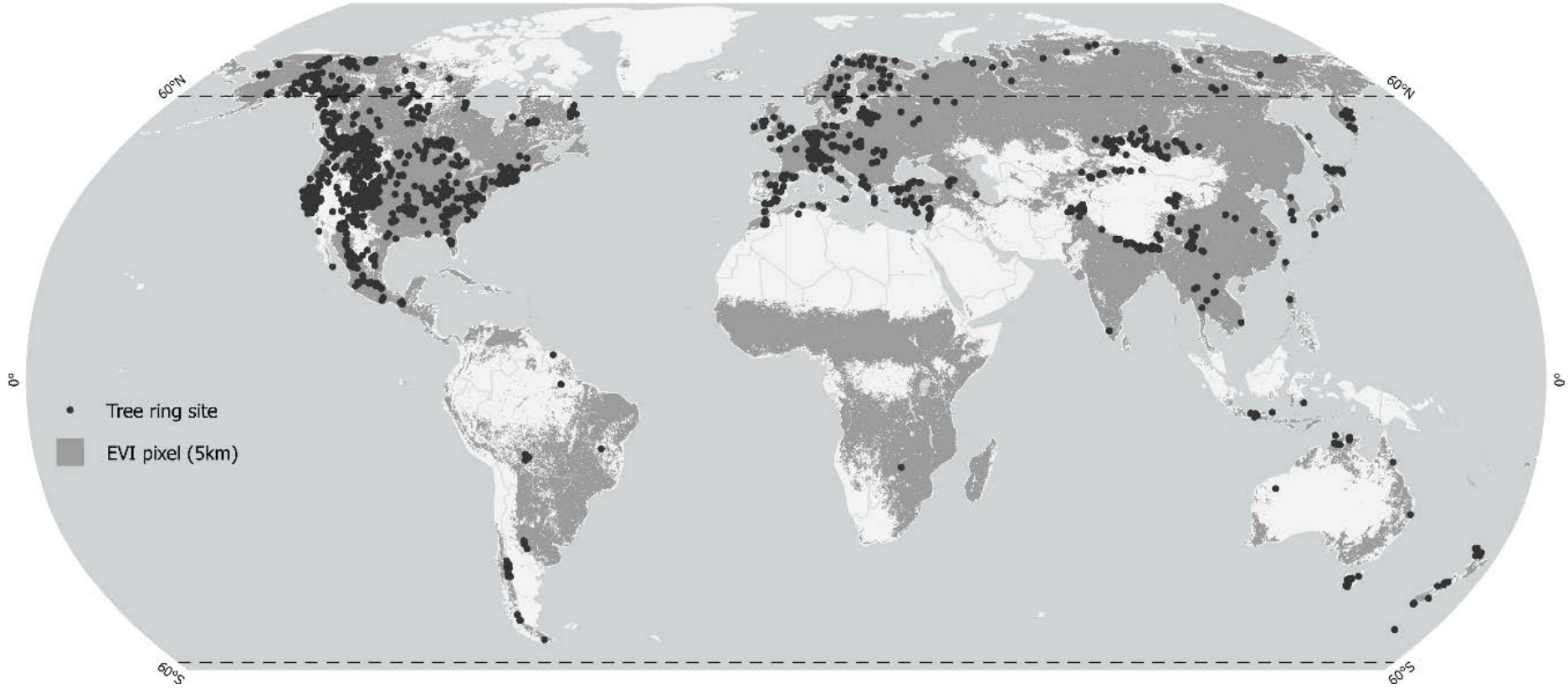

Figure 3.2. Spatial coverage of tree ring chronologies and remotely sensed vegetation greenness. Remotely sensed enhanced vegetation index (EVI) coverage is restricted to pixels with a dominant growing season, allowing for an annual area under the curve estimate from EVI data as a proxy for vegetation productivity, equivalent to tree ring widths. The figure uses public domain spatial data from Natural Earth (http://www.naturalearthdata.com/) and an original spatial layer developed from open-access EVI2 data (https://lpdaac.usgs.gov/products/mcd12q2v006/).

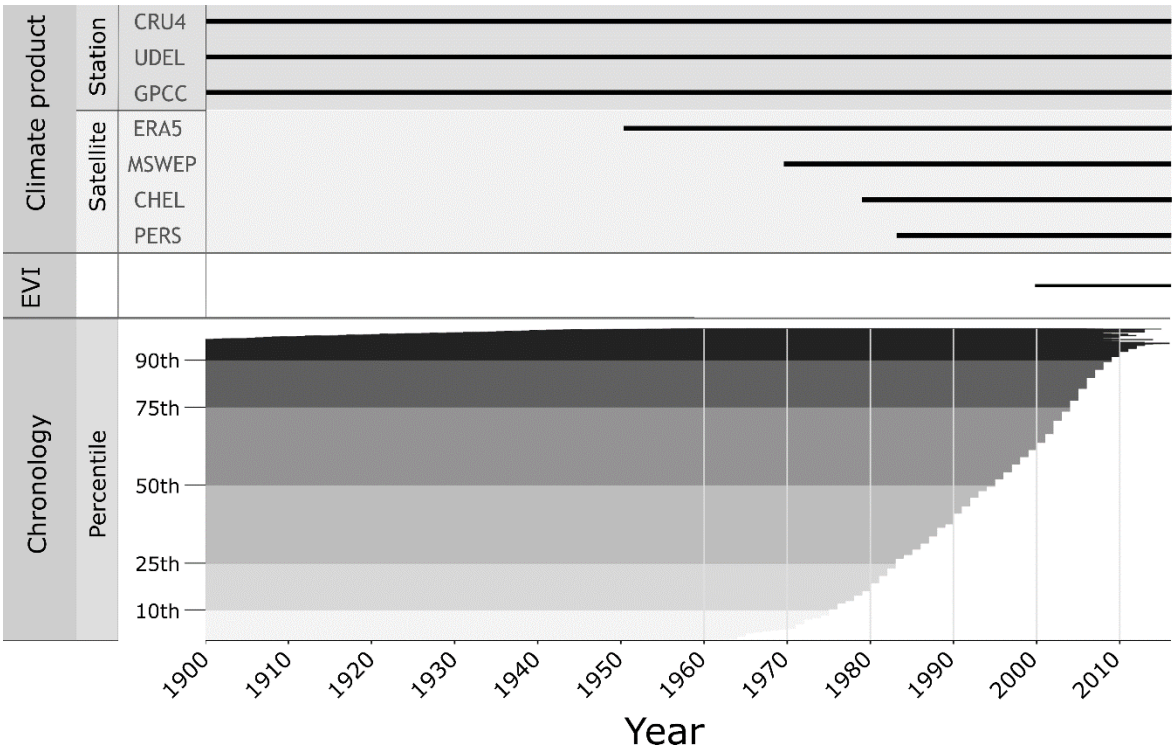

Figure 3.3. Temporal data coverage of climate products, remotely sensed EVI data, and tree ring chronologies. Tree ring chronologies are ordered by end year and truncated at 1900s to match climate data (total of 4422 sites). Shades of grey in lower panel represent the percentiles of the dataset. Only temporally pairwise-complete data was used for climate product comparisons.

3.3.3. Remote sensing data

The most widely used vegetation indices to assess vegetation greenness and draw inferences on vegetation health and productivity are the Normalized Difference Vegetation Index (NDVI) and the Enhanced Vegetation Index (EVI) (Xue and Su 2017). While both have been used widely, EVI is less prone to noise from atmospheric and soil conditions and less easily saturated by dense vegetation, and therefore more sensitive to interannual variation of forested areas, particularly in temperate and tropical regions (Myneni et al. 2002; Huang et al. 2021). Here we use an annual EVI data from the NASA Earth Observing System Data and Information System (EOSDIS) website, where an annual area under the curve has been integrated (collection MCD12Q2 v006, product MOD13A1), which represents photosynthesis over the entire growth cycle from greenup to dormancy (Friedl et al. 2019). This data is similar in principle to tree-ring records, where the ring width represents the integration of a growing season's growth. Also

similar to tree ring data the EVI area under the curve records are only available for climate regions with a distinct growing seasons (Fig 2, shown as dark gray data coverage). We aggregated the original 500 m resolution EVI area under the curve data to 5 km resolution and included only pixels that had time series with at least 50% non-missing values for a 5 km aggregated grid cell. Our analysis focuses on forested areas, by excluding croplands, grasslands and other non-forested areas using the vegetation continuous fields product (MOD44B) (DiMiceli et al. 2015). This aggregated 5 km resolution dataset is available through a data repository (http://doi.org/ 10.6084/m9.figshare.24540928), and could be used to test other climate products.

3.3.4. Statistical analyses

For each tree ring site and for each pixel of the EVI dataset we carry out an 8-months lagged correlation analysis. We assumed the growing season to have ended at the end of August for the northern hemisphere and at the end of February for the southern hemisphere, evaluating cumulative annual EVI or tree ring width with 8 months of climate data with a simple linear model, implemented with the *lm()* function of the R base package (R Core Team 2022). Although more sophisticated multivariate response function analysis methods are available for research in dendroclimatology, this is not needed in this study. For comparisons of climate data products with all factors held identical, a simple statistic from a correlative model is sufficient. We therefore chose an un-adjusted variance explained (R^2) from a multiple regression model, where the EVI area under the curve or tree ring width was specified as response variable, and the 8 month of monthly climate data prior to the end of the growing season were the predictor variables. This generally captures the growing season and several month prior where precipitation-growth correlations are expected to be reasonably strong.

To concisely report results for thousands of tree ring chronologies and millions of EVI grid cells, we used regional aggregation of the resulting R^2 values. EVI data was aggregated using ecozone delineations from the Terrestrial Ecoregions of the World product (Olson et al. 2001). To enable regional choices of the best climate data product, an assessment of the best dataset for an ecoregion was made using the Condorcet voting algorithm. The Condorcet method is a ranked pair-wise balloting system. In our case, the ranked ballots are the ranked R^2 statistics for each

tree ring chronology or EVI pixel that belong to the same ecoregion. A ranked ballot not only evaluates how often a product is ranked first in regional summaries. Last place rankings (and intermediate rankings) carry negative (or neutral) weight in the evaluation as well. The ranked ballot procedure was implemented with the *Condorcet()* function of the *Vote* package (Version 2.3-2) (Sevcikova et al. 2022) for the R programming environment (R Core Team 2022).

Lastly, for the long-term historical analysis, using the 120-year dendrochronology dataset, we used the same multiple regression approach described above using 21-year moving windows in single year increment steps, covering the period 1901 to 2000, and therefore reporting moving average statistics from 1911 to 1990. This allows the evaluation of how data quality has developed over time. All graphical representation of quantitative data were generated with the *ggplot2* package (Wickham 2016) for the R programming environment, and maps of data coverage and results were generated with ArcGIS Pro v3.0.0 (ESRI 2022).

3.4. Results & discussion

3.4.1. Regional comparisons based on EVI data

Remote-sensing based validation statistics of precipitation products for recent climate data since 2000 are very similar, when summarized by continent or subcontinent (

Figure 3.4, bar charts). It should be noted that the analysis is restricted to forested areas with seasonal growth patterns and therefore excludes ecoregions with aseasonal tropical rainforests and areas with minimal tree coverage. Regional Condorcet ranked-ballot winners by ecoregions provides spatially more explicit results (Figure 3.4, map). All data products appear as the best choice in some regions of the world, notably, however, MSWEP is more frequently the winner dominating large area of several ecosystems. For North America, MSWEP, CHELSA and UDEL dominate as the preferred data products by a small margin. Northern Asia is dominated by MSWEP and CRU4. For sub-Saharan Africa and the Sierras of Mexico, MSWEP wins by relatively large margin when compared to all others.

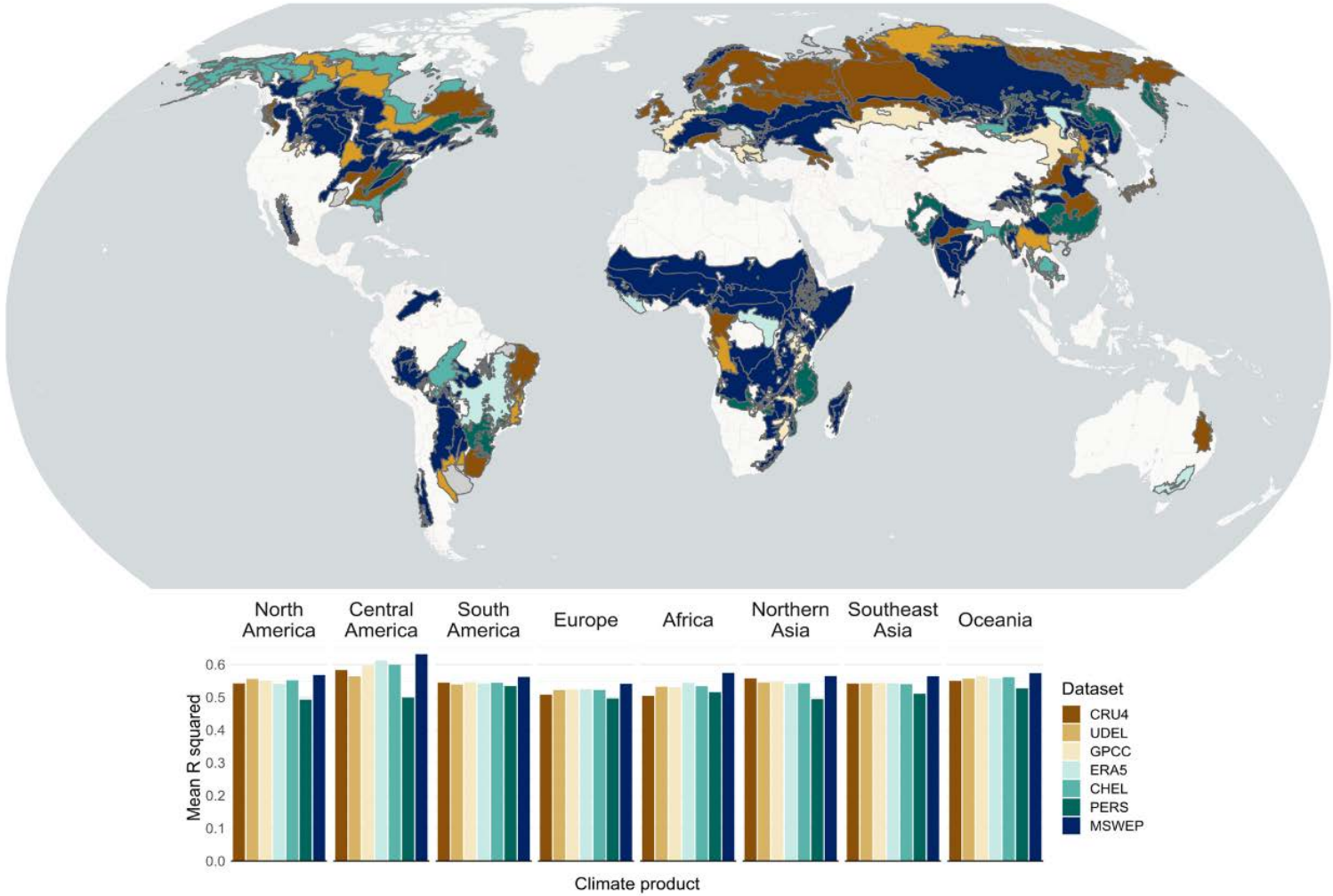

Figure 3.4. Best regional interpolated precipitation products for a recent 2000-2017 period against remotely sensed vegetation greenness. The comparisons are based on the strongest correlation with Enhanced Vegetation Index (EVI) annual area under the curve values. The map by ecoregions represents the best performing precipitation product, using the Condorcet winner method, where R^2 values of individual EVI pixels are used equivalently to ranked ballots. The figure uses public domain data from Natural Earth (http://www.naturalearthdata.com/) and original results generated in this study.

A fairly consistent result is that the remotely-sensed PERSIANN precipitation product under-performs in most regions of the world (most frequently ranked last), although the product does come out as ranked-ballot winner for mid- to high-latitude eastern continental regions, i.e. the east coast of Canada, the US, Russia and China, as well as similarly positioned mid-latitude eastern regions of South America and the Africa on the southern hemisphere. Climatic patterns, typically with year-round intermediate amounts of rainfall in these regions appear to favor accurate estimates of precipitation via remote sensing. We speculate that both passive and active microwave sensors may be less likely to be saturated, and therefore allow for better precision in regions with intermediate rainfall. While the remote-sensing based PERSIANN product was not superior to gauge-based products where weather station coverage is sparse, a multi-source models that combines gauge, satellite, and re-analysis data (MSWEP) could yield better precipitation estimates. While superiority of MSWEP compared to other products was not very closely linked to poor weather station coverage (c.f., Figure 3.1 and Figure 3.4), impressive margins of improvement were observed for some regions with few ground-based climate stations, such as Africa and parts of South America

3.4.2. Validation against long-term tree ring data

While validation against EVI time series provides spatially explicit results, tree ring records can evaluate quality of data products over long time periods. For this second comparison, only gauge-based products (CRU, UDEL and GPCC) can be included, where data coverage is available since the beginning of the century.

Variance explained by moving averages of 21-year windows reveal that the UDEL is generally superior for early climate estimates based on data from 1901-1940, corresponding to R^2 values of moving windows from 1910-1930 (Figure 3.5, global panel). Subsequently, R^2 values are fairly similar for moving window mid-points from 1930 to 1960, and then separate by a moderate amount for the most recent decades, with GPCC performing best, followed by UDEL and CRU4. It is important to note that the superior performance of UDEL in the early decades only applies to specific regions, namely Northern Asia and the Himalayas region, where whether station coverage is generally sparse, and we speculate that the researchers developing the UDEL product may have had access to station records not available for interpolation in CRU and GPCC

products. However, UDEL data is also marginally better in early century climate estimates for North America, Europe, South America and Southeast Asia. Their method of interpolation, an angular-distance weighting (ADW) method, appears superior to those used in other products for early century reconstructions, where weather station coverage is generally sparse. AWD can make use of directional information from data nodes, and has been found to handle sparse data coverage reasonably well (Shepard 1968, 1984; Willmott et al. 1985).

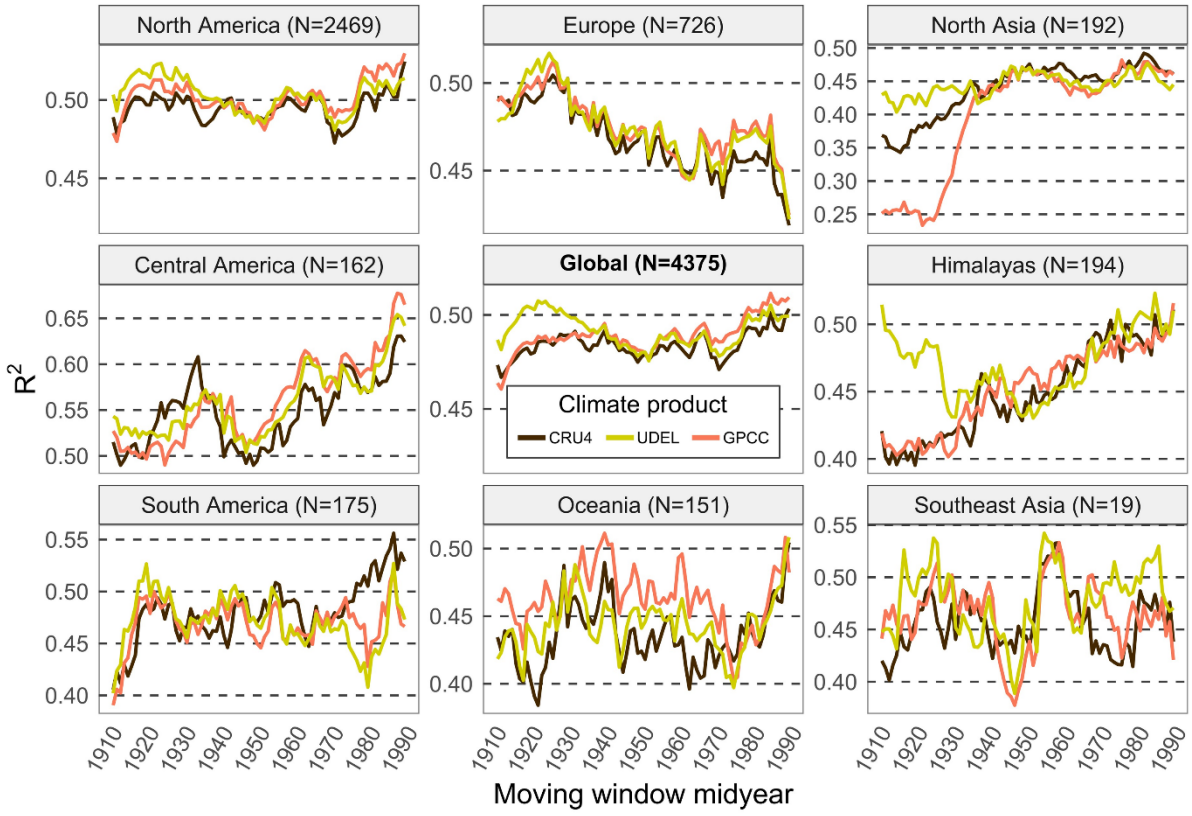

Figure 3.5. Best regional interpolated precipitation products in a long term (1901-2017) evaluation against tree ring records. Trends over time in validation statistics for the three global interpolated precipitation products that extend back to the 1900s. The lines represent variance explained in tree ring width by precipitation using 20-year moving windows.

Regional breakdowns suggest that all three gauge-based climate data products perform fairly similarly besides regional differences in the early decades (Figure 3.5, regional panels). That said, a small but notable difference among data products is CRU outperforming other data

products for recent climate since the 1970s for South America. For the Oceania region GPCC appears to be the best choice for most of the evaluated time series.

As a side note, not directly related to this study's objectives, we should also briefly interpret trends and variability in validation statistics over time that are visible in all data products. A general increase in the strength of the association between precipitation variables and chronology time series indicates that biological response has become more dependent on variability in precipitation over time. This is apparent for Northern Asia, the Himalayas region, and Central America. An opposite trend can be observed for Europe, indicating a weakening of the dependence of tree growth on variability in precipitation. Directional climate change towards drier conditions and/or warmer temperatures would be a plausible explanation for positive trends, and this has in fact been observed, especially for Central America (with a strong trend toward less precipitation (Magrin et al. 2014; Herrera and Ault 2017; WMO 2021), and the Himalayas with a strong warming trend of high elevation ecosystems where trees were sampled (Liu et al. 2009; Shrestha et al. 2012; Garg et al. 2022). The weakening in of plant-climate interactions in Europe can be explained by increased water-use efficiency from cumulative NO_x pollution due to industrialization over the century, where increases in water-use efficiency can over-compensate for any negative climate change effects on tree growth (e.g., Guerrieri (2010)).

3.5. Limitations of the analysis

As noted previously, our contribution is only a *partial* validation of climate data products, because the accuracy of absolute climate values cannot be assessed with biological data sources. Our evaluation is therefore only relevant for a specific target audience of researchers who analyze historical time series in biological or geophysical data. To establish a putatively causal link between climate and biological response, with correlative or associative methods using time series data, bias is not an important metric. Climate data can actually be extremely biased without compromising such analyses. To give an example, consider the usage of coarse resolution gridded temperature data used in mountainous terrain. Widely used datasets for this purpose such as CRU or UDEL have 0.5° resolution, and absolute temperature values along elevation gradients can vary extremely across an approximately 50×50 km grid cell in mountainous terrain. Yet, in the field of dendroclimatology this poses no problem, because a

warmer than average growing season in a particular year is warmer than average at all elevations. That said, our evaluation should not inform data selection for types of analysis that require unbiased estimates. To give an example, analysis types that build on climatic comparisons among different locations for a fixed time period, such as ecological niche modeling or species distribution modeling should not rely on climate data recommendations from this analysis.

3.6. Conclusions

For researchers who analyze historical time series in biological or geophysical data, our analysis allows to infer the best regional choice of time-series precipitation products. That said we should emphasize that for applications that require unbiased estimate of differences among locations for a fixed time period, our recommendations are not applicable. The results for the 20-year time series of remotely sensed EVI allows for comprehensive regional comparisons. All gauge and re-analysis based data products performed similarly, but they were outperformed by the multi-source MSWEP product that utilizes gauge, re-analysis, and remote sensing data. Especially for regions with low weather station coverage, such as Africa and parts of South America, the margin of improvement in how well MSWEP time series data tracks vegetation greenness was impressive. The analysis confirmed our working hypothesis that satellite-based or multi-source products have the potential to provide better precipitation estimates in regions of low weather station coverage. Unfortunately, satellite or re-analysis based products are not available prior to the 1980s. For applications that require longer time series analysis, gauge based products are the only option. Of the three gauge-based data products included in the analysis against 120-year tree ring records (CRU, GPCC and UDEL), the results showed that UDEL had superior performance prior to the 1940s, with especially large margins for northern Asia and the Himalayas region. From the 1940s onward, all three gauge-based climate data products perform fairly similarly. Locally, CRU outperformed other data products after the 1960s for South America. For the Oceania region GPCC was the best choice for analysis of long time series.

3.7. References

Augustine DJ (2010) Spatial versus temporal variation in precipitation in a semiarid ecosystem. Landsc Ecol 25:913–925. https://doi.org/10.1007/S10980-010-9469-Y/FIGURES/6

Beck HE, Wood EF, Pan M, et al (2019) MSWep v2 Global 3-hourly 0.1° precipitation:

Methodology and quantitative assessment. Bull Am Meteorol Soc 100:473–500. https://doi.org/10.1175/BAMS-D-17-0138.1

Bunn A, Korpela M, Biondi F, et al (2022) dplR: Dendrochronology Program Library in R

Bunn AG (2010) Statistical and visual crossdating in R using the dplR library. Dendrochronologia 28:251–258. https://doi.org/10.1016/j.dendro.2009.12.001

Bunn AG (2008) A dendrochronology program library in R (dplR). Dendrochronologia 26:115–124. https://doi.org/10.1016/j.dendro.2008.01.002

Castellanos-Acuña D, Hamann A (2020) A cross-checked global monthly weather station database for precipitation covering the period 1901 to 2010. Geosci Data J in press:1–11. https://doi.org/10.1002/gdj3.88

DiMiceli C, Carroll M, Sohlberg R, et al (2015) MOD44B MODIS/Terra Vegetation Continuous Fields Yearly L3 Global 250m SIN Grid V006 [Data set]. In: NASA EOSDIS L. Process. DAAC. https://lpdaac.usgs.gov/products/mod44bv006/. Accessed 12 Oct 2022

Dinku T, Connor SJ, Ceccato P, Ropelewski CF (2008) Comparison of global gridded precipitation products over a mountainous region of Africa. Int J Climatol 28:1627–1638. https://doi.org/10.1002/JOC.1669

ESRI (2022) ArcGIS Pro

Fontana C, Reis-Avila G, Nabais C, et al (2018) Dendrochronology and climate in the Brazilian atlantic forest: Which species, where and how. Neotrop Biol Conserv 13:321–333. https://doi.org/10.4013/nbc.2018.134.06

Friedl M, Gray J, Sulla-Menashe D (2019) MCD12Q2 MODIS/terra+aqua land cover dynamics yearly L3 global 500m SIN grid V006 [Data set]. In: NASA EOSDIS L. Process. DAAC. https://lpdaac.usgs.gov/products/mcd12q2v006/. Accessed 13 Oct 2022

Fung KF, Chew KS, Huang YF, et al (2022) Evaluation of spatial interpolation methods and spatiotemporal modeling of rainfall distribution in Peninsular Malaysia. Ain Shams Eng J 13:101571. https://doi.org/10.1016/j.asej.2021.09.001

García-Suárez AM, Butler CJ, Baillie MGL (2009) Climate signal in tree-ring chronologies in a temperate climate: A multi-species approach. Dendrochronologia 27:183–198. https://doi.org/10.1016/j.dendro.2009.05.003

Garg PK, Shukla A, Yousuf B, Garg S (2022) Temperature and precipitation changes over the

glaciated parts of Indian Himalayan region during 1901–2016. Environ Monit Assess 194:1–27. https://doi.org/10.1007/S10661-021-09689-5/TABLES/8

Golian S, Javadian M, Behrangi A (2019) On the use of satellite, gauge, and reanalysis precipitation products for drought studies. Environ Res Lett 14:075005. https://doi.org/10.1088/1748-9326/AB2203

Grissino-Mayer HD, Fritts HC (1997) The International Tree-Ring Data Bank: an enhanced global database serving the global scientific community. The Holocene 7:235–238. https://doi.org/10.1177/095968369700700212

Guerrieri R, Siegwolf R, Saurer M, et al (2010) Anthropogenic NOx emissions alter the intrinsic water-use efficiency (WUEi) for *Quercus cerris* stands under Mediterranean climate conditions. Environ Pollut 158:2841–2847. https://doi.org/10.1016/J.ENVPOL.2010.06.017

Harris I, Osborn TJ, Jones P, Lister D (2020) Version 4 of the CRU TS monthly high-resolution gridded multivariate climate dataset. Sci Data 7:109. https://doi.org/10.1038/s41597-020-0453-3

Herrera D, Ault T (2017) Insights from a new high-resolution drought atlas for the Caribbean spanning 1950–2016. J Clim 30:7801–7825. https://doi.org/10.1175/JCLI-D-16-0838.1

Huang S, Tang L, Hupy JP, et al (2021) A commentary review on the use of normalized difference vegetation index (NDVI) in the era of popular remote sensing. J For Res 32:1–6. https://doi.org/10.1007/S11676-020-01155-1/FIGURES/2

Karger DN, Wilson AM, Mahony C, et al (2021) Global daily 1 km land surface precipitation based on cloud cover-informed downscaling. Sci Data 8:. https://doi.org/10.1038/S41597-021-01084-6

Kluver D, Mote T, Leathers D, et al (2016) Creation and validation of a comprehensive 1° by 1° daily gridded north american dataset for 1900–2009: Snowfall. J Atmos Ocean Technol 33:857–871. https://doi.org/10.1175/JTECH-D-15-0027.1

Liu X, Cheng Z, Yan L, Yin ZY (2009) Elevation dependency of recent and future minimum surface air temperature trends in the Tibetan Plateau and its surroundings. Glob Planet Change 68:164–174. https://doi.org/10.1016/J.GLOPLACHA.2009.03.017

Magrin GO, Marengo JA, Boulanger J-P, et al (2014) Central and South America. In: Field CB, Barros VR, Dokken DJ, et al. (eds) Climate change 2014: Impacts, adaptation, and

vulnerability. Part B: Regional aspects. Contribution of working group II to the fifth assessment report of the Intergovernmental Panel on Climate Change. Cambridge University Press, Cambridge, United Kingdom and New York, NY, USA, pp 1499–1566

Matsuura K, Willmott CJ (2018) Terrestrial Precipitation: 1900-2017 Gridded Monthly Time Series. Arch. (Version 5.01)

Myneni RB, Hoffman S, Knyazikhin Y, et al (2002) Global products of vegetation leaf area and fraction absorbed PAR from year one of MODIS data. Remote Sens Environ 83:214–231. https://doi.org/10.1016/S0034-4257(02)00074-3

New M, Lister D, Hulme M, Makin I (2002) A high-resolution data set of surface climate over global land areas. Clim Res 21:1–25. https://doi.org/10.3354/CR021001

Nguyen P, Shearer EJ, Tran H, et al (2019) The CHRS Data Portal, an easily accessible public repository for PERSIANN global satellite precipitation data. Sci Data 6:180296. https://doi.org/10.1038/sdata.2018.296

Olson DM, Dinerstein E, Wikramanayake ED, et al (2001) Terrestrial ecoregions of the world: a new map of life on Earth. Bioscience 51:933–938

R Core Team (2022) R: A language and environment for statistical computing. Vienna, Austria

Schneider U, Becker A, Finger P, et al (2018) GPCC full data monthly product version 2018 at 0.25°: Monthly land-surface precipitation from rain-gauges built on GTS-based and historical data. ftp://ftp.dwd.de/pub/data/gpcc/html/fulldata-monthly_v2018_doi_download.html. Accessed 1 Aug 2021

Serrano-Notivoli R, Tejedor E, Roberto Serrano-Notivoli C (2021) From rain to data: A review of the creation of monthly and daily station-based gridded precipitation datasets. Wiley Interdiscip Rev Water 8:e1555. https://doi.org/10.1002/WAT2.1555

Sevcikova H, Silverman B, Raftery A (2022) vote: Election Vote Counting

Shepard D (1968) A two-dimensional interpolation for irregularly-spaced data function. In: Proc 23rd Assoc Computing Machinery (ACM) Natl Conf ACM New York. New York, NY, pp 517–524

Shepard DS (1984) Computer mapping: The SYMAP interpolation algorithm. In: Gaile GL, Willmott CJ (eds) Spatial statistics and models. Springer Netherlands, Dordrecht, pp 133–145

Shrestha UB, Gautam S, Bawa KS (2012) Widespread climate change in the Himalayas and

associated changes in local ecosystems. PLoS One 7:. https://doi.org/10.1371/JOURNAL.PONE.0036741

Simmons A, Hersbach H, Muñoz-Sabater J, et al (2021) Low frequency variability and trends in surface air temperature and humidity from ERA5 and other datasets. ECMWF Tech Memo 811:. https://doi.org/10.21957/ly5vbtbfd

Speer JH (2010) Fundamentals of tree-ring research. The University of Arizona Press, Tucson, Arizona

Sun C, Liu Y (2016) Climate response of tree radial growth at different timescales in the Qinling Mountains. PLoS One 11:e0160938. https://doi.org/10.1371/JOURNAL.PONE.0160938

Sun Q, Miao C, Duan Q, et al (2018) A review of global precipitation data sets: Data dources, estimation, and intercomparisons. Rev Geophys 56:79–107. https://doi.org/10.1002/2017RG000574

Wickham H (2016) ggplot2: Elegant Graphics for Data Analysis. Springer-Verlag New York

Willmott CJ, Rowe CM, Philpot WD (1985) Small-scale climate maps: A sensitivity analysis of some common assumptions associated with grid-point interpolation and contouring. Am Cartogr 12:5–16. https://doi.org/10.1559/152304085783914686

WMO (2021) State of the Climate in Latin America and the Caribbean. World Meteorological Organization (WMO), Geneva 2, Switzerland

Xu X, Zhang X, Li X (2023) Evaluation of the applicability of three methods for climatic spatial interpolation in the Hengduan mountains region. J Hydrometeorol 24:35–51. https://doi.org/10.1175/JHM-D-22-0039.1

Xue J, Su B (2017) Significant remote sensing vegetation indices: A review of developments and applications. J Sensors 2017:. https://doi.org/10.1155/2017/1353691

Zandler H, Haag I, Samimi C (2019) Evaluation needs and temporal performance differences of gridded precipitation products in peripheral mountain regions. Sci Reports 2019 91 9:1–15. https://doi.org/10.1038/s41598-019-51666-z

Zhao S, Pederson N, Orangeville LD, et al (2018) The International Tree-Ring Data Bank (ITRDB) revisited: Data availability and global ecological representativity. J Biogeogr 46:355–368. https://doi.org/https://doi.org/10.1111/jbi.13488

Chapter 4. Climate sensitivity of global seasonal forests inferred from remote sensing versus dendrochronology

4.1. Summary

Dendroclimatology research offers insights on how trees respond to climate anomalies and climate trends through historical analysis. However, tree ring databases cannot be easily updated with recent observations. Here, we test if a remotely sensed area under the curve metric from the Enhanced Vegetation Index (EVI) can serve as a tree ring equivalent to study growth–climate relationships. The results show that EVI-inferred vegetation sensitivity to climate broadly mirrors forest growth limitations inferred from tree ring analysis. A univariate drought sensitivity index correlates between r=0.35 (individual trees vs. single grid cells) and 0.52 (ecoregion averages). A cluster-based multivariate response function analysis shows misclassification error rates between 32 and 55% depending on how narrow the required match in multiple variables is defined. While there are apparent differences in response functions derived from tree rings versus EVI, the discrepancies arise primarily from how trees partition photosynthate into current and next year's growth, and the differences do not affect inferences on climatic growth limitations. We conclude that dendroclimatology methods applied to remotely sensed time series of EVI data can provide global, regional, and local characterization of climatic limiting factors of forest ecosystems with global coverage, spatial resolution, and timeliness that could not be obtained from dendrochronology research alone.

4.2. Introduction

Dendroclimatological analysis has been an important tool to reconstruct historical climate conditions, but more recently the approach has also been used to analyze anthropogenic climate change impacts, such as drought-related dieback (Gazol et al. 2018; Hevia et al. 2019; Sánchez-Salguero et al. 2020) and forecasting changes in productivity associated with climate change (Xu et al. 2017; Salas-Eljatib 2021; Martinez del Castillo et al. 2022). Although insightful, the research approach is time-consuming and limited by sample size to make broader inferences on ecosystems at landscape scales. When reanalyzing chronologies from databases such as the International Tree Ring Databank, it must also be kept in mind that contributing authors had different original study objectives, leading to sample selection that may be biased towards maximizing the climate signal, e.g. by sampling trees in exposed topo-edaphic positions (Sullivan and Csank 2016). Therefore, inferences from dendroclimatological research are difficult to extend to regional, continental or global scales. Lastly, the arguably most restrictive limitation of dendroclimatological research is that existing historical tree ring data cannot practically be updated, and only a very small fraction of globally available chronologies cover recent decades. The approach is therefore generally unsuitable for monitoring tree growth response to recent climate change at scale.

Remote sensing technology could be an excellent complement to address these limitations. High quality time-series data from the satellite borne MODIS sensors provides vegetation reflectance data that is updated every year with global coverage (Xue and Su 2017; Huang et al. 2021). Notably, the normalized difference vegetation index (NDVI) and the enhanced vegetation index (EVI) (Xue and Su 2017) are available as mature and well validated products that have been widely used to quantify vegetation productivity (Ogaya et al. 2015; Jaafar and Ahmad 2015; von Keyserlingk et al. 2021; Xiong et al. 2021; Kang et al. 2022; Wang et al. 2022). Of the two indices, EVI is less prone to noise from atmospheric and soil conditions and is also more sensitive to interannual variation forest greenness by not being easily saturated by dense vegetation coverage (Myneni et al. 2002; Huang et al. 2021). With more than 20 years of high quality remote sensing data available today, it becomes possible to analyze interannual variability in inferred forest growth at local, continental or global scales and derive similar

insights regarding climatic limiting factors to those from dendroclimatological research (Sang and Hamann 2022).

Remote sensing approaches have already been widely used to make inferences on vegetation sensitivity to climate change and climate extreme events. For example, both EVI and NDVI indices have been used for monitoring vegetation health over time, and infer sensitivity to climatic anomalies and climate extremes, including many recent contributions to the field (Dong et al. 2022; Wang et al. 2022; Das et al. 2022; Sang and Hamann 2022). Correspondence of remote sensing data and tree ring anomalies in response to frost and drought have also been documented (Kharuk et al. 2013; Pasho and Alla 2015; Correa-Díaz et al. 2021; Tonelli et al. 2023), including inferred water stress validated against isotope-based water-use efficiency in tree rings (Correa-Díaz et al. 2020, 2021). Other studies that tried to match inferred interannual variation in forest productivity from tree ring records with historical time series of remote sensing data found discrepancies, however, for example in cold-limited growing environments such as subalpine and boreal ecosystems (Brehaut and Danby 2018; Erasmi et al. 2021).

In this study we investigate under what circumstances inferred climate dependencies match between tree ring records and remotely sensed vegetation greenness, and for what reasons we may see discrepancies. We contribute a global analysis based on more than 100,000 tree cores from 4422 sites from the International Tree Ring Databank, primarily representing seasonal temperate forests. We quantify how well remotely sensed time series records of vegetation greenness (EVI) can replicate annual, seasonal or monthly growth limitations inferred from dendroclimatology analysis. Our specific objectives are: (1) to validate a simple EVI-derived univariate index of drought vulnerability against tree ring records, similar to previous local studies; (2) investigate tree-ring and EVI based correspondence in monthly climatic sensitivity through the year; and (3) test if any discrepancies observed can be explained through lagged growth effects in tree rings versus the more immediate metric of remotely sensed canopy greenness. Our overall goal is to contribute insights that may help to complement dendroclimatology research approaches with remote sensing data, allowing a spatial and temporal expansion of vulnerability assessments of seasonal forest ecosystems to climate change.

4.3. Material and Methods

4.3.1. Remote sensing data and processing

For remote sensing data we use the MCD12Q2 v006 Enhanced Vegetation Index (EVI) product developed by NASA and obtained from the Earth Observing System Data and Information System website (Friedl et al. 2019). We selected an EVI metric that closely corresponds to tree ring data: an area under the curve estimate (product MOD13A1), derived by applying a cubic smoothing spline to EVI time series data taken at 16-days intervals (Friedl et al. 2019). This layer was chosen as proxy for annual vegetation growth, representing the full vegetation cycle from green-up to dormancy in a year (Friedl et al. 2019), comparable to a single-year growth increments in tree ring chronologies. It should be noted that this metric is not available for aseasonal forests, such as evergreen tropical regions. The same limitation actually applies to tree ring records, where trees in aseasonal ecosystems do not produce rings that can be dated. We filtered the EVI data for forested grid cells with the Vegetation Continuous Fields product MOD44B (DiMiceli et al., 2015), and then averaged 250m grid cells that were classified as forested to 5 km resolution for further analysis. We required at least 3% non-missing values (i.e. 3% 250m grid cells classified as forested) within a 5 km grid-cell. The 5 km grid cell values may therefore only represent a small area of forest cover contained within. In other words, the analysis and derived visualizations do not represent the overall response of various vegetation classes across the full 25 km² extent of the aggregated 5 km grid cells, but represents forest stands with seasonal growth patterns only.

4.3.2. Tree ring data and pre-processing

Tree ring data were obtained from the International Tree Ring Data Bank (ITRDB) for 4422 sample locations (NOAA 2023). We used approximately 100,000 raw tree ring measurements that were detrended using Friedman's super-smoother method to remove both long and medium-frequency variability, emphasizing short frequency (year-to-year) variability (Friedman 1984), implanted with the package dplR (Bunn 2008, 2010; Bunn et al. 2022) for the R programming environment (R Core Team 2022). Raw ring width records for individual cores from the same tree, and individual trees of the same species and the same forest stand were then combined into a site chronology using the function *chron()* of the package dplR, which applies a robust

biweight mean on all measurements of a given year. This robust mean assigns a weight of zero to outliers (values over ± 6 SD), i.e., removing them from site chronology calculations (Mosteller and Tukey 1977; Cook and Kairiukstis 1990). Because tree ring growth data is temporally auto correlated, we further employed autoregressive modelling (Brockwell and Davis 1991) to remove temporal autocorrelations, also implemented with the dplR package for the R programming environment (R Core Team 2022).

4.3.3. Climate data

Time series of monthly precipitation were obtained from the University of Delaware Terrestrial Precipitation product from the University of Delaware (UDEL) (Matsuura and Willmott, 2018) for the coordinates of the tree ring chronologies and the corresponding center coordinates of 5 km aggregated EVI grid cells. Similarly, time series of monthly minimum, maximum and average temperature were obtained from dataset from the Climatic Research Unit of the University of East Anglia (CRU-TS v4.05) (Harris et al. 2020). The datasets were chosen from three options: UDEL, CRU-TS, and the monthly precipitation product v2018 from the Global Precipitation Climatology Centre (GPCC) (Schneider et al. 2018), based on an initial exploratory analysis of the amount of variance they explain in tree ring data. Both CRU and GPCC performed well for temperature data, and the UDEL dataset, specialized on modeling precipitation, outperformed both CRU and GPCC for precipitation variables (data not shown).

4.3.4. Response function analysis and sensitivity indices

Growth sensitivity to climate was based on a lagged monthly correlation analysis between annual growth data and monthly climatic variables for average temperature and precipitation. For each tree ring site and each individual EVI grid cell, we calculated Pearson correlation coefficients for the 18 months prior to the presumed end of the growing season. These periods were April of the previous year to September of the current year for the northern hemisphere, and October of the previous year to March of the current year for the northern hemisphere (i.e., a 6-month shift). Therefore, the analysis also captures potential legacy effects of previous year growing conditions on current year ring width or vegetation greenness.

Next, a simple univariate index of drought sensitivity was derived from 36 correlation coefficients (18 lagged temperature and 18 lagged precipitation correlation coefficients). To obtain a univariate index of climate sensitivity, we subtracted the average of all precipitation coefficients from the average of all temperature coefficients, with the resulting index value theoretically ranging from 2 to -2, where positive values indicate primarily cold-limited and light- or cloud-limited growing environments (i.e., positive correlation with temperature anomalies and negative correlation with precipitation anomalies) and negative value indicate drought limited conditions (i.e., negative response to high temperature anomalies and positive response to high precipitation anomalies).

For a more complex representation of monthly vegetation sensitivity to climate, we follow the approach of Sang & Hamann (2022) that groups time series of individual remote sensing pixels (or tree ring chronologies) via a cluster analysis. Cluster identity represents a specific pattern of vegetation responses across 18 months of historical temperature and precipitation variability. For clustering we used the Partition Around Medoids (PAM) algorithm, implemented with the *cluster* package (Maechler et al. 2023) for the R programming environment (R Core Team 2022). To map visualization of global patterns, the clusters were ordered from cold-limited to drought-limited in the same way as for the univariate index, by subtracting the average precipitation coefficient from the average temperature coefficient. This ordering was only for visualization purposes to convey one aspect of the clusters by colors in maps. However, clusters with similar overall sensitivity to climate may still differ in the seasonal timing of drought or cold limitations.

4.3.5. Correspondence of EVI and tree ring data

To evaluate the extent to which the univariate and multivariate vegetation sensitivity indices derived from tree ring vs EVI data match, we calculated Pearson correlation coefficients for the univariate climate sensitivity index of each tree ring chronology to the respective EVI grid cell into which the tree ring chronology site falls. To investigate how well correlations hold at larger scales for broader inferences, we also aggregate tree ring data and EVI data at the level of mapped ecosystems. Correlations and root mean square errors were then calculated between ecosystem means of EVI and tree ring data to estimate precision and bias. For this purpose, we used the high-resolution ecosystem variant delineation compiled by Roberts and Hamann (2012)

that tracks elevation gradients for western North America, where a large amount of tree ring data was available along complex climatic gradients. For the rest of the world, we used the Terrestrial Ecoregions of the World (TEOW) delineation at the ecoregion level (Olson et al. 2001).

4.4. Results and Discussion

4.4.1. Overall climatic sensitivity

The univariate vegetation sensitivity index, which ranges from primarily cold-limited (blue) to heat- and drought-limited (red) broadly matches between remotely sensed EVI data and tree-ring inferred values (cf., Figure 4.1a versus Figure 4.1b). It should be noted that geographic coverage of tree rings and remote sensing data is quite different. For example, drought-limited ecosystems in the southwestern U.S. are well researched by dendrochronologists, but there is not enough continuous canopy coverage in these savannah-type ecosystems to allow inferences on tree sensitivity to climate from moderate resolution remote sensing. Conversely, large regions of seasonal forests of the world that can be evaluated through remote sensing have sparse or no dendrochronology sample coverage.

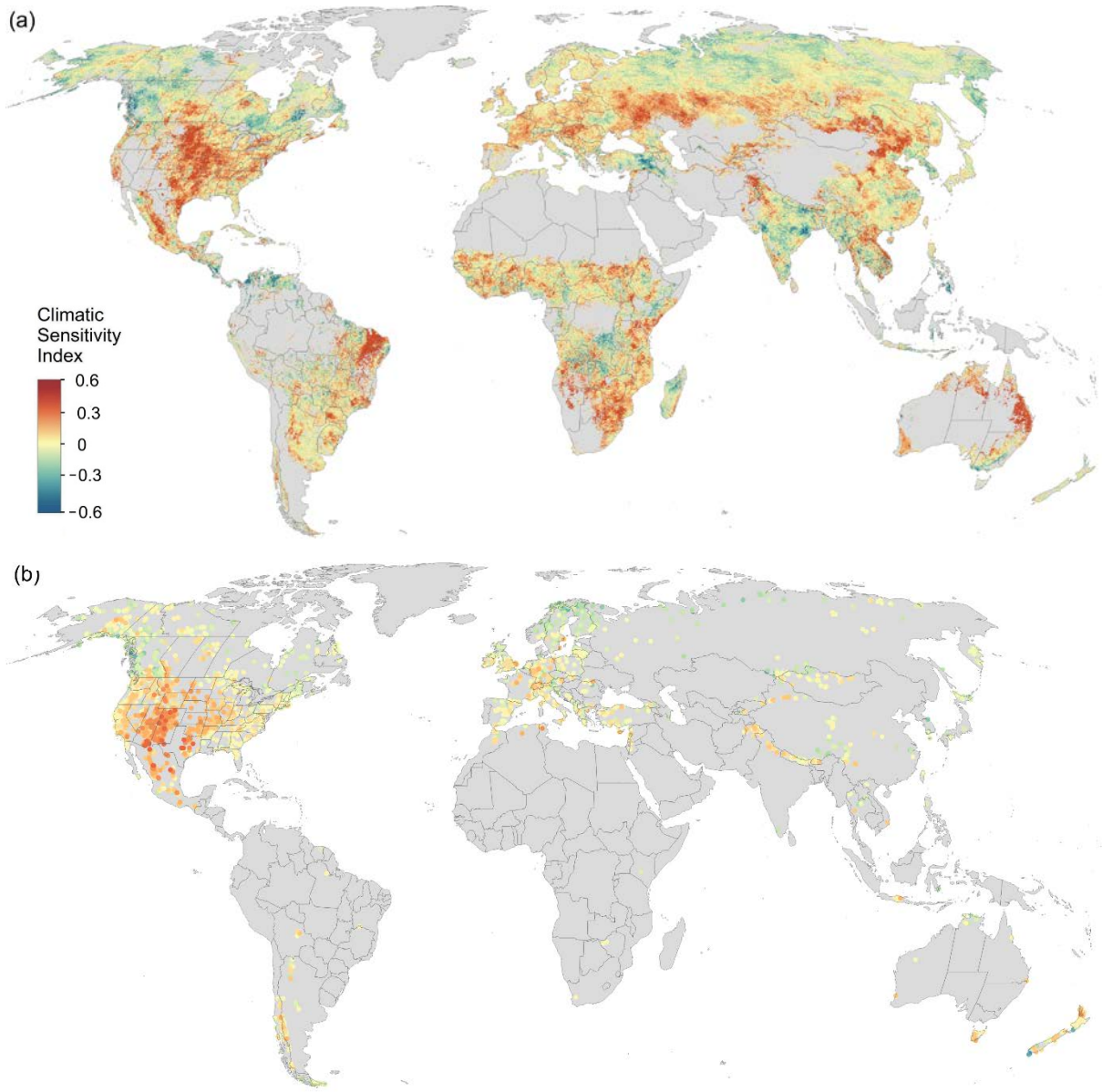

Figure 4.1. Forest sensitivity to drought, measured as average monthly precipitation correlations minus average monthly temperature correlations, for (a) remotely sensed EVI area under the curve for 250m grid cells classified as forests, aggregated to 5 km cells and (b) tree ring chronology locations. Red indicates drought limited regions while blue areas indicate cold or cloud/light limited environments.

Where chronology- and EVI-derived climate sensitivity overlaps, we find that remote sensing-based index has a somewhat larger range, but is otherwise unbiased (Figure 4.2). The correlation between chronology- and EVI-derived indices is relatively low (0.36), but it needs to be kept in

mind that EVI grid cells represent an aggregated tree response within 25 km² areas that may contain several hundreds of thousands of trees and other vegetation, whereas tree ring chronologies are typically built from no more than 25 individual trees in a specific location (Cook and Kairiukstis 1990; Nehrbass-Ahles et al. 2014b). When both tree ring chronology data and EVI data was aggregated by ecoregion, the correlation improved to r=0.56 and the small bias, indicated by the regression line deviating from the diagonal, is further reduced. Bias correction, if desired, would be straight forward, but normally such indices are used for relative vulnerability assessments, and bias correction should therefore not be required.

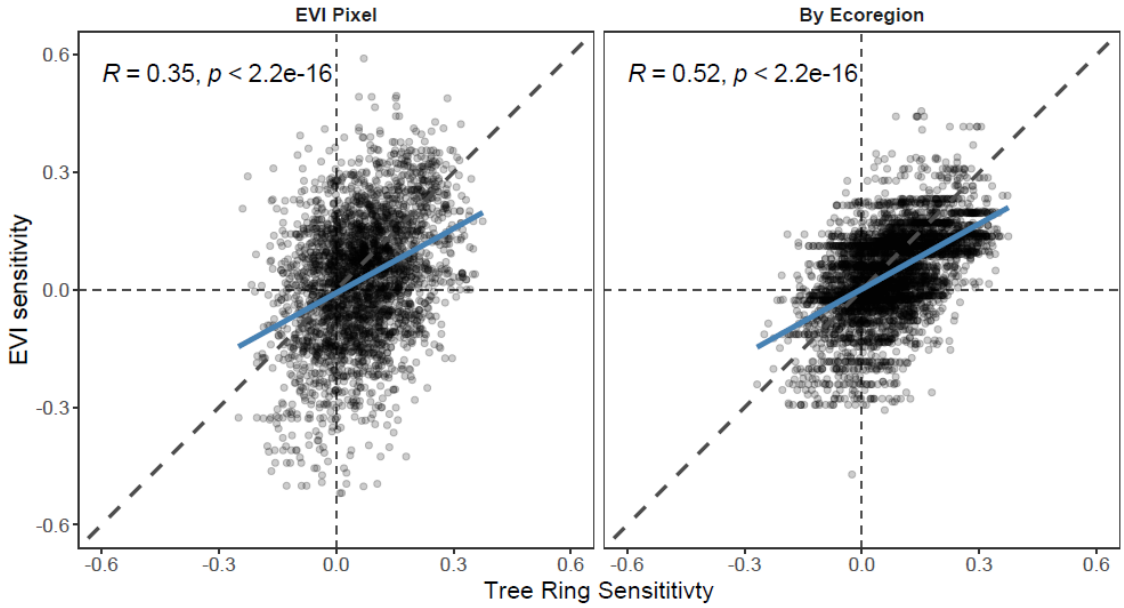

Figure 4.2. Comparison of forest drought sensitivity inferred from tree ring chronologies versus remotely sensed EVI area under the curve. Blue line is simple linear regression on actual data. for (a) the EVI grid cell that contains the tree ring sample location, and (b) sensitivity estimates from EVI grid cells and tree rings averaged by ecoregion.

The direction of the bias is slightly to the right towards more apparent drought-sensitivity in tree rings relative to the corresponding EVI pixel (Figure 4.2), and we speculate that this may be due to sampling bias in site and tree species selection for dendrochronology analysis. Investigators of local studies, who submit their chronologies to the ITRDB, usually select species, study locations, topo-edaphic positions or crown positions for chronology samples that are exposed and not buffered by deep soils and readily accessible ground water, so that the climate signal in

tree ring chronologies is maximized, for example for the purpose of reconstructing past climate trends. Although this sampling does not bias direction and relative magnitude of tree responses to short-term climate variability, inferences from individual dendrochronology samples to overall forest stand productivity are rather susceptible to biases (Nehrbass-Ahles et al. 2014b). As such it seems plausible that the observed shifts to right in Figure 4.2, implying a somewhat higher drought sensitivity from tree rings than EVI estimates, could well be due to sampling bias in the tree ring data set.

4.4.2. Monthly climatic limiting factors

When comparing clusters of similar response functions in tree rings with the corresponding response function derived from time series of EVI grid cells, the seasonal timing and magnitude of climate sensitivities also correspond reasonably well (Figure 4.3). Although the clusters are categorical, we applied a color ramp equivalent to Figure 4.1 for visualization of geographic patterns (Figure 4.4). Again, clusters that are limited by low precipitation and/or high temperatures are indicated by red, and those limited by high precipitation and/or cold temperatures appear in blue. The latter applies to northern environments, but blue grid cells are also visible in seasonal forests in tropical regions. Here, the inter-annually varying growth limitation is neither cold nor water availability, but light-limitations associated with cloudy skies during years with high precipitation.

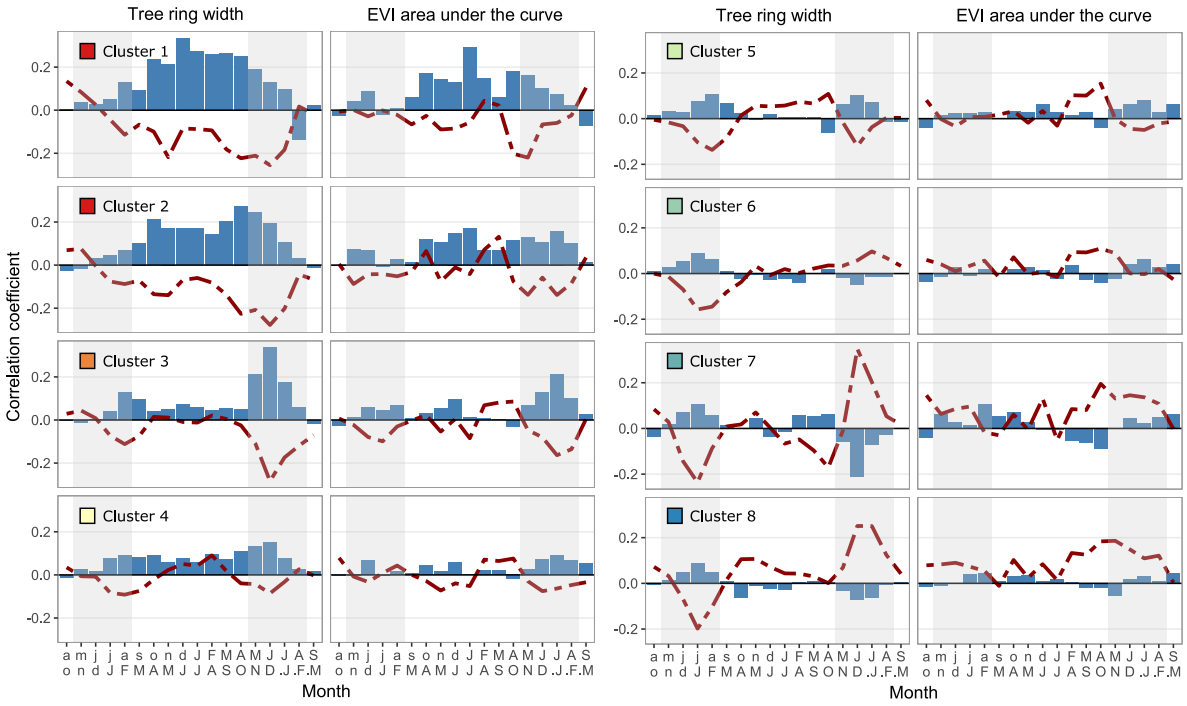

Figure 4.3. Comparison of tree-ring versus EVI-based monthly temperature (red line) and precipitation (blue bars) limitations for 18 months prior to the end of the current growing season. The values are averages for chronology sites, and corresponding EVI grid cells that contain the tree ring sample locations. Typical growing season periods are highlighted in gray, and months in the top and bottom row are for the northern and southern hemisphere, respectively.

At the hottest and driest end of the spectrum, trees are limited by higher-than-normal temperatures and lower than normal precipitation (Figure 4.3, Clusters 1 and 2, red). The period of these limitations spans approximately for a full year prior the end of the current growing season, i.e. August of the previous year to July of the current year's growing season (for the northern hemisphere). Clusters 3 and 4 show similar limitations, but to a lesser extent and more narrowly restricted to the current and the end of the prior growing season. The next set of climate response types, Clusters 5 and 6, show a generally more neutral response. For the tree ring-based climate dependencies, growth is still somewhat positively influenced during years with high precipitation during the growing season, but temperature dependencies flip from negative (Cluster 5) to positive (Cluster 6), indicating the emergence of cold limitations. The corresponding EVI-inferred growth limitations are somewhat divergent, with clusters 5 and 6 showing moderate pre-growing season cold limitations (February to April). This suggests

negative effects of a late spring or late snowmelt on overall growth during the current growing season.

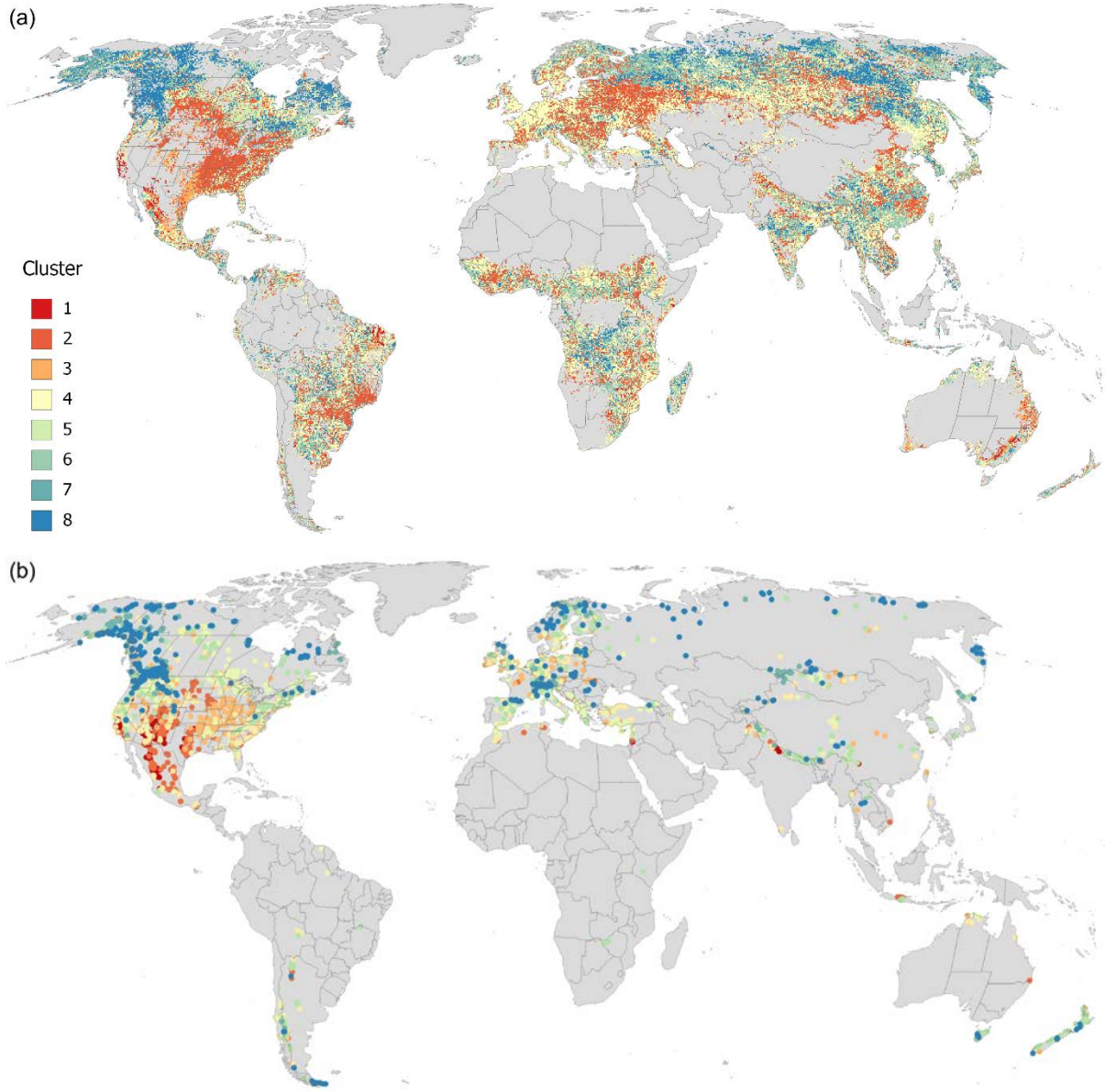

Figure 4.4. Cluster membership of (a) EVI grid cells and (b) tree ring chronologies, representing multivariate climatic limitations as shown in Figure 4.3.

Lastly, Cluster 7 and 8 are most cold-limited during the current season. High temperatures in June and July are most strongly correlated with a large ring width, while years with high precipitation have a small to moderate negative effect on growth, possibly due to cloud cover being correlated with lower temperatures. In these two clusters, we see a very pronounced

difference compared to the EVI counterpart. First, for EVI inferred productivity, substantial pre-growing season cold limitations apply, which is not at all the case tree ring data. Secondly, in the tree ring data temperature and precipitation dependencies for the previous year growing season are reversed, apparently suggesting heat- and drought limitations. We think the reason for this apparently paradoxical response type is lagged partitioning of photosynthate, also observed in other studies (e.g., Kannenberg et al., 2019). If the previous growing season is warm and long, then the carbohydrates get laid down in latewood growth of that growing season, and are thus not available for early wood growth in the subsequent year. If the previous growing season is cool and short (i.e. unfavorable), then carbohydrates get stored in the wood and roots over winter and contribute to next year's early-wood growth, thus explaining the correlation reversal (poor previous growing season conditions causing increased ring width in the current year).

A misclassification analysis between EVI versus tree-ring inferred growth limitations suggests that error rates are high, and the overall match of cluster membership of a tree ring chronology and the corresponding aggregated forests within 25 km² grid cells is low (Table 1). The highest EVI error rates occur in the intermediate Cluster 5 with overall low climate dependencies (i.e., a total of only 166 correct classifications, and 71% misclassified). The type of errors are not unexpected, with EVI-inferred Cluster 5 response types that were misclassified actually containing tree ring chronologies of Cluster 4 and 6 response types (i.e. a total of 150 and 110 misclassifications with adjacent cluster types). As noted earlier when discussing correlations of the univariate drought sensitivity index, exact matches between a single site chronology for ground truthing, versus hundreds of thousands of trees (and other vegetation types that could not be filtered at 250m resolution) should not be expected. When relaxing the matching criteria to accept adjacent response types as matching, then the overall misclassification error rate drops to 32% (Table 4.1, off-diagonal in italics).

Table 4.1. Misclassification matrix of tree ring versus remote sensing based grouping of climatic limiting factors. We show the matrix for five clusters with an overall out of bag (OOB) error rate of 55.5%. Allowing for an adjacent cluster counting as match (*italic*), the OOB misclassification rate drops to 32.6%.

EVI	Tree ring cluster								
cluster	1	2	3	4	5	6	7	8	Error
1	**188**	*39*	53	83	10	15	1	22	0.54
2	*57*	**167**	*17*	35	6	6	0	3	0.43
3	25	*1*	**407**	*138*	65	47	4	28	0.43
4	38	13	*119*	**347**	*84*	90	4	57	0.54
5	4	2	89	*150*	**166**	*110*	7	38	0.71
6	10	5	71	118	*71*	**251**	*15*	111	0.62
7	1	0	19	35	15	*52*	**96**	*70*	0.67
8	7	3	31	68	23	102	*31*	**233**	0.53

4.5. Conclusion

Overall, the results demonstrate potential value of remote sensing data to obtain insights equivalent to those from dendroclimatology research in identifying specific types of climatic limitations and implied sensitivity to observed and projected climate change. While there is no perfect correspondence in the response types that we inferred from tree ring versus EVI data, these are neither needed nor necessarily desired. For example, sampling biases present in tree ring research to maximize the climate signal are not expected in remote sensing data. Lagged growth effects in tree rings versus the more immediate metric of remotely sensed canopy greenness, while interesting, does not cause any issues in inferring climatic limiting factors and potential climate change vulnerabilities, as long as the timing of the limitations is correctly interpreted. We think that overall the findings highlight the potential of remote sensing data for assessing the timing and magnitude of climate sensitivities throughout the year. The approach provides a foundation for complementing dendroclimatological research with remote sensing, and enabling broader vulnerability assessments of seasonal forest ecosystems to climate change, where tree ring data is sparse or unavailable. Furthermore, changes in climate dependencies can be analyzed as remote sensing records are added every year, enabling monitoring and forecasting of the impacts of climate change on forest growth at regional, continental, and global scales.

4.6. References

Brehaut, L., Danby, R.K., 2018. Inconsistent relationships between annual tree ring-widths and satellite-measured NDVI in a mountainous subarctic environment. Ecol. Indic. 91, 698–711. https://doi.org/10.1016/j.ecolind.2018.04.052

Brockwell, P.J., Davis, R.A., 1991. Multivariate Time Series, in: Time Series: Theory and Methods. Springer, New York, NY, pp. 401–462. https://doi.org/10.1007/978-1-4419-0320-4_11

Bunn, A., Korpela, M., Biondi, F., Campelo, F., Mérian, P., Qeadan, F., Zang, C., 2022. dplR: Dendrochronology Program Library in R.

Bunn, A.G., 2010. Statistical and visual crossdating in R using the dplR library. Dendrochronologia 28, 251–258. https://doi.org/10.1016/j.dendro.2009.12.001

Bunn, A.G., 2008. A dendrochronology program library in R (dplR). Dendrochronologia 26, 115–124. https://doi.org/10.1016/j.dendro.2008.01.002

Cook, E.R., Kairiukstis, L.A., 1990. Methods of dendrochronology: Applications in the environmental sciences, Arctic and Alpine Research. Springer-Science+Business Media, B. V., Dordrecht, Holland. https://doi.org/10.1007/9789401578790

Correa-Díaz, A., Romero-Sánchez, M.E., Villanueva-Díaz, J., 2021. The greening effect characterized by the Normalized Difference Vegetation Index was not coupled with phenological trends and tree growth rates in eight protected mountains of central Mexico. For. Ecol. Manage. 496. https://doi.org/10.1016/j.foreco.2021.119402

Correa-Díaz, A., Silva, L.C.R., Horwath, W.R., Gómez-Guerrero, A., Vargas-Hernández, J., Villanueva-Díaz, J., Suárez-Espinoza, J., Velázquez-Martínez, A., 2020. From trees to ecosystems: Spatiotemporal scaling of climatic impacts on montane landscapes using dendrochronological, isotopic, and remotely sensed data. Global Biogeochem. Cycles 34, 1–20. https://doi.org/10.1029/2019GB006325

Das, A.J., Slaton, M.R., Mallory, J., Asner, G.P., Martin, R.E., Hardwick, P., 2022. Empirically validated drought vulnerability mapping in the mixed conifer forests of the <scp>Sierra Nevada</scp>. Ecol. Appl. 32. https://doi.org/10.1002/eap.2514

Dong, C., Wang, X., Ran, Y., Nawaz, Z., 2022. Heatwaves significantly slow the vegetation growth rate on the Tibetan Plateau. Remote Sens. 14, 1–17. https://doi.org/10.3390/rs14102402

Erasmi, S., Klinge, M., Dulamsuren, C., Schneider, F., Hauck, M., 2021. Modelling the productivity of Siberian larch forests from Landsat NDVI time series in fragmented forest stands of the Mongolian forest-steppe. Environ. Monit. Assess. 193, 1–18. https://doi.org/10.1007/s10661-021-08996-1

Friedl, M., Gray, J., Sulla-Menashe, D., 2019. MCD12Q2 MODIS/Terra+Aqua Land Cover Dynamics Yearly L3 Global 500m SIN Grid V006 [Data set] [WWW Document]. NASA EOSDIS L. Process. DAAC. URL https://lpdaac.usgs.gov/products/mcd12q2v006/ (accessed 10.13.22).

Friedman, J.H., 1984. A variable span smoother, Journal of American Statistical Association. https://doi.org/10.21236/ADA148241

Gazol, A., Camarero, J.J., Vicente-Serrano, S.M., Sánchez-Salguero, R., Gutiérrez, E., de Luis, M., Sangüesa-Barreda, G., Novak, K., Rozas, V., Tíscar, P.A., Linares, J.C., Martín-Hernández, N., Martínez del Castillo, E., Ribas, M., García-González, I., Silla, F., Camisón, A., Génova, M., Olano, J.M., Longares, L.A., Hevia, A., Tomás-Burguera, M., Galván, J.D., 2018. Forest resilience to drought varies across biomes. Glob. Chang. Biol. 24, 2143–2158. https://doi.org/10.1111/gcb.14082

Harris, I., Osborn, T.J., Jones, P., Lister, D., 2020. Version 4 of the CRU TS monthly high-resolution gridded multivariate climate dataset. Sci. Data 7, 109. https://doi.org/10.1038/s41597-020-0453-3

Hevia, A., Sánchez-Salguero, R., Camarero, J.J., Querejeta, J.I., Sangüesa-Barreda, G., Gazol, A., 2019. Long-term nutrient imbalances linked to drought-triggered forest dieback. Sci. Total Environ. 690, 1254–1267. https://doi.org/10.1016/J.SCITOTENV.2019.06.515

Huang, S., Tang, L., Hupy, J.P., Wang, Y., Shao, G., 2021. A commentary review on the use of normalized difference vegetation index (NDVI) in the era of popular remote sensing. J. For. Res. 32, 1–6. https://doi.org/10.1007/S11676-020-01155-1/FIGURES/2

Jaafar, H.H., Ahmad, F.A., 2015. Crop yield prediction from remotely sensed vegetation indices and primary productivity in arid and semi-arid lands. http://dx.doi.org/10.1080/01431161.2015.1084434 36, 4570–4589. https://doi.org/10.1080/01431161.2015.1084434

Kang, W., Liu, S., Chen, X., Feng, K., Guo, Z., Wang, T., 2022. Evaluation of ecosystem stability against climate changes via satellite data in the eastern sandy area of northern

China. J. Environ. Manage. 308, 114596. https://doi.org/10.1016/j.jenvman.2022.114596

Kannenberg, S.A., Novick, K.A., Alexander, M.R., Maxwell, J.T., Moore, D.J.P., Phillips, R.P., Anderegg, W.R.L., 2019. Linking drought legacy effects across scales: From leaves to tree rings to ecosystems. Glob. Chang. Biol. 25, 2978–2992. https://doi.org/10.1111/GCB.14710

Kharuk, V.I., Ranson, K.J., Oskorbin, P.A., Im, S.T., Dvinskaya, M.L., 2013. Climate induced birch mortality in Trans-Baikal lake region, Siberia. For. Ecol. Manage. 289, 385–392. https://doi.org/10.1016/j.foreco.2012.10.024

Maechler, M., Rousseeuw, P., Struyf, A., Hubert, M., Hornik, K., 2022. cluster: Cluster Analysis Basics and Extensions.

Martinez del Castillo, E., Zang, C.S., Buras, A., Hacket-Pain, A., Esper, J., Serrano-Notivoli, R., Hartl, C., Weigel, R., Klesse, S., Resco de Dios, V., Scharnweber, T., Dorado-Liñán, I., van der Maaten-Theunissen, M., van der Maaten, E., Jump, A., Mikac, S., Banzragch, B.E., Beck, W., Cavin, L., Claessens, H., Čada, V., Čufar, K., Dulamsuren, C., Gričar, J., Gil-Pelegrín, E., Janda, P., Kazimirovic, M., Kreyling, J., Latte, N., Leuschner, C., Longares, L.A., Menzel, A., Merela, M., Motta, R., Muffler, L., Nola, P., Petritan, A.M., Petritan, I.C., Prislan, P., Rubio-Cuadrado, Á., Rydval, M., Stajić, B., Svoboda, M., Toromani, E., Trotsiuk, V., Wilmking, M., Zlatanov, T., de Luis, M., 2022. Climate-change-driven growth decline of European beech forests. Commun. Biol. 5, 1–9. https://doi.org/10.1038/s42003-022-03107-3

Mosteller, F., Tukey, J.W., 1977. Data Analysis and Regression: a second course in statistics. Addison-Wesley.

Myneni, R.B., Hoffman, S., Knyazikhin, Y., Privette, J.L., Glassy, J., Tian, Y., Wang, Y., Song, X., Zhang, Y., Smith, G.R., Lotsch, A., Friedl, M., Morisette, J.T., Votava, P., Nemani, R.R., Running, S.W., 2002. Global products of vegetation leaf area and fraction absorbed PAR from year one of MODIS data. Remote Sens. Environ. 83, 214–231. https://doi.org/10.1016/S0034-4257(02)00074-3

Nehrbass-Ahles, C., Babst, F., Klesse, S., Nötzli, M., Bouriaud, O., Neukom, R., Dobbertin, M., Frank, D., 2014. The influence of sampling design on tree-ring-based quantification of forest growth. Glob. Chang. Biol. 20, 2867–2885. https://doi.org/10.1111/GCB.12599

NOAA, 2023. International Tree-Ring Data Bank [WWW Document]. URL

https://www.ncei.noaa.gov/access/paleo-search/?dataTypeId=18 (accessed 3.31.23).

Ogaya, R., Barbeta, A., Başnou, C., Peñuelas, J., 2015. Satellite data as indicators of tree biomass growth and forest dieback in a Mediterranean holm oak forest. Ann. For. Sci. 72, 135–144. https://doi.org/10.1007/S13595-014-0408-Y/FIGURES/9

Olson, D.M., Dinerstein, E., Wikramanayake, E.D., Burgess, N.D., Powell, G.V.N., Underwood, E.C., Amico, J.A.D., Itoua, I., Strand, H.E., Morrison, J.C., Loucks, J., Allnutt, T.F., Ricketts, T.H., Kura, Y., Lamoreux, J.F., Wesley, W., Hedao, P., Kassem, K.R., 2001. Terrestrial ecoregions of the world: a new map of life on Earth. Bioscience 51, 933–938.

Pasho, E., Alla, A.Q., 2015. Climate impacts on radial growth and vegetation activity of two co-existing Mediterranean pine species. Can. J. For. Res. 45, 1748–1756. https://doi.org/10.1139/cjfr-2015-0146

R Core Team, 2022. R: A language and environment for statistical computing. Vienna, Austria.

Roberts, D.R., Hamann, A., 2012. Predicting potential climate change impacts with bioclimate envelope models: A palaeoecological perspective. Glob. Ecol. Biogeogr. 21, 121–133. https://doi.org/10.1111/j.1466-8238.2011.00657.x

Salas-Eljatib, C., 2021. An approach to quantify climate–productivity relationships: an example from a widespread *Nothofagus* forest. Ecol. Appl. 31, 1–14. https://doi.org/10.1002/eap.2285

Sánchez-Salguero, R., Colangelo, M., Matías, L., Ripullone, F., Camarero, J.J., 2020. Shifts in growth responses to climate and exceeded drought-vulnerability thresholds characterize dieback in two Mediterranean deciduous oaks. Forests 11. https://doi.org/10.3390/F11070714

Sang, Z., Hamann, A., 2022. Climatic limiting factors of North American ecosystems: a remote-sensing based vulnerability analysis. Environ. Res. Lett. 17, 094011. https://doi.org/10.1088/1748-9326/AC8608

Schneider, U., Becker, A., Finger, P., Meyer-Christoffer, A., Ziese, M., 2018. GPCC Full Data Monthly Product Version 2018 at 0.25°: monthly land-surface precipitation from rain-gauges built on GTS-based and historical data [WWW Document]. https://doi.org/10.5676/DWD_GPCC/FD_M_V2018_025

Schuur, E.A., Matson, P.A., 2001. Net primary productivity and nutrient cycling across a mesic

to wet precipitation gradient in Hawaiian montane forest. Oecologia 128, 431–442. https://doi.org/10.1007/S004420100671/METRICS

Silver, W.L., Lugo, A.E., Keller, M., 1999. Soil oxygen availability and biogeochemistry along rainfall and topographic gradients in upland wet tropical forest soils. Biogeochem. 1999 443 44, 301–328. https://doi.org/10.1007/BF00996995

Sullivan, P.F., Csank, A.Z., 2016. Contrasting sampling designs among archived datasets: implications for synthesis efforts. Tree Physiol. 36, 1057–1059. https://doi.org/10.1093/treephys/tpw067

Tonelli, E., Vitali, A., Malandra, F., Camarero, J.J., Colangelo, M., Nolè, A., Ripullone, F., Carrer, M., Urbinati, C., 2023. Tree-ring and remote sensing analyses uncover the role played by elevation on European beech sensitivity to late spring frost. Sci. Total Environ. 857. https://doi.org/10.1016/j.scitotenv.2022.159239

von Keyserlingk, J., de Hoop, M., Mayor, A.G., Dekker, S.C., Rietkerk, M., Foerster, S., 2021. Resilience of vegetation to drought: Studying the effect of grazing in a Mediterranean rangeland using satellite time series. Remote Sens. Environ. 255, 112270. https://doi.org/10.1016/j.rse.2020.112270

Wang, S., Jia, L., Cai, L., Wang, Y., Zhan, T., Huang, A., Fan, D., 2022. Assessment of grassland degradation on the Tibetan Plateau based on multi-source data. Remote Sens. 14. https://doi.org/10.3390/rs14236011

Xiong, Q., Xiao, Y., Liang, P., Li, L., Zhang, L., Li, T., Pan, K., Liu, C., 2021. Trends in climate change and human interventions indicate grassland productivity on the Qinghai–Tibetan Plateau from 1980 to 2015. Ecol. Indic. 129, 108010. https://doi.org/10.1016/j.ecolind.2021.108010

Xu, K., Wang, X., Liang, P., An, H., Sun, H., Han, W., Li, Q., 2017. Tree-ring widths are good proxies of annual variation in forest productivity in temperate forests. Sci. Rep. 7, 1–8. https://doi.org/10.1038/s41598-017-02022-6

Xue, J., Su, B., 2017. Significant remote sensing vegetation indices: A review of developments and applications. J. Sensors 2017. https://doi.org/10.1155/2017/1353691

Chapter 5. A standardized resilience index to ecological droughts (RED50) reveals local adaptation of tree species and their populations

5.1. Summary

Climate change adaptation in forestry requires metrics that identify species and populations with the capacity to tolerate and recover from drought. Yet, empirical comparisons of drought resilience are challenging due to inconsistent drought definitions and confounding effects of species composition, regional population adaptation and local site factors. To address this, we develop a standardized Resilience to Ecological Drought index (RED50), which quantifies the ability of trees to recover from a modeled drought event that causes a 50% growth reduction. Applied to 718 tree-ring sites globally, including detailed analyses of 20 North American species, RED50 enables consistent, cross-species assessments of recovery potential. First, we found a moderate negative correlation between drought resistance and recovery ($r = –0.24$, $p < 0.0001$), indicating a trade-off: species that suppress growth during drought tend to recover more fully afterward. Second, recovery potential varied within species across their ranges, with trailing-edge and interior populations generally showing the highest RED50 values. Third, within-region comparisons revealed that drought-adapted species occupying more xeric sites consistently outperformed mesic-site species in post-drought recovery. These patterns suggest that both species- and population-level adaptations to water limitation enhance resilience. Two complementary, low-risk assisted migration strategies emerge for climate-informed forest management from this analysis: seed sourcing from resilient populations within the species range (e.g., from dry-edge provenances), and RED50-informed species selection within regions when water limitations are expected (i.e. a short-distance version of assisted migration among local sites). Together, these approaches offer practical pathways for reforestation, restoration, and gene conservation planning under climate change.

5.2. Introduction

Under observed climate change over the last several decades, droughts have caused tree mortality, dieback and growth reductions through impacts that include disruptions of the water conduction systems (Choat et al. 2018), dieback of the fine root system (Hartmann et al. 2013), carbon starvation (Hartmann et al. 2013; Kono et al. 2019; Prats et al. 2023) or a combination of these factors. Mortality can be a direct effect of a single drought event, an outcome of additive effects of consecutive droughts (Anderegg et al. 2013), or may also be an indirect outcome through pests and diseases that can more easily overwhelm the defense mechanisms of weakened trees (Babst et al. 2013; Macalady and Bugmann 2014).

Not all species and ecosystems are equally vulnerable to such drought impacts, however. The general expectation is that drought impacts will be most severe in forest communities where tree growth is already water-limited, and where tree populations are located in transition zones toward macroclimatic conditions that no longer support forested ecosystems. That said, tree species and their populations are also locally adapted to the environments in which they occur (Sniderhan et al. 2018; Vizcaíno-Palomar et al. 2019; Silvestro et al. 2023), which could explain more widespread drought impacts observed across forested ecosystems. In other words, if climate change increases the evapotranspirative demand relative to the tolerances of locally adapted species populations, drought impacts may be observed throughout the species range and not only at the drier portion of their range.

This introduces a central challenge for comparative drought vulnerability assessments: the same climatic event may produce very different biological outcomes depending on local site factors, species traits and population-level adaptation. For example, rooting depth and hydraulic architecture strongly shape drought response (Nardini et al. 2013, 2016), while topographic position, soil properties, and competition modulate stress exposure and recovery potential (Galiano et al. 2010; Cavin et al. 2013). These differences align with the concept of ecological drought, defined as an episodic deficit in water availability that causes negative impacts on individual species, natural ecosystems, or managed landscapes (Crausbay et al. 2017). In this framing, even moderate climatic deviations become biologically meaningful if they exceed the adaptive capacity of particular species or populations. Recognizing ecological drought shifts attention from absolute climatic thresholds toward context-specific biological impacts, and

highlights why standardized, relative metrics, such as measuring recovery from a fixed decline in growth, are needed. These approaches can help identify vulnerable species and populations more effectively and support decision-making in reforestation planning, assisted migration, and regional conservation strategies.

In order to assess the capacity of trees to recover from drought events, tracking historical time series of tree growth in response to climate conditions has proven to be a useful approach. Lloret et al (2011) proposed a number of widely used metrics that describe the immediate drought impact on growth (resistance), the ability to resume growth post-drought (recovery) and the degree of return to pre-drought growth levels within a defined period (resilience). The resilience metric is important as an indicator of physical drought damage that requires time to repair. These metrics are used to identify vulnerability of forest ecosystems to climate change in various studies (Das et al. 2007; Grant et al. 2013; Sohn et al. 2016a; Matusick et al. 2018; Senf et al. 2020; Zald et al. 2022).

Such dendroclimatological analyses offer the potential to inform climate change adaptation by guiding management interventions (Oggioni et al. 2024; D'Orangeville et al. 2025). If drought-sensitive species or forest ecosystems can be identified, they may benefit from targeted silvicultural practices, such as thinning, which reduces water demand and thereby enhance drought recovery and reduce mortality (Sohn et al. 2016b). Adaptation to changing environmental conditions could also involve the selection of drought-adapted planting stock through assisted migration (Oggioni et al. 2024), or the use of species sourced from historically drier environments that match planting site conditions under observed or anticipated climate change (Vizcaíno-Palomar et al. 2019; Silvestro et al. 2023; Bower et al. 2024).

To prioritize such climate change adaptation and mitigation efforts, comparative drought vulnerability assessments of tree species and their populations are essential. However, in empirical tree ring research, where environmental conditions are not directly controlled, it has been difficult to compare drought vulnerability metrics across species and regions (Schwarz et al. 2020; DeSoto et al. 2020b). First, climatic drought events occur with different severity in different years and regions. Second, even identical climatic conditions (climatic drought) may be perceived differently, reflected in the concept of an ecological drought. Such differences can

arise between species, populations, or communities, depending on their local adaptation and physiological thresholds. Third, local site factors mediate how sensitive individual trees are to climatic or ecological droughts. Such site factors can vary in scale and include topographic positions (Galiano et al. 2010; Gutierrez Lopez et al. 2021), soil water holding capacity (Paz-Kagan et al. 2017), rooting depth (Nardini et al. 2013, 2016), or competition for available water resources (Cavin et al. 2013).

While site factors are difficult to account for in large-scale comparative studies (except through representative sampling of site conditions), variation in drought severity and local adaptations of species and their populations can be addressed through analytical and methodological choices. Standardized dryness indices like Standardized Precipitation Evapotranspiration Index (SPEI) can be used as a proxy for ecological drought conditions. The SPEI represents an accumulated water deficit that is standardized by its long-term average for a specific location. Thus, it does not represent an absolute climatic value, but a deviation from normal conditions.

The issue of droughts differing in severity, location and timing in empirical studies can also be addressed through standardization approaches. Schwarz et al. (2020) proposed fitting a curve of observed recovery over observed resilience across multiple different drought events in tree ring chronologies. By fitting different curves to samples from different species or regions, and comparing their deviation to the curve that represents complete recovery, a standardized resilience metric can be obtained that is independent of the severity of individual drought events. The standardized resilience metric is a conceptual analogue to physiological vulnerability curves and calculating P50 metrics in tree physiology, indicating the capacity of xylem to withstand progressively drier conditions until 50% of conduits embolize (Meinzer and McCulloh 2013; Wagner et al. 2023).

Here, we apply this standardization approach to obtain a Resilience index to Ecological Drought (RED50), which measures the capacity to recover from a hypothetical ecological drought that causes a 50% growth reduction. We apply the RED50 metric to compare drought vulnerability among species and regions based on 718 tree ring chronology sites obtained from the ITRDB. Our objectives are to (1) discover general patterns of how standardized drought vulnerability is related to macroclimatic site environments; (2) to test if populations of species regionally differ

in their capacity to withstand standardized drought events, and (3) to compare the standardized resilience of different species within the same regions. Our working hypothesis is that due to adaptation of tree species and populations to local climate conditions, the most severe drought impacts are not limited to the trailing edge of forested ecosystems. However, if drought resilience can adequately be quantified, the information may guide species selection and population movements through assisted migration to address climate change.

5.3. Methods

1.3.1. Chronology and climate data

The analysis of damage-dependent recovery capacity of trees across global forest ecosystems was carried out for the period 1971-2005, which had a high number of complete chronologies available from the from the International Tree-Ring Data Bank (ITRDB), good quality of global historical climate records (Manvailer and Hamann 2024), and also coverage of published research on drought impacts on forested ecosystems for validating our definition of ecological drought events (Hammond et al. 2022).

Tree ring width measurements were detrended using the Friedman Super-Smoother 'spline' to preserve short-term variability, which is preferable for assessing year-to-year growth responses to drought events (Friedman 1984). We employed autoregressive modeling to mitigate temporal autocorrelation effects, thereby amplifying the climate signal in our growth data. These two steps were implemented with the *dplR* package (Bunn 2008, 2010; Bunn et al. 2022) for the R programming environment (R Core Team 2024).

As the climatic drought metric we used the Standardized Precipitation Evapotranspiration Index (SPEI) with monthly values aggregated to an annual drought index (Sep to Aug for the northern hemisphere and Mar to Feb for the southern hemisphere) to ensure alignment of prior climatic events with the end of growing season tree ring records. SPEI calculations were implemented with the *SPEI* package (Beguería and Vicente-Serrano 2023) for the R programming environment, based on precipitation and temperature interpolations by (Matsuura and Willmott 2018), which were chosen for their superior correlation with biological data (Manvailer and Hamann 2024).

Ecological drought events were defined as reductions of ≥1 standard deviation in both SPEI and ring width index within the same or subsequent year, ensuring that our analysis had a focus on climatically-induced growth reductions (See Appendix 5 for all cases considered). To validate our drought detection method, we cross-referenced our identified drought events with a global drought-induced mortality dataset (Hammond et al. 2022). By linking ecological drought events as defined above to the published mortality database, allowing for a distance of up to 150 km between chronology sites and mortality records, then from a total of 170 mortality event locations within the range of chronology sites, 82% (140 mortality events) were preceded within 3 years by an ecological drought as defined above (see Appendix 6 for details on this analysis supporting the method development).

For reporting purposes, we group chronologies into clusters of site chronologies that had similar climatologies and growth responses. For this purpose, we employed the Partition Around Medoids (PAM) algorithm to cluster chronology sites based on 35 annual SPEI values and 35 corresponding ring width values. PAM was implemented with the function *pam()* of the package *cluster* (Struyf et al. 1997; Maechler et al. 2023) while the optimal number of clusters was determined using the elbow method implemented with the function *fviz_nbclust()* of the package *factoextra* (Kassambara and Mundt 2020) for the R programming environment. See Appendix 7 for more details.

After applying filtering criteria, 718 site chronologies, grouped into 26 clusters, were used for the drought response analysis (Figure 5.1). Filtering criteria included the following: (1) a minimum of 30 years of data within the 1971-2005 period, (2) at least 6 chronology sites within a PAM cluster, (3) at least 3 ecological drought events identified in a site chronology, (4) some outlier removal of less than 5% of the remaining chronology sites due to various issues, including spatially disjunct cluster members, and outliers in calculations of drought metrics. See Appendix **8** for visualization of sites filtered.

A large number of chronology sites (43%) were removed because chronologies did not contain at least three drought events during the study period, or because PAM clusters contained less than 6 site chronologies with at least three droughts (Figure 5.1, gray sample points and clusters). These

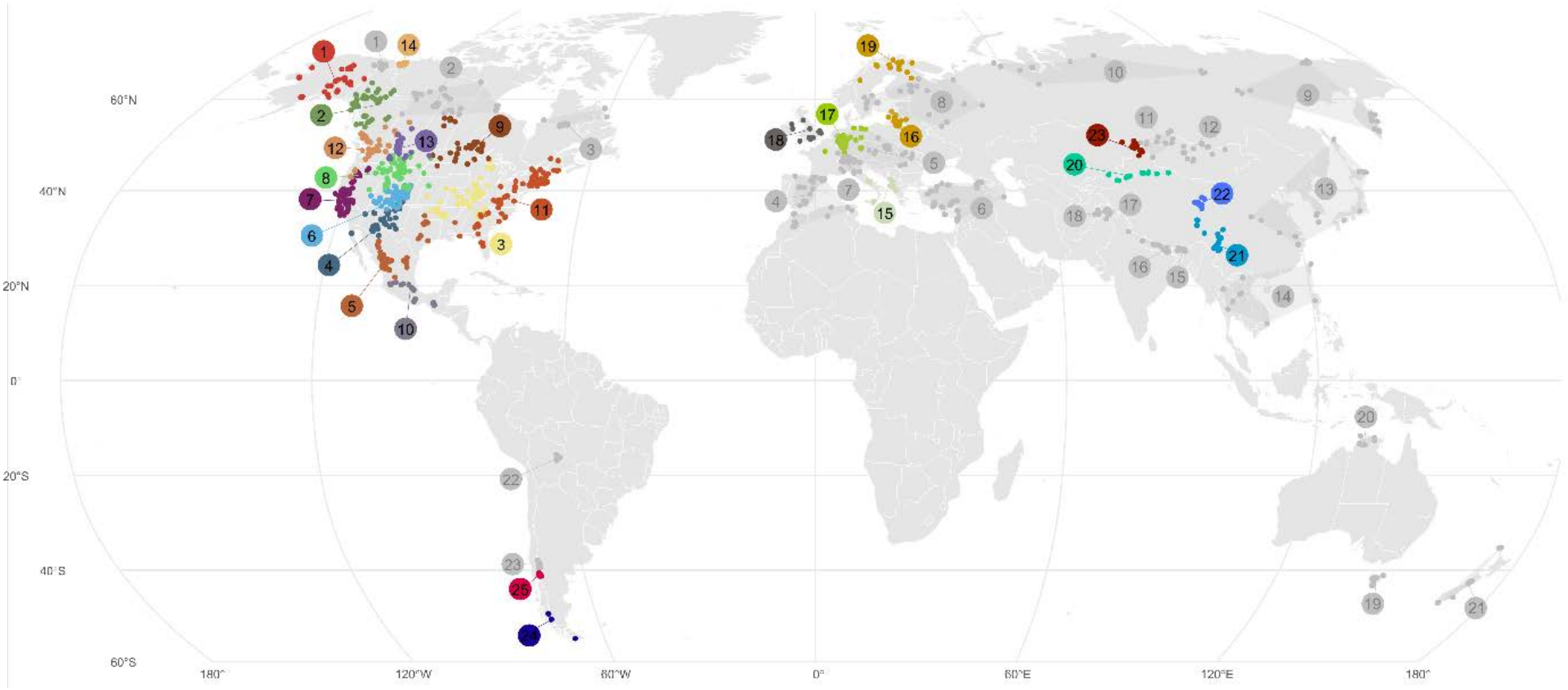

Figure 5.1. Chronology sites and clusters of sites with similar climatologies and growth response. Approximately 40% of chronology sites were removed to satisfy filtering criteria that ensured that drought metrics could be estimated, and reliable inferences could be drawn for clusters with regards to their drought vulnerability.

filtering criteria ensured that drought response metrics could reliably be estimated, and subsequent statistical analysis of precision of estimates within clusters could be carried out.

Drought responses were quantified with both the widely used metrics resistance, recovery, and resilience (Loret et al. (2011), and a “recovery capacity” metric as described by Schwarz et al. (2020). This drought recovery capacity metric is based on a negative exponential function fitted to recovery over resistance metrics for individual drought events (colored points in Figure 5.2 a). The recovery capacity is then defined by how much the fitted curve deviates from complete recovery (solid line vs dashed line in Figure 5.2 b). This recovery capacity metric is independent of the severity of the actually observed individual drought events. We calculate this recovery capacity metric for a resistance value of 0.5, meaning that the growth is reduced by 50% as a consequence of a hypothetical ecological drought event.

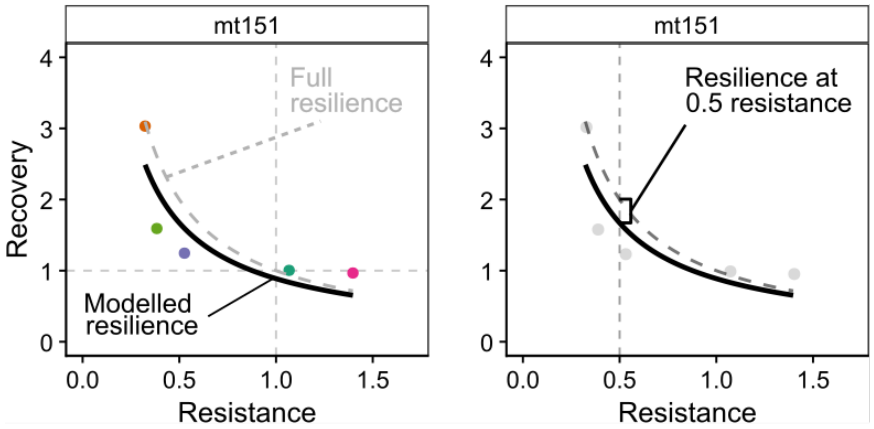

Figure 5.2. Estimation of a recovery capacity metric by fitting a curve to resistance and recovery values. The deviation of the fitted lines (solid) to full recovery (dashed lines) for a hypothetical drought event that causes 50% growth reduction (Resistance = 0.5) is interpreted as a recovery capacity metric that is independent of the severity of the observed individual drought events (colored dots).

5.4. Results

5.4.1. Resilience in relation to ecological drought severity

While one might expect that severe drought impacts on growth (i.e., low resistance values) would be associated with impaired recovery, this pattern does not hold for the standardized RED50 metric (Figure 5.3). Across species and regions, sites with more pronounced growth reductions during drought—indicated by low resistance—often exhibit more complete recovery. In contrast, sites with high resistance values—where drought had only minor effects on growth—tend to show incomplete recovery, with elevated RED50 values. This counterintuitive pattern suggests that resilience, as quantified here, is not simply a function of how severely a tree was affected during drought, but may also reflect underlying physiological or ecological strategies that influence both sensitivity and recovery.

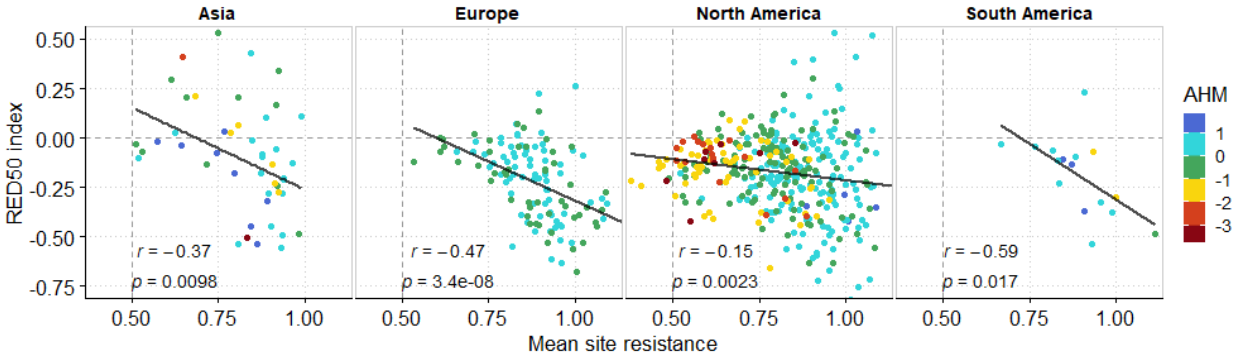

Figure 5.3. Resilience to ecological droughts (RED50) as a function of the ecological drought severity (resistance), and their relationships with a non-standardized annual heat-moisture index (AHM, log transformed values with smaller values indicate a drier climate normal values). Data points represent chronologies averaged by species and sites. A RED50 value of zero indicates complete recovery to pre-drought levels, a resistance value of 0.5 indicates a 50% growth reduction (indicated by dashed lines).

This general inverse relationship between resistance and RED50 is consistent across most regions and taxa, indicating that trees which experience larger growth reductions during drought are often capable of more complete recovery. This pattern suggests that the ability to sharply reduce growth during drought—a form of drought avoidance or protective shutdown—may be advantageous for subsequent recovery. In contrast, trees that maintain moderate growth during drought conditions may accumulate greater physiological damage, resulting in slower or incomplete recovery.

5.4.2. Recovery across species and regions

To compare species and regional differences under equivalent drought stress, we modeled RED50 values assuming a uniform growth reduction of 50% (resistance = 0.5) across all sites. This approach isolates recovery capacity from variation in drought severity, thereby enabling a standardized comparison. Results reveal substantial variation in RED50 both across and within species and regions (Table 4.1). Species-specific averages ranged from near-complete lack of recovery—such as *Pinus strobus* in region 9 (RED50 = –0.50, SE = 0.07) to full recovery, as observed in *Pseudotsuga menziesii* in region 13 (RED50 = 0.01, SE = 0.09). Overall, the mean RED50 across all chronologies was –0.16, suggesting that most populations exhibit incomplete recovery from a hypothetical drought event causing 50% growth reduction. This modeled drought severity is relatively uncommon in the full dataset, occurring in approximately 30% of the identified drought years. For context, the average resistance across all observations was 0.83, indicating that most drought events in the data produced milder growth reductions. RED values exceeding zero (at the top) that are well beyond the uncertainty indicated by the standard error would suggest overcompensation or unexpected additional growth enabled by prior drought conditions (or cyclical climate patterns where very favorable growth conditions regularly follow drought periods).

Table 5.1 Average drought recovery statistics across sites for each species–cluster combination, sorted from most to least resilient within each continent. Columns include the number of sites (N Sites), number of drought events analyzed (N Droughts), the standardized recovery metric (RED50) at 50% growth reduction, standard error of the RED statistic (SE), mean resistance (Resistance), and traditional resilience (Resilience).

Continent Cluster #	Species	N Sites	N Droughts	RED50	SE	Resistance	Resilience
North America							
7	*Quercus douglasii*	29	6	0.28	0.09	0.79	1.10
14	*Picea glauca*	24	4	0.12	0.04	0.83	0.98
11	*Quercus prinus*	7	3	0.03	0.13	0.89	0.97
12	*Tsuga mertensiana*	14	3	0.03	0.16	0.95	1.14
13	*Pseudotsuga menziesii*	33	6	0.01	0.09	0.90	1.03
11	*Chamaecyparis thyoides*	18	3	-0.05	0.10	0.91	1.02
7	*Pinus ponderosa*	7	6	-0.06	0.04	0.87	1.06

6	*Pinus edulis*	33	7.6	-0.07	0.02	0.73	0.97
3	*Quercus alba*	12	5	-0.09	0.09	0.88	1.01
13	*Pinus flexilis*	10	6	-0.11	0.06	0.86	1.05
6	*Pseudotsuga menziesii*	28	7.7	-0.11	0.02	0.73	0.94
3	*Liriodendron tulipifera*	12	5	-0.12	0.08	0.84	0.99
3	*Quercus spp*	7	5	-0.12	0.07	0.91	0.98
5	*Quercus stellata*	6	6	-0.14	0.06	0.99	0.99
6	*Pinus ponderosa*	15	7.6	-0.14	0.04	0.79	0.96
10	*Taxodium mucronatum*	12	5	-0.15	0.06	0.86	1.03
4	*Pseudotsuga menziesii*	34	5.9	-0.15	0.03	0.57	0.91
12	*Abies lasiocarpa*	8	3	-0.15	0.13	0.94	1.05
5	*Pseudotsuga menziesii*	27	6	-0.16	0.02	0.74	0.94
12	*Pseudotsuga menziesii*	7	3	-0.17	0.13	0.90	0.96
10	*Pseudotsuga menziesii*	9	5	-0.17	0.05	0.77	1.05
1	*Picea glauca*	32	3	-0.17	0.03	0.92	1.06
11	*Quercus rubra*	6	3	-0.18	0.07	0.78	0.97
11	*Tsuga canadensis*	12	3	-0.18	0.05	0.97	1.03
4	*Pinus ponderosa*	25	5.3	-0.18	0.02	0.63	0.89
8	*Pinus ponderosa*	13	5	-0.22	0.05	0.84	0.95
8	*Pseudotsuga menziesii*	34	5	-0.24	0.03	0.84	0.93
9	*Quercus macrocarpa*	11	4	-0.25	0.08	0.85	0.95
8	*Pinus flexilis*	10	5	-0.29	0.06	0.89	0.95
11	*Quercus alba*	8	3	-0.30	0.05	0.83	0.96
2	*Abies lasiocarpa*	7	3	-0.31	0.05	0.98	1.04
9	*Pinus resinosa*	9	4	-0.36	0.07	0.89	0.93
9	*Pinus strobus*	13	4	-0.50	0.07	1.00	1.02
Europe							
16	*Larix decidua*	10	6	-0.09	0.02	0.70	0.99
17	*Fagus sylvatica*	26	5	-0.09	0.02	0.78	0.97
15	*Pinus heldreichii*	10	3	-0.14	0.04	0.87	0.95
17	*Picea abies*	21	5	-0.17	0.05	0.87	1.00
17	*Pinus sylvestris*	7	5	-0.25	0.09	1.00	1.03
18	*Quercus spp*	10	4	-0.30	0.04	0.90	1.03
19	*Pinus sylvestris*	11	3	-0.31	0.05	0.90	0.95
17	*Quercus petraea*	19	5	-0.36	0.03	1.01	1.10
17	*Quercus robur*	9	5	-0.45	0.06	0.96	1.08
Asia							
22	*Juniperus przewalskii*	9	3	0.17	0.07	0.62	0.99
21	*Juniperus tibetica*	6	3.8	0.00	0.05	0.90	1.14
20	*Picea schrenkiana*	13	4	-0.14	0.05	0.83	0.93
24	*Larix sibirica*	13	4	-0.20	0.10	0.86	0.97
21	*Abies forestii*	6	4	-0.35	0.11	0.91	0.99
South America							
25	*Nothofagus pumilio*	10	3	-0.17	0.07	0.87	0.96
24	*Nothofagus pumilio*	6	4	-0.22	0.07	0.93	1.06

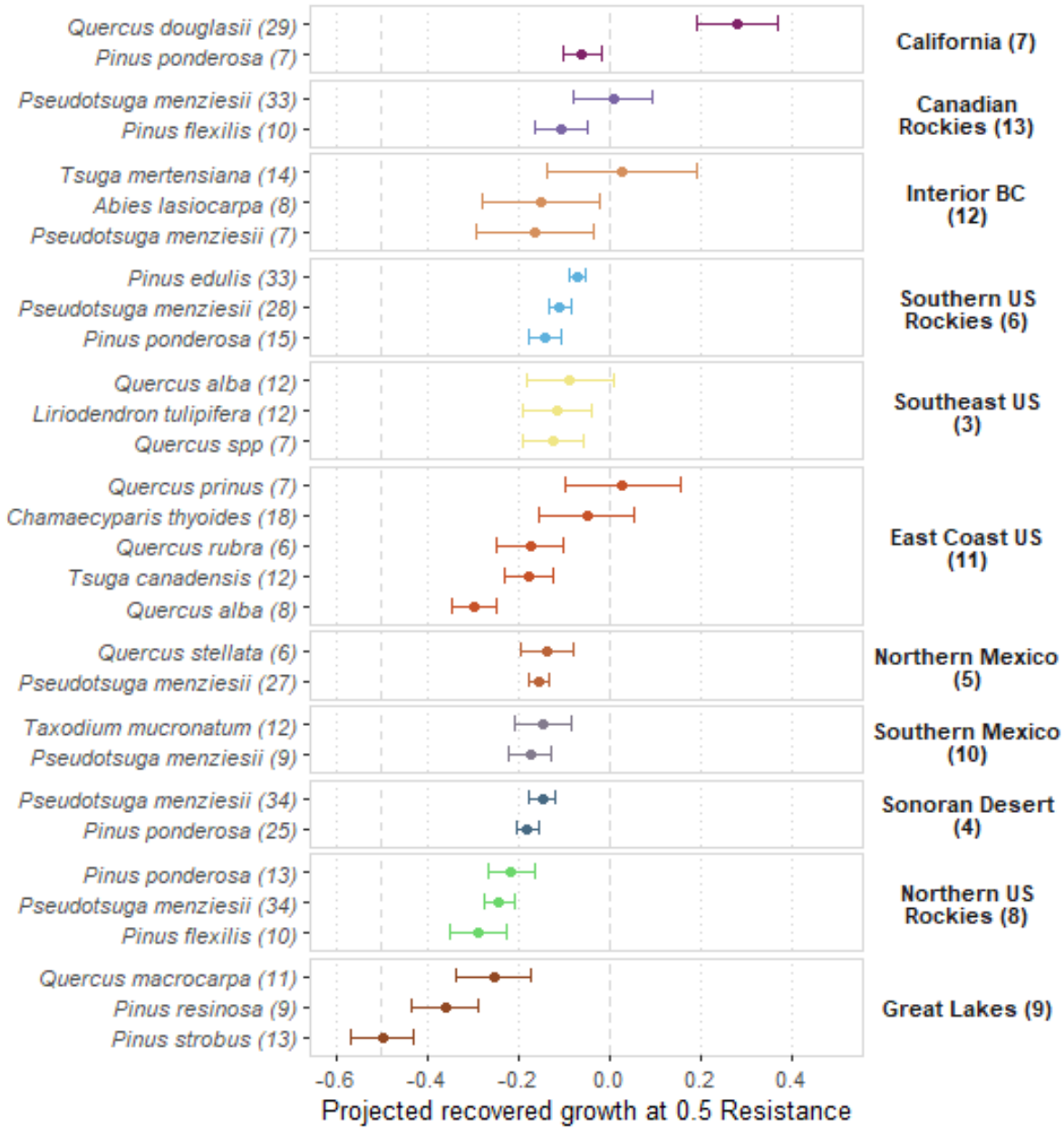

Figure 5.4. Average RED50 across clusters and species. Points represent average RED50 species recovery for a given cluster in a given region. Horizontal bars show one standard error. Only species with more than six sites are shown (N = 718). A RED50 value of zero indicates complete recovery to pre-drought levels, while –0.5 represents no recovery at all (dashed lines). Points to the left of –0.5 indicate that growth during the recovery period was lower than during drought. Positions to the right of zero indicate growth rates exceeding pre-drought levels.

5.4.1. Species comparisons with regions of North America

For a comparative assessment of species performance we plotted standardized drought recovery values (RED50) within North American regions. Only North America had sufficient sample sizes across multiple species and clusters to enable this analysis. Figure 4.4 summarizes species-level RED50 values averaged by regional clusters (as indicated by their names and the corresponding numbers shown in Figure 4.1), allowing for intra-regional comparisons of drought recovery.

Across regions, some of the highest RED50 values were observed in species and clusters associated with moderate to high annual precipitation, including the California, The Canadian Rockies, Interior BC, and East Coast US clusters (Fig. 5.4). Species with notably high resilience values include *Quercus douglasii* and *Pinus ponderosa* in California (cluster 7), which showed unexpectedly high post-drought growth and near-complete recovery, respectively. In the Canadian Rockies (cluster 13), *Pseudotsuga menziesii* also demonstrated complete recovery. On the East Coast (cluster 11), *Quercus prinus* and *Chamaecyparis thyoides* showed strong recovery, with RED50 values close to zero, suggesting effective recovery capacity in these mesic forest types.

Several regional clusters exhibit strong interspecific gradients in drought resilience, with non-overlapping standard errors indicating statistically significant differences among species. In the East Coast US (cluster 11), *Quercus prinus*, a species typically found on dry, rocky ridges, south- or west-facing slopes, showed the highest RED50 values (~0.03), while *Quercus alba*, typically found on well-drained but moisture-retentive soils exhibited the lowest value (–0.30), reflecting a marked contrast in recovery capacity among co-occurring hardwood species. In the Great Lakes cluster (9), *Pinus strobus* shows the lowest drought resilience (–0.50), consistent with its shallow roots and mesic-site preference in this region. *Pinus resinosa* performs slightly better but still poorly (–0.36), matching its moderate drought tolerance. *Quercus macrocarpa* has the highest RED50 value of the group (–0.25), which fits its dry-site adaptation and deep-rooted physiology, though overall recovery remains incomplete under a 50% drought impact, underscoring the limited drought adaptation of these mesic species. In the Southern Rockies (cluster 6), *Pinus edulis* is the top performer (–0.07), as expected from a specialist in arid

environments. *Pseudotsuga menziesii* (–0.11) and *Pinus ponderosa* (–0.14) trail comparatively in RED50 values.

5.4.2. Population variations in wide-ranging species

Several wide-ranging species were present in multiple clusters across North America, enabling comparisons of RED50 values across different parts of their range. These comparisons can reveal whether drought recovery potential is influenced by local environmental conditions and/or population-level differentiation.

With species ordered from most to least resilient overall in Fig. 4.5, *Picea glauca* shows substantial regional variation in drought recovery. In the Northern Yukon cluster (14) a very dry interior region, RED50 reached 0.12, suggesting higher values than indicative of recovery. In contrast, populations in the Boreal Alaska cluster (1), which experiences stronger coastal climatic influence and higher precipitation, showed lower recovery (–0.17).

Pseudotsuga menziesii (Douglas-fir) is present in six clusters. Recovery potential was highest in the Southwest US and Interior California (clusters 4 and 5), where RED50 values ranged from –0.15 to –0.16, suggesting relatively strong recovery in some trailing-edge populations. In contrast, more southerly and interior populations, such as those in the Southern US Rockies and Southern Mexico (clusters 6 and 10), showed lower recovery values (–0.17), under equivalent relative drought impacts.

Pinus ponderosa occurs in four regional clusters, showing a gradient in drought recovery performance. The highest RED50 value is observed in the California cluster (7; –0.06), representing the trailing western edge of the species' distribution, conforming to patterns observed in other trailing-edge noted above. Recovery is somewhat lower in the Southern Rockies (cluster 6; –0.14), and further declines towards the Northern US Rockies (cluster 8; –0.22) show the lowest recovery. However, the Sonoran Desert region (cluster 4; –0.18), which represents the driest portion of the species' interior range, where one might have expected the greatest drought resilience showed intermediate RED50 values. The low resilience may indicate a limit to the species adaptive capacity to an extremely marginal environment.

Quercus alba (White oak) shows higher RED50 values in the Southeast US cluster (3), closer to the great plains biome, compared to the East Coast (cluster 11), a more mesic region where recovery was minimal.

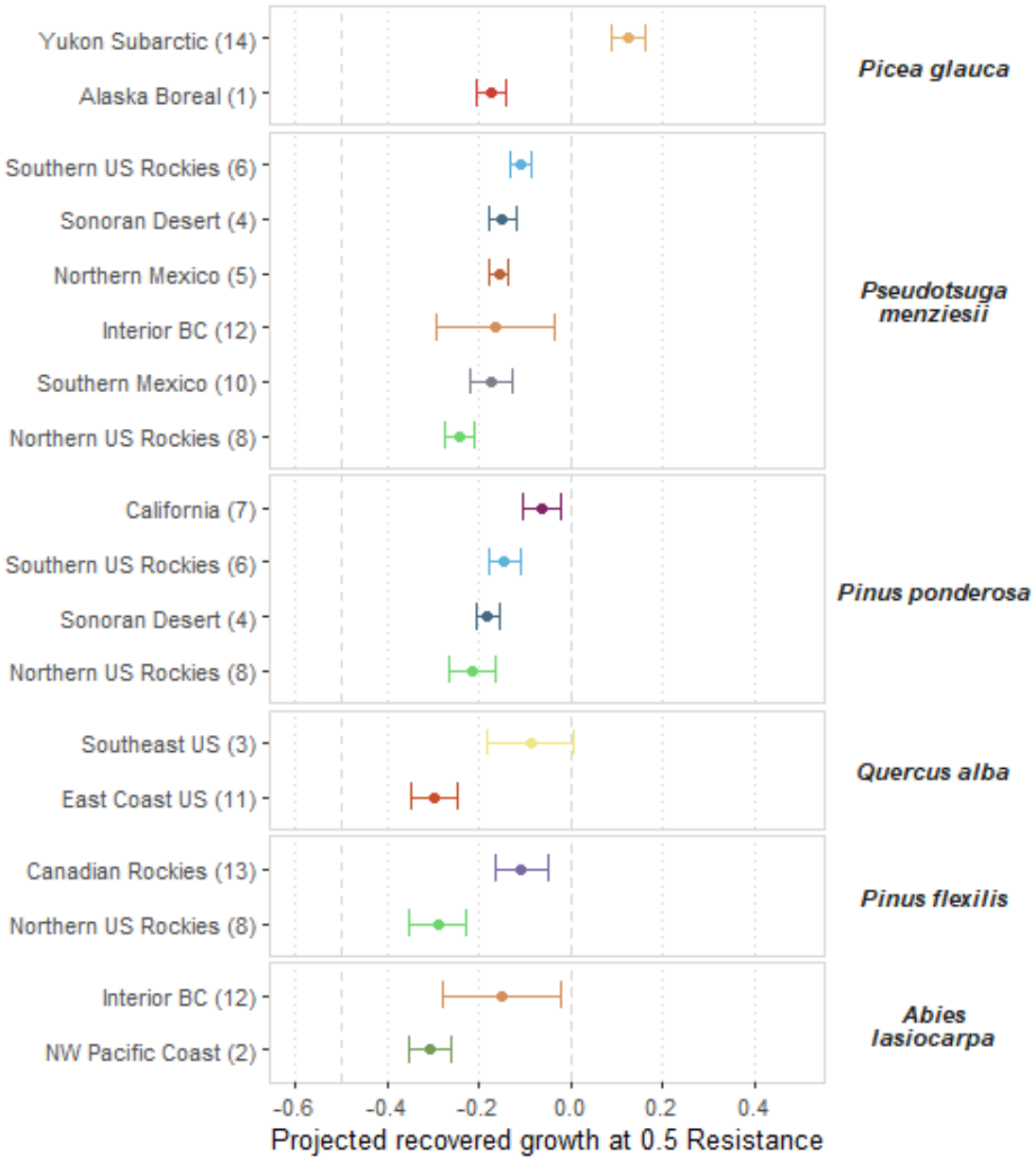

Figure 5.5. Same as Figure 5.4 but RED50 averages are grouped by species for population comparisons.

Pinus flexilis appears in two regional clusters and shows differentiation that are consistent with general trends observed in other species. In the Southern Rockies (cluster 4), RED50 was relatively high at –0.11, indicating reasonable recovery following severe drought. In contrast, populations in the Northern US Rockies (cluster 8) showed substantially lower recovery (–0.29).

Abies lasiocarpa again shows an expected difference in RED50 values between two interior and coastal clusters. In the dry Interior BC (cluster 12), RED50 was –0.15, while in the Pacific Coast (cluster 2) it declined to –0.31, indicating substantially reduced recovery in more mesic coastal populations, in fact one of the weakest resilience values overall. This pattern aligns with observations for other species, where interior or trailing-edge populations demonstrate stronger recovery capacity under standardized drought impacts.

5.5. Discussion

5.5.1. Adaptive resilience in dry environments

Our analysis reveals that many species demonstrate higher resilience where historical drought severity has been most pronounced. This includes populations of species toward the dry and warm end of their distribution, e.g., *Quercus douglasii, Pinus ponderosa* in California, *Pinus edulis* in the Southern Rockies, and *Picea glauca* in the interior Yukon. Even species not typically associated with arid conditions, such as *Quercus alba*, exhibited improved drought recovery in drier southwestern regions compared to more mesic eastern sites. These patterns suggest that local adaptation to long-term water limitation can enhance post-drought recovery, aligning with the expectation that trailing-edge or interior populations often harbor traits conferring greater resilience (Choat et al. 2012; Aitken and Whitlock 2013).

Rather than uniformly increasing vulnerability, chronic drought exposure appears to select for conservative water use strategies, deeper rooting systems, and hydraulic traits that facilitate recovery once favorable conditions return (Anderegg et al. 2016; Peters et al. 2021; Bachofen et al. 2024). For instance, *Pinus ponderosa* shows precise timing of xylogenesis regulated by moisture availability (Ziaco et al. 2018), while *Pinus edulis* exhibits deep rooting and strong drought avoidance traits (Ronco Jr. 1990). Even among mesic conifers like *Pseudotsuga*

menziesii, populations in drier areas show improved post-drought performance, likely reflecting stomatal control and greater hydraulic safety margins (Choat et al. 2012; Leuschner et al. 2024).

We found no evidence for uniformly reduced resilience in more arid regions. Instead, populations at the trailing or driest interior edge of species distributions often exhibit the strongest recovery potential, likely due to long-term selection for drought-avoidance and hydraulic safety traits (Choat et al. 2018; Blumstein et al. 2023). This aligns with studies showing greater non-structural carbohydrate reserves and enhanced root investment in dry-adapted populations, supporting faster regrowth after stress events (Blumstein et al. 2023; Bachofen et al. 2024).

5.5.2. Trade-offs between drought resistance and recovery

A consistent global pattern in our results is a negative correlation between drought resistance and recovery capacity: sites or species that maintained high growth during drought (high resistance) often had lower RED50 values, and vice versa ($r = –0.24$, $p < 0.0001$). This suggests a trade-off between strategies: conservative species that shut down growth rapidly during drought may avoid hydraulic damage and thereby enable faster recovery when conditions improve (McDowell et al. 2008; Hesse et al. 2023). In contrast, species that sustain moderate growth under drought, possibly maintaining carbon gain or competitive advantage, may suffer longer-term physiological costs (e.g., embolism, carbon depletion), impairing recovery.

This supports recent syntheses showing that resistance-focused strategies often carry a cost to resilience, especially when droughts are severe or recurrent (Li et al. 2020; Trugman et al. 2021). The RED50 trade-off observed here reflects that sustaining productivity during drought may heighten vulnerability to carbon starvation or hydraulic failure during prolonged stress (Hartmann et al. 2013; Kono et al. 2019). The mechanisms behind this trade-off are well-documented by empirical studies showing that trees with high resistance often operate closer to hydraulic failure thresholds (McDowell et al. 2008; Choat et al. 2012), whereas species with low resistance may conserve hydraulic integrity and maintain non-structural carbohydrate reserves essential for regrowth (Hartmann et al. 2013; Hesse et al. 2023). This trade-off helps explain why

species adapted to arid environments often show both low resistance and high RED50 values. For example, *Pinus edulis* and *Pseudotsuga menziesii* in the Southern Rockies exhibit this pattern, where the capacity to limit growth during drought appears to support faster rebound post-drought.

5.5.3. Intra- and inter-specific variation conform

Across multiple species, drought recovery generally aligns with geographic expectations of adaptation, where trailing-edge, interior, and dry-site populations show higher RED50 values. For example, *Picea glauca* and *Abies lasiocarpa* demonstrated better recovery in interior continental regions than in coastal, wetter environments. *Pseudotsuga menziesii* and *Pinus ponderosa* also exhibited patterns of stronger recovery in dry Californian or interior populations, compared to their more northern or mesic counterparts. These results reflect local adaptation of species populations and conform to the expectation that resilience traits are not uniformly distributed across a species' range, but instead shaped by climatic selection pressures, especially at ecotones where moisture availability varies sharply (Aitken et al. 2008; Isaac-Renton et al. 2018).

This spatial perspective also complements findings from provenance trials and trait-based studies that highlight local adaptation in hydraulic safety margins and rooting architecture across climatic gradients (Montwé et al. 2016; Silvestro et al. 2023; D'Orangeville et al. 2025). In other research, drought-tolerant provenances of black spruce (*Picea mariana*) and red spruce (*Picea rubens*), for example, have shown superior recovery under stress, even within mesic landscapes, likely due to inherited physiological adaptations (Sniderhan et al. 2018; Vizcaíno-Palomar et al. 2019).

Moreover, inter-specific differences within regions showed similar contrasts. In the East Coast US cluster, *Quercus prinus* had much higher RED50 than *Quercus alba*, matching their ecological preferences. *Quercus prinus* is commonly associated with dry, rocky ridge sites and south- or west-facing slopes, where its drought adaptations such as deep rooting are advantageous (Abrams 1990). In contrast, *Q. alba* typically occurs on well-drained but moisture-retentive soils, making it less suited to drought-prone microsites (Burns and Honkala 1990a). In the Great Lakes region, the drought-tolerant *Quercus macrocarpa*, which is often found on dry

prairie-forest transition zones (Burns and Honkala 1990a), exhibited significantly better resilience than *Pinus strobus*, a species more commonly associated with cooler, mesic sites (Burns and Honkala 1990b).

Thus, differences that we observed among regions at the intra-species level, namely greater resilience in populations adapted to drier regions, can also be seen at the inter-species level within regions. Drought-resilient species are prevalent at dry sites within regions precisely because they are better adapted there, and they demonstrate better recovery capacity under drought.

5.6. Conclusions and management implications

The observation that drought-resilient species dominate drier sites within regions, and that dry-adapted populations exhibit higher recovery across regions, tells a consistent story: local adaptation plays a critical role in shaping resilience to drought. This pattern, observed both at the intra- and interspecific level, has implications for forest management and climate change adaptation.

Two complementary strategies emerge. First, within-species variation can be harnessed by relocating drought-resilient populations, typically from trailing edges or interior dry zones, to regions where climate change is expected to increase drought exposure. This supports regionally informed seed transfer that leverages adaptive traits already present in natural populations. Second, at the interspecific level, species selection can be modified within regions to match changing conditions. For example, managers might favor drought-adapted species from nearby xeric microsites for planting in areas becoming drier under climate change. These short-distance "assisted migration" strategies remain ecologically conservative yet climate-informed.

We should note, however, that even with these management interventions adaptive capacity remains limited. Further warming and intensification of drought may exceed physiological thresholds even in currently resilient populations. Future work could extend this framework to examine tipping points and multi-year drought impacts. Nonetheless, our results strengthen the rationale for conserving trailing-edge and dry-site populations, which are increasingly recognized as important reservoirs of adaptive genetic diversity (Hampe and Petit 2005;

Hoffmann and Sgró 2011; Aitken and Whitlock 2013; Vizcaíno-Palomar et al. 2019). This study adds empirical support to the value of gene conservation efforts that prioritize these marginal populations under a rapidly changing climate.

5.7. References

Abrams MD (1990) Adaptations and responses to drought in Quercus species of North America . Tree Physiol 7:227–238. https://doi.org/10.1093/treephys/7.1-2-3-4.227

Aitken SN, Whitlock MC (2013) Assisted gene flow to facilitate local adaptation to climate change. Annu Rev Ecol Evol Syst 44:367–388. https://doi.org/10.1146/annurev-ecolsys-110512-135747

Aitken SN, Yeaman S, Holliday JA, et al (2008) Adaptation, migration or extirpation: climate change outcomes for tree populations. Evol Appl 1:95–111. https://doi.org/10.1111/j.1752-4571.2007.00013.x

Anderegg WRL, Klein T, Bartlett M, et al (2016) Meta-analysis reveals that hydraulic traits explain cross-species patterns of drought-induced tree mortality across the globe. Proc Natl Acad Sci U S A 113:5024–5029. https://doi.org/10.1073/pnas.1525678113

Anderegg WRL, Plavcová L, Anderegg LDL, et al (2013) Drought's legacy: Multiyear hydraulic deterioration underlies widespread aspen forest die-off and portends increased future risk. Glob Chang Biol 19:1188–1196. https://doi.org/10.1111/gcb.12100

Babst F, Poulter B, Trouet V, et al (2013) Site- and species-specific responses of forest growth to climate across the European continent. Glob Ecol Biogeogr 22:706–717. https://doi.org/10.1111/GEB.12023

Bachofen C, Tumber-Dávila SJ, Mackay DS, et al (2024) Tree water uptake patterns across the globe. New Phytol 242:1891–1910. https://doi.org/10.1111/nph.19762

Beguería S, Vicente-Serrano SM (2023) SPEI: Calculation of the Standardized Precipitation-Evapotranspiration Index

Blumstein M, Gersony J, Martínez-Vilalta J, Sala A (2023) Global variation in nonstructural carbohydrate stores in response to climate. Glob Chang Biol 29:1854–1869. https://doi.org/10.1111/gcb.16573

Bower AD, Frerker KL, Pike CC, et al (2024) A practical framework for applied forestry assisted migration. Front For Glob Chang 7:1–16. https://doi.org/10.3389/ffgc.2024.1454329

Bunn A, Korpela M, Biondi F, et al (2022) dplR: Dendrochronology program library in R

Bunn AG (2010) Statistical and visual crossdating in R using the dplR library. Dendrochronologia 28:251–258. https://doi.org/10.1016/j.dendro.2009.12.001

Bunn AG (2008) A dendrochronology program library in R (dplR). Dendrochronologia 26:115–124. https://doi.org/10.1016/j.dendro.2008.01.002

Burns RM, Honkala BH (eds) (1990a) Silvics of North America: 2. Hardwoods. U.S. Department of Agriculture, Forest Service, Washington, DC

Burns RM, Honkala BH (eds) (1990b) Silvics of North America: 1. Conifers. U.S. Department of Agriculture, Forest Service, Washington, DC

Cavin L, Mountford EP, Peterken GF, Jump AS (2013) Extreme drought alters competitive dominance within and between tree species in a mixed forest stand. Funct Ecol 27:1424–1435. https://doi.org/10.1111/1365-2435.12126

Choat B, Brodribb TJ, Brodersen CR, et al (2018) Triggers of tree mortality under drought. Nature 558:531–539. https://doi.org/10.1038/s41586-018-0240-x

Choat B, Jansen S, Brodribb TJ, et al (2012) Global convergence in the vulnerability of forests to drought. Nature 491:752–755. https://doi.org/10.1038/nature11688

Crausbay SD, Ramirez AR, Carter SL, et al (2017) Defining ecological drought for the twenty-first century. Bull Am Meteorol Soc 98:2543–2550. https://doi.org/10.1175/BAMS-D-16-0292.1

D'Orangeville L, Itter MS, Dos Santos JM, Taylor AR (2025) Can tree-rings inform assisted migration? Revisiting provenance trials across Atlantic Canada to compare local adaptation between red spruce populations. For Ecol Manage 578:122482. https://doi.org/10.1016/j.foreco.2024.122482

Das AJ, Battles JJ, Stephenson NL, Van Mantgem PJ (2007) The relationship between tree growth patterns and likelihood of mortality: A study of two tree species in the Sierra Nevada. Can J For Res 37:580–597. https://doi.org/10.1139/X06-262

DeSoto L, Cailleret M, Sterck F, et al (2020) Low growth resilience to drought is related to future mortality risk in trees. Nat Commun 11:545. https://doi.org/10.1038/s41467-020-

14300-5

Friedman JH (1984) A Variable Span Smoother

Galiano L, Martínez-Vilalta J, Lloret F (2010) Drought-induced multifactor decline of Scots Pine in the Pyrenees and potential vegetation change by the expansion of co-occurring Oak species. Ecosystems 13:978–991. https://doi.org/10.1007/s10021-010-9368-8

Grant GE, Tague CL, Allen CD (2013) Watering the forest for the trees: an emerging priority for managing water in forest landscapes. Front Ecol Environ 11:314–321. https://doi.org/10.1890/120209

Gutierrez Lopez J, Tor-ngern P, Oren R, et al (2021) How tree species, tree size, and topographical location influenced tree transpiration in northern boreal forests during the historic 2018 drought. Glob Chang Biol 27:3066–3078. https://doi.org/10.1111/gcb.15601

Hammond WM, Williams AP, Abatzoglou JT, et al (2022) Global field observations of tree die-off reveal hotter-drought fingerprint for Earth's forests. Nat Commun 13:. https://doi.org/10.1038/s41467-022-29289-2

Hampe A, Petit RJ (2005) Conserving biodiversity under climate change: The rear edge matters. Ecol Lett 8:461–467. https://doi.org/10.1111/j.1461-0248.2005.00739.x

Hartmann H, Ziegler W, Trumbore S (2013) Lethal drought leads to reduction in nonstructural carbohydrates in Norway spruce tree roots but not in the canopy. Funct Ecol 27:413–427. https://doi.org/10.1111/1365-2435.12046

Hesse BD, Gebhardt T, Hafner BD, et al (2023) Physiological recovery of tree water relations upon drought release—response of mature beech and spruce after five years of recurrent summer drought. Tree Physiol 43:522–538. https://doi.org/10.1093/treephys/tpac135

Hoffmann AA, Sgró CM (2011) Climate change and evolutionary adaptation. Nature 470:479–485. https://doi.org/10.1038/nature09670

Isaac-Renton M, Montwé D, Hamann A, et al (2018) Northern forest tree populations are physiologically maladapted to drought. Nat Commun 9:1–9. https://doi.org/10.1038/s41467-018-07701-0

Kassambara A, Mundt F (2020) factoextra: Extract and visualize the results of multivariate data analyses

Kono Y, Ishida A, Saiki S-T, et al (2019) Initial hydraulic failure followed by late-stage carbon

starvation leads to drought-induced death in the tree *Trema orientalis*. Commun Biol 2:8. https://doi.org/10.1038/s42003-018-0256-7

Leuschner C, Fuchs S, Wedde P, et al (2024) A multi-criteria drought resistance assessment of temperate Acer, Carpinus, Fraxinus, Quercus, and Tilia species. Perspect Plant Ecol Evol Syst 62:125777. https://doi.org/10.1016/j.ppees.2023.125777

Li X, Piao S, Wang K, et al (2020) Temporal trade-off between gymnosperm resistance and resilience increases forest sensitivity to extreme drought. Nat Ecol Evol 4:1075–1083. https://doi.org/10.1038/s41559-020-1217-3

Lloret F, Keeling EG, Sala A (2011) Components of tree resilience: Effects of successive low-growth episodes in old ponderosa pine forests. Oikos 120:1909–1920. https://doi.org/10.1111/j.1600-0706.2011.19372.x

Macalady AK, Bugmann H (2014) Growth-mortality relationships in piñon pine (Pinus edulis) during severe droughts of the past century: Shifting processes in space and time. PLoS One 9:. https://doi.org/10.1371/journal.pone.0092770

Maechler M, Rousseeuw P, Struyf A, et al (2023) cluster: Cluster Analysis Basics and Extensions

Manvailer V, Hamann A (2024) Validation of global precipitation time series products against tree ring records and remotely sensed vegetation greenness. PLoS One 19:1–13. https://doi.org/10.1371/journal.pone.0299111

Matsuura K, Willmott CJ (2018) Terrestrial Precipitation: 1900-2017 Gridded Monthly Time Series. Arch. (Version 5.01)

Matusick G, Ruthrof KX, Kala J, et al (2018) Chronic historical drought legacy exacerbates tree mortality and crown dieback during acute heatwave-compounded drought. Environ Res Lett 13:. https://doi.org/10.1088/1748-9326/aad8cb

McDowell N, Pockman WT, Allen CD, et al (2008) Mechanisms of plant survival and mortality during drought: Why do some plants survive while others succumb to drought? New Phytol 178:719–739. https://doi.org/10.1111/j.1469-8137.2008.02436.x

Meinzer FC, McCulloh KA (2013) Xylem recovery from drought-induced embolism: Where is the hydraulic point of no return? Tree Physiol 33:331–334. https://doi.org/10.1093/treephys/tpt022

Montwé D, Isaac-Renton M, Hamann A, Spiecker H (2016) Drought tolerance and growth in

populations of a wide-ranging tree species indicate climate change risks for the boreal north. Glob Chang Biol 22:806–815. https://doi.org/10.1111/gcb.13123

Nardini A, Battistuzzo M, Savi T (2013) Shoot desiccation and hydraulic failure in temperate woody angiosperms during an extreme summer drought. New Phytol 200:322–329. https://doi.org/10.1111/nph.12288

Nardini A, Casolo V, Dal Borgo A, et al (2016) Rooting depth, water relations and non-structural carbohydrate dynamics in three woody angiosperms differentially affected by an extreme summer drought. Plant Cell Environ 39:618–627. https://doi.org/10.1111/pce.12646

Oggioni S, Rossi L, Avanzi C, et al (2024) Drought responses of Italian silver fir provenances in a climate change perspective. Dendrochronologia 85:126184. https://doi.org/10.1016/j.dendro.2024.126184

Paz-Kagan T, Brodrick PG, Vaughn NR, et al (2017) What mediates tree mortality during drought in the southern Sierra Nevada. Ecol Appl 27:2443–2457. https://doi.org/10.1002/eap.1620

Peters JMR, López R, Nolf M, et al (2021) Living on the edge: A continental-scale assessment of forest vulnerability to drought. Glob Chang Biol 27:3620–3641. https://doi.org/10.1111/gcb.15641

Prats KA, Fanton AC, Brodersen CR, Furze ME (2023) Starch depletion in the xylem and phloem ray parenchyma of grapevine stems under drought. AoB Plants 15:1–12. https://doi.org/10.1093/aobpla/plad062

R Core Team (2024) R: A language and environment for statistical computing. Vienna, Austria

Ronco Jr. FP (1990) *Pinus edulis* Engelm. Pinyon. In: Burns RM, Honkala BH (eds) Silvics of North America Volume 1. Conifers. United States Department of Agriculture, Washington, D.C., pp 327–337

Schwarz J, Skiadaresis G, Kohler M, et al (2020) Quantifying growth responses of trees to drought—a critique of commonly used resilience indices and recommendations for future studies. Curr For Reports 6:185–200. https://doi.org/10.1007/s40725-020-00119-2

Senf C, Buras A, Zang CS, et al (2020) Excess forest mortality is consistently linked to drought across Europe. Nat Commun 11:1–8. https://doi.org/10.1038/s41467-020-19924-1

Silvestro R, Mura C, Alano Bonacini D, et al (2023) Local adaptation shapes functional traits

and resource allocation in black spruce. Sci Rep 13:1–11. https://doi.org/10.1038/s41598-023-48530-6

Sniderhan AE, McNickle GG, Baltzer JL (2018) Assessing local adaptation vs. plasticity under different resource conditions in seedlings of a dominant boreal tree species. AoB Plants 10:1–13. https://doi.org/10.1093/aobpla/ply004

Sohn JA, Hartig F, Kohler M, et al (2016a) Heavy and frequent thinning promotes drought adaptation in Pinus sylvestris forests. Ecol Appl 26:2190–2205. https://doi.org/10.1002/eap.1373

Sohn JA, Saha S, Bauhus J (2016b) Potential of forest thinning to mitigate drought stress: A meta-analysis. For Ecol Manage 380:261–273. https://doi.org/10.1016/j.foreco.2016.07.046

Struyf A, Hubert M, Rousseeuw PJ (1997) Clustering in an object-oriented environment. J Stat Softw 1:1–30

Trugman AT, Anderegg LDL, Anderegg WRL, et al (2021) Why is tree drought mortality so hard to predict? Trends Ecol Evol 36:520–532. https://doi.org/10.1016/j.tree.2021.02.001

Vizcaíno-Palomar N, González-Muñoz N, González-Martínez SC, et al (2019) Most southern scots pine populations are locally adapted to drought for tree height growth. Forests 10:. https://doi.org/10.3390/f10070555

Wagner Y, Volkov M, Nadal-Sala D, et al (2023) Relationships between xylem embolism and tree functioning during drought, recovery, and recurring drought in Aleppo pine. Physiol Plant 175:1–11. https://doi.org/10.1111/ppl.13995

Zald HSJ, Callahan CC, Hurteau MD, et al (2022) Tree growth responses to extreme drought after mechanical thinning and prescribed fire in a Sierra Nevada mixed-conifer forest, USA. For Ecol Manage 510:120107. https://doi.org/10.1016/j.foreco.2022.120107

Ziaco E, Truettner C, Biondi F, Bullock S (2018) Moisture-driven xylogenesis in *Pinus ponderosa* from a Mojave Desert mountain reveals high phenological plasticity. Plant Cell Environ 41:823–836. https://doi.org/10.1111/pce.13152

Chapter 6. Thesis conclusion

This thesis set out to explore how tree species and populations respond to drought by drawing on long-term growth records, satellite observations, and climate data. The analyses presented here do not claim to resolve all challenges in understanding forest vulnerability but offer a contribution toward improving the consistency and ecological relevance of comparative assessments at larger spatial scales.

One of the first goals of this work was to make existing datasets more accessible and analytically robust. Revisiting foundational data sources such as the International Tree-Ring Data Bank helped identify and address recurring issues that often complicate their reuse in large-scale studies. Likewise, comparisons among commonly used climate products, evaluated against independent growth responses, highlighted the importance of selecting appropriate environmental inputs for ecological inference. While these steps are incremental, they help lay a stronger foundation for future research that relies on compiled or repurposed datasets.

A central theme of the thesis is the value of standardized drought response metrics that account for the environmental conditions under which each tree population has developed. Rather than applying fixed thresholds across all sites, this approach emphasizes relative change—measuring recovery against a population's typical growth patterns and climate background. Doing so can help account for the effects of exposure and distinguish them from intrinsic sensitivity. The approach may allow for more meaningful comparisons among species, regions, or ecological settings. The findings suggest that populations exposed to more frequent or intense droughts in the past often display greater recovery capacity, consistent with the idea that local adaptation or acclimation plays a role in shaping drought responses.

The methods developed and applied here are intended as tools rather than prescriptions. In practical terms, they may assist in identifying populations with greater or lesser resilience, which in turn could inform decisions around reforestation, assisted migration, or other adaptation strategies. Integrating tree-ring data with remote sensing further extends the reach of these analyses, making it possible to explore climate–growth relationships in areas with limited field data. While the agreement between data sources is not perfect, the general correspondence

suggests that combining different lines of evidence may offer a more comprehensive view of forest vulnerability.

It is important to recognize that no single metric, such as the proposed resilience-based drought index, can capture the complexity of forest adaptation needs or serve as a stand-alone guide for management decisions. Drought-resilient populations may not perform as well in other dimensions, such as productivity or pest resistance, and moving genotypes outside their historical range always involves some uncertainty. Therefore, any decisions based on drought vulnerability assessments should be weighed alongside other ecological, silvicultural, and operational considerations.

In summary, this thesis offers a set of approaches aimed at improving how forest vulnerability to drought can be assessed across broad spatial scales. The findings reflect both the complexity and variability of drought responses and suggest that careful standardization and ecological framing can improve the interpretability of large-scale analyses. While the work here represents only one step in an ongoing effort to understand and manage forests under climate change, it highlights ways in which existing data and tools might be used more effectively to inform adaptive strategies.

Bibliography

Abrams MD (1990) Adaptations and responses to drought in Quercus species of North America . Tree Physiol 7:227–238. https://doi.org/10.1093/treephys/7.1-2-3-4.227

Aitken SN, Whitlock MC (2013) Assisted gene flow to facilitate local adaptation to climate change. Annu Rev Ecol Evol Syst 44:367–388. https://doi.org/10.1146/annurev-ecolsys-110512-135747

Aitken SN, Yeaman S, Holliday JA, et al (2008) Adaptation, migration or extirpation: climate change outcomes for tree populations. Evol Appl 1:95–111. https://doi.org/10.1111/j.1752-4571.2007.00013.x

Anderegg WRL, Klein T, Bartlett M, et al (2016) Meta-analysis reveals that hydraulic traits explain cross-species patterns of drought-induced tree mortality across the globe. Proc Natl Acad Sci U S A 113:5024–5029. https://doi.org/10.1073/pnas.1525678113

Anderegg WRL, Meinzer FC (2015) Wood anatomy and plant hydraulics in a changing climate. In: Hacke UG (ed) Functional and Ecological Xylem Anatomy. Springer International Publishing, Cham, pp 235–253

Anderegg WRL, Plavcová L, Anderegg LDL, et al (2013) Drought's legacy: Multiyear hydraulic deterioration underlies widespread aspen forest die-off and portends increased future risk. Glob Chang Biol 19:1188–1196. https://doi.org/10.1111/gcb.12100

Anderegg WRL, Schwalm C, Biondi F, et al (2015) Pervasive drought legacies in forest ecosystems and their implications for carbon cycle models. Science (80-) 349:528–532. https://doi.org/10.1126/science.aab1833

Augustine DJ (2010) Spatial versus temporal variation in precipitation in a semiarid ecosystem. Landsc Ecol 25:913–925. https://doi.org/10.1007/S10980-010-9469-Y/FIGURES/6

Babst F, Poulter B, Trouet V, et al (2013) Site- and species-specific responses of forest growth to climate across the European continent. Glob Ecol Biogeogr 22:706–717. https://doi.org/10.1111/GEB.12023

Bachofen C, Tumber-Dávila SJ, Mackay DS, et al (2024) Tree water uptake patterns across the globe. New Phytol 242:1891–1910. https://doi.org/10.1111/nph.19762

Beck HE, Wood EF, Pan M, et al (2019) MSWep v2 Global 3-hourly 0.1° precipitation:

Methodology and quantitative assessment. Bull Am Meteorol Soc 100:473–500. https://doi.org/10.1175/BAMS-D-17-0138.1

Beguería S, Vicente-Serrano SM (2023) SPEI: Calculation of the Standardized Precipitation-Evapotranspiration Index

Blumstein M, Gersony J, Martínez-Vilalta J, Sala A (2023) Global variation in nonstructural carbohydrate stores in response to climate. Glob Chang Biol 29:1854–1869. https://doi.org/10.1111/gcb.16573

Bond-Lamberty B, Rocha A V., Calvin K, et al (2014) Disturbance legacies and climate jointly drive tree growth and mortality in an intensively studied boreal forest. Glob Chang Biol 20:216–227. https://doi.org/10.1111/gcb.12404

Bose AK, Scherrer D, Camarero JJ, et al (2021) Climate sensitivity and drought seasonality determine post-drought growth recovery of *Quercus petraea* and *Quercus robur* in Europe. Sci Total Environ 784:147222. https://doi.org/10.1016/j.scitotenv.2021.147222

Bower AD, Frerker KL, Pike CC, et al (2024) A practical framework for applied forestry assisted migration. Front For Glob Chang 7:1–16. https://doi.org/10.3389/ffgc.2024.1454329

Brandes AF das N, Sánchez-Tapia A, Sansevero JBB, et al (2019) Fire records in tree rings of moquiniastrum polymorphum: Potential for reconstructing fire history in the Brazilian atlantic forest. Acta Bot Brasilica 33:61–66. https://doi.org/10.1590/0102-33062018abb0282

Brehaut L, Danby RK (2018) Inconsistent relationships between annual tree ring-widths and satellite-measured NDVI in a mountainous subarctic environment. Ecol Indic 91:698–711. https://doi.org/10.1016/j.ecolind.2018.04.052

Brienen RJW, Caldwell L, Duchesne L, et al (2020a) Forest carbon sink neutralized by pervasive growth-lifespan trade-offs. Nat Commun 11:1–10. https://doi.org/10.1038/s41467-020-17966-z

Brienen RJW, Caldwell L, Duchesne L, et al (2020b) Forest carbon sink neutralized by pervasive growth-lifespan trade-offs. Nat Commun 11:1–10. https://doi.org/10.1038/s41467-020-17966-z

Brockwell PJ, Davis RA (1991) Multivariate time series. In: Time series: theory and methods. Springer, New York, NY, pp 401–462

Brown SR, Baysinger A, Brown PM, et al (2020) Fire history across forest types in the Southern

Beartooth Mountains, Wyoming. Tree-Ring Res 76:27. https://doi.org/10.3959/TRR2018-11

Bunn A, Korpela M, Biondi F, et al (2022) dplR: Dendrochronology program library in R

Bunn AG (2010) Statistical and visual crossdating in R using the dplR library. Dendrochronologia 28:251–258. https://doi.org/10.1016/j.dendro.2009.12.001

Bunn AG (2008) A dendrochronology program library in R (dplR). Dendrochronologia 26:115–124. https://doi.org/10.1016/j.dendro.2008.01.002

Büntgen U, Allen K, Anchukaitis KJ, et al (2021) The influence of decision-making in tree ring-based climate reconstructions. Nat Commun 12:. https://doi.org/10.1038/s41467-021-23627-6

Buras A (2017) A comment on the expressed population signal. Dendrochronologia 44:130–132. https://doi.org/10.1016/j.dendro.2017.03.005

Burns RM, Honkala BH (eds) (1990a) Silvics of North America: 2. Hardwoods. U.S. Department of Agriculture, Forest Service, Washington, DC

Burns RM, Honkala BH (eds) (1990b) Silvics of North America: 1. Conifers. U.S. Department of Agriculture, Forest Service, Washington, DC

Carlquist S (2012) How wood evolves: a new synthesis. Botany 90:901–940. https://doi.org/10.1139/b2012-048

Castellanos-Acuña D, Hamann A (2020) A cross-checked global monthly weather station database for precipitation covering the period 1901 to 2010. Geosci Data J in press:1–11. https://doi.org/10.1002/gdj3.88

Cavin L, Mountford EP, Peterken GF, Jump AS (2013) Extreme drought alters competitive dominance within and between tree species in a mixed forest stand. Funct Ecol 27:1424–1435. https://doi.org/10.1111/1365-2435.12126

Cayuela L, Macarro I, Stein A, Oksanen J (2021) Taxonstand: taxonomic standardization of plant species names

Charney ND, Babst F, Poulter B, et al (2016) Observed forest sensitivity to climate implies large changes in 21st century North American forest growth. Ecol Lett 19:1119–1128. https://doi.org/10.1111/ele.12650

Choat B, Brodribb TJ, Brodersen CR, et al (2018) Triggers of tree mortality under drought. Nature 558:531–539. https://doi.org/10.1038/s41586-018-0240-x

Choat B, Jansen S, Brodribb TJ, et al (2012) Global convergence in the vulnerability of forests to drought. Nature 491:752–755. https://doi.org/10.1038/nature11688

Ciais P, Reichstein M, Viovy N, et al (2005) Europe-wide reduction in primary productivity caused by the heat and drought in 2003. Nature 437:529–533. https://doi.org/10.1038/nature03972

Clark JS, Iverson L, Woodall CW, et al (2016) The impacts of increasing drought on forest dynamics, structure, and biodiversity in the United States. Glob Chang Biol 22:2329–2352. https://doi.org/10.1111/gcb.13160

Cook BI, Cook ER, Smerdon JE, et al (2016) North American megadroughts in the Common Era: Reconstructions and simulations. Wiley Interdiscip Rev Clim Chang 7:411–432. https://doi.org/10.1002/wcc.394

Cook ER, Briffa KR, Meko DM, et al (1995) The 'segment length curse' in long tree-ring chronology development for palaeoclimatic studies. The Holocene 5:229–237

Cook ER, Kairiukstis LA (1990) Methods of Dendrochronology: Applications in the environmental sciences. Springer-Science+Business Media, B. V., Dordrecht, Holland

Cook ER, Seager R, Cane MA, Stahle DW (2007) North American drought: Reconstructions, causes, and consequences. Earth-Science Rev 81:93–134. https://doi.org/10.1016/j.earscirev.2006.12.002

Cook ER, Seager R, Kushnir Y, et al (2015) Old World megadroughts and pluvials during the Common Era. Sci Adv 1:1–10. https://doi.org/10.1126/sciadv.1500561

Cook ER, Solomina O, Matskovsky V, et al (2020) The European Russia Drought Atlas (1400–2016 CE). Clim Dyn 54:2317–2335. https://doi.org/10.1007/s00382-019-05115-2

Correa-Díaz A, Romero-Sánchez ME, Villanueva-Díaz J (2021) The greening effect characterized by the Normalized Difference Vegetation Index was not coupled with phenological trends and tree growth rates in eight protected mountains of central Mexico. For Ecol Manage 496:. https://doi.org/10.1016/j.foreco.2021.119402

Correa-Díaz A, Silva LCR, Horwath WR, et al (2019) Linking remote sensing and dendrochronology to quantify climate-induced shifts in high-elevation forests over space and time. J Geophys Res Biogeosciences 124:166–183. https://doi.org/10.1029/2018JG004687

Correa-Díaz A, Silva LCR, Horwath WR, et al (2020) From trees to ecosystems: spatiotemporal

scaling of climatic impacts on montane landscapes using sendrochronological, isotopic, and remotely sensed data. Global Biogeochem Cycles 34:1–20. https://doi.org/10.1029/2019GB006325

Coulthard BL, St. George S, Meko DM (2020) The limits of freely-available tree-ring chronologies. Quat Sci Rev 234:106264. https://doi.org/10.1016/j.quascirev.2020.106264

Crausbay SD, Ramirez AR, Carter SL, et al (2017) Defining ecological drought for the twenty-first century. Bull Am Meteorol Soc 98:2543–2550. https://doi.org/10.1175/BAMS-D-16-0292.1

Cui W, Dong X, Xi B, Kennedy A (2017) Evaluation of reanalyzed precipitation variability and trends using the gridded gauge-based analysis over the CONUS. J Hydrometeorol 18:2227–2248. https://doi.org/10.1175/JHM-D-17-0029.1

D'Orangeville L, Itter MS, Dos Santos JM, Taylor AR (2025) Can tree-rings inform assisted migration? Revisiting provenance trials across Atlantic Canada to compare local adaptation between red spruce populations. For Ecol Manage 578:122482. https://doi.org/10.1016/j.foreco.2024.122482

Das AJ, Battles JJ, Stephenson NL, Van Mantgem PJ (2007) The relationship between tree growth patterns and likelihood of mortality: A study of two tree species in the Sierra Nevada. Can J For Res 37:580–597. https://doi.org/10.1139/X06-262

Das AJ, Slaton MR, Mallory J, et al (2022) Empirically validated drought vulnerability mapping in the mixed conifer forests of the <scp>Sierra Nevada</scp>. Ecol Appl 32:. https://doi.org/10.1002/eap.2514

David Robinson (2020) fuzzyjoin: Join Tables Together on Inexact Matching

DeSoto L, Cailleret M, Sterck F, et al (2020a) Low growth resilience to drought is related to future mortality risk in trees. Nat Commun 11:1–9. https://doi.org/10.1038/s41467-020-14300-5

DeSoto L, Cailleret M, Sterck F, et al (2020b) Low growth resilience to drought is related to future mortality risk in trees. Nat Commun 11:545. https://doi.org/10.1038/s41467-020-14300-5

DiMiceli C, Carroll M, Sohlberg R, et al (2015) MOD44B MODIS/Terra Vegetation Continuous Fields Yearly L3 Global 250m SIN Grid V006 [Data set]. In: NASA EOSDIS L. Process. DAAC. https://lpdaac.usgs.gov/products/mod44bv006/. Accessed 12 Oct 2022

Dinku T, Connor SJ, Ceccato P, Ropelewski CF (2008) Comparison of global gridded precipitation products over a mountainous region of Africa. Int J Climatol 28:1627–1638. https://doi.org/10.1002/JOC.1669

Dong C, Wang X, Ran Y, Nawaz Z (2022) Heatwaves significantly slow the vegetation growth rate on the Tibetan Plateau. Remote Sens 14:1–17. https://doi.org/10.3390/rs14102402

Dorman M, Svoray T, Perevolotsky A, et al (2015) What determines tree mortality in dry environments? A multi-perspective approach. Ecol Appl 25:1054–1071. https://doi.org/10.1890/14-0698.1

Eliades F, Sarris D, Bachofer F, et al (2024) Understanding tree mortality patterns: a comprehensive review of temote sensing and ground-based studies

Erasmi S, Klinge M, Dulamsuren C, et al (2021) Modelling the productivity of Siberian larch forests from Landsat NDVI time series in fragmented forest stands of the Mongolian forest-steppe. Environ Monit Assess 193:1–18. https://doi.org/10.1007/s10661-021-08996-1

ESRI (2011) ArcGIS Desktop: Release 10

ESRI (2022) ArcGIS Pro

Folland CK, Karl TR, Christy JR, et al (2001) Observed climate variability and change. In: T HJ, Ding Y, Griggs DJ, et al. (eds) Climate Change 2001: the scientific basis. Contribution of working group I to the third assessment report of the Intergovernmental panel on climate change. Cambridge University Press, Cambridge, United Kingdom and New York, NY, USA, p 881

Fontana C, Reis-Avila G, Nabais C, et al (2018) Dendrochronology and climate in the Brazilian atlantic forest: Which species, where and how. Neotrop Biol Conserv 13:321–333. https://doi.org/10.4013/nbc.2018.134.06

Friedl M, Gray J, Sulla-Menashe D (2019) MCD12Q2 MODIS/Terra+Aqua Land Cover Dynamics Yearly L3 Global 500m SIN Grid V006 [Data set]. In: NASA EOSDIS L. Process. DAAC. https://lpdaac.usgs.gov/products/mcd12q2v006/. Accessed 13 Oct 2022

Friedman JH (1984) A Variable Span Smoother

Fung KF, Chew KS, Huang YF, et al (2022) Evaluation of spatial interpolation methods and spatiotemporal modeling of rainfall distribution in Peninsular Malaysia. Ain Shams Eng J 13:101571. https://doi.org/10.1016/j.asej.2021.09.001

Galiano L, Martínez-Vilalta J, Lloret F (2010) Drought-induced multifactor decline of Scots Pine

in the Pyrenees and potential vegetation change by the expansion of co-occurring Oak species. Ecosystems 13:978–991. https://doi.org/10.1007/s10021-010-9368-8

García-Suárez AM, Butler CJ, Baillie MGL (2009) Climate signal in tree-ring chronologies in a temperate climate: A multi-species approach. Dendrochronologia 27:183–198. https://doi.org/10.1016/j.dendro.2009.05.003

Garg PK, Shukla A, Yousuf B, Garg S (2022) Temperature and precipitation changes over the glaciated parts of Indian Himalayan Region during 1901–2016. Environ Monit Assess 194:1–27. https://doi.org/10.1007/S10661-021-09689-5/TABLES/8

Gavin DG, Gunning C, Veblen TT (2007) Drought induces lagged tree mortality in a subalpine forest in the Rocky Mountains. Oikos 116:1983–1994

Gazol A, Camarero JJ, Vicente-Serrano SM, et al (2018) Forest resilience to drought varies across biomes. Glob Chang Biol 24:2143–2158. https://doi.org/10.1111/gcb.14082

Golian S, Javadian M, Behrangi A (2019) On the use of satellite, gauge, and reanalysis precipitation products for drought studies. Environ Res Lett 14:075005. https://doi.org/10.1088/1748-9326/AB2203

Grant GE, Tague CL, Allen CD (2013) Watering the forest for the trees: an emerging priority for managing water in forest landscapes. Front Ecol Environ 11:314–321. https://doi.org/10.1890/120209

Greenwood S, Ruiz-Benito P, Martínez-Vilalta J, et al (2017) Tree mortality across biomes is promoted by drought intensity, lower wood density and higher specific leaf area. Ecol Lett 20:539–553. https://doi.org/10.1111/ele.12748

Grissino-Mayer HD, Fritts HC (1997) The International Tree-Ring Data Bank: an enhanced global database serving the global scientific community. The Holocene 7:235–238. https://doi.org/10.1177/095968369700700212

Guerrieri R, Siegwolf R, Saurer M, et al (2010) Anthropogenic NOx emissions alter the intrinsic water-use efficiency (WUEi) for *Quercus cerris* stands under Mediterranean climate conditions. Environ Pollut 158:2841–2847. https://doi.org/10.1016/J.ENVPOL.2010.06.017

Gutierrez Lopez J, Tor-ngern P, Oren R, et al (2021) How tree species, tree size, and topographical location influenced tree transpiration in northern boreal forests during the historic 2018 drought. Glob Chang Biol 27:3066–3078. https://doi.org/10.1111/gcb.15601

Hammond WM, Williams AP, Abatzoglou JT, et al (2022) Global field observations of tree die-

off reveal hotter-drought fingerprint for Earth's forests. Nat Commun 13:. https://doi.org/10.1038/s41467-022-29289-2

Hampe A, Petit RJ (2005) Conserving biodiversity under climate change: The rear edge matters. Ecol Lett 8:461–467. https://doi.org/10.1111/j.1461-0248.2005.00739.x

Harris I, Osborn TJ, Jones P, Lister D (2020) Version 4 of the CRU TS monthly high-resolution gridded multivariate climate dataset. Sci Data 7:109. https://doi.org/10.1038/s41597-020-0453-3

Hartmann H, Ziegler W, Trumbore S (2013) Lethal drought leads to reduction in nonstructural carbohydrates in Norway spruce tree roots but not in the canopy. Funct Ecol 27:413–427. https://doi.org/10.1111/1365-2435.12046

Herrera D, Ault T (2017) Insights from a new high-resolution drought atlas for the Caribbean spanning 1950–2016. J Clim 30:7801–7825. https://doi.org/10.1175/JCLI-D-16-0838.1

Herweijer C, Seager R, Cook ER, Emile-Greay J (2007) North American droughts of the last millennium from a gridded network of tree-ring data. J Clim 20:1353–1376. https://doi.org/10.1175/JCLI4042.1

Hesse BD, Gebhardt T, Hafner BD, et al (2023) Physiological recovery of tree water relations upon drought release—response of mature beech and spruce after five years of recurrent summer drought. Tree Physiol 43:522–538. https://doi.org/10.1093/treephys/tpac135

Hevia A, Sánchez-Salguero R, Camarero JJ, et al (2019) Long-term nutrient imbalances linked to drought-triggered forest dieback. Sci Total Environ 690:1254–1267. https://doi.org/10.1016/J.SCITOTENV.2019.06.515

Hijmans RJ (2021) geosphere: Spherical Trigonometry

Hoffmann AA, Sgró CM (2011) Climate change and evolutionary adaptation. Nature 470:479–485. https://doi.org/10.1038/nature09670

Hogg EH, Brandt JP, Kochtubajda B (2005) Factors affecting interannual variation in growth of western Canadian aspen forests during 1951-2000. Can J For Res 35:610–622. https://doi.org/10.1139/x04-211

Huang M, Wang X, Keenan TF, Piao S (2018) Drought timing influences the legacy of tree growth recovery. Glob Chang Biol 24:3546–3559. https://doi.org/10.1111/gcb.14294

Huang S, Tang L, Hupy JP, et al (2021) A commentary review on the use of normalized difference vegetation index (NDVI) in the era of popular remote sensing. J For Res 32:1–6.

https://doi.org/10.1007/S11676-020-01155-1/FIGURES/2

Isaac-Renton M, Montwé D, Hamann A, et al (2018) Northern forest tree populations are physiologically maladapted to drought. Nat Commun 9:1–9. https://doi.org/10.1038/s41467-018-07701-0

Jaafar HH, Ahmad FA (2015) Crop yield prediction from remotely sensed vegetation indices and primary productivity in arid and semi-arid lands. http://dx.doi.org/101080/0143116120151084434 36:4570–4589. https://doi.org/10.1080/01431161.2015.1084434

Kang W, Liu S, Chen X, et al (2022) Evaluation of ecosystem stability against climate changes via satellite data in the eastern sandy area of northern China. J Environ Manage 308:114596. https://doi.org/10.1016/j.jenvman.2022.114596

Kannenberg SA, Novick KA, Alexander MR, et al (2019) Linking drought legacy effects across scales: From leaves to tree rings to ecosystems. Glob Chang Biol 25:2978–2992. https://doi.org/10.1111/GCB.14710

Karger DN, Wilson AM, Mahony C, et al (2021) Global daily 1 km land surface precipitation based on cloud cover-informed downscaling. Sci Data 8:. https://doi.org/10.1038/S41597-021-01084-6

Kassambara A, Mundt F (2020) factoextra: extract and visualize the results of multivariate data analyses

Kharuk VI, Ranson KJ, Oskorbin PA, et al (2013) Climate induced birch mortality in Trans-Baikal lake region, Siberia. For Ecol Manage 289:385–392. https://doi.org/10.1016/j.foreco.2012.10.024

Klockow PA, Vogel JG, Edgar CB, Moore GW (2018) Lagged mortality among tree species four years after an exceptional drought in east Texas. Ecosphere 9:. https://doi.org/10.1002/ecs2.2455

Kluver D, Mote T, Leathers D, et al (2016) Creation and validation of a comprehensive 1° by 1° daily gridded North American dataset for 1900–2009: snowfall. J Atmos Ocean Technol 33:857–871. https://doi.org/10.1175/JTECH-D-15-0027.1

Knutzen F, Averbeck P, Barrasso C, et al (2023) Impacts and damages of the European multi-year drought and heat event 2018 - 2022 on forests, a review. Egusph Prepr 1–56

Kono Y, Ishida A, Saiki S-T, et al (2019) Initial hydraulic failure followed by late-stage carbon

starvation leads to drought-induced death in the tree *Trema orientalis*. Commun Biol 2:8. https://doi.org/10.1038/s42003-018-0256-7

Krusic PJ, Cook ER, Dukpa D, et al (2015) Six hundred thirty-eight years of summer temperature variability over the Bhutanese Himalaya. Geophys Res Lett 42:2988–2994. https://doi.org/10.1002/2015GL063566

Leuschner C, Fuchs S, Wedde P, et al (2024) A multi-criteria drought resistance assessment of temperate Acer, Carpinus, Fraxinus, Quercus, and Tilia species. Perspect Plant Ecol Evol Syst 62:125777. https://doi.org/10.1016/j.ppees.2023.125777

Li X, Piao S, Wang K, et al (2020) Temporal trade-off between gymnosperm resistance and resilience increases forest sensitivity to extreme drought. Nat Ecol Evol 4:1075–1083. https://doi.org/10.1038/s41559-020-1217-3

Liu X, Cheng Z, Yan L, Yin ZY (2009) Elevation dependency of recent and future minimum surface air temperature trends in the Tibetan Plateau and its surroundings. Glob Planet Change 68:164–174. https://doi.org/10.1016/J.GLOPLACHA.2009.03.017

Lloret F, Keeling EG, Sala A (2011) Components of tree resilience: Effects of successive low-growth episodes in old ponderosa pine forests. Oikos 120:1909–1920. https://doi.org/10.1111/j.1600-0706.2011.19372.x

Luo K, Wang X, de Jong M, Flannigan M (2024) Drought triggers and sustains overnight fires in North America. Nature 627:321–327. https://doi.org/10.1038/s41586-024-07028-5

Macalady AK, Bugmann H (2014) Growth-mortality relationships in piñon pine (*Pinus edulis*) during severe droughts of the past century: Shifting processes in space and time. PLoS One 9:. https://doi.org/10.1371/journal.pone.0092770

Maechler M, Rousseeuw P, Struyf A, et al (2023) cluster: Cluster Analysis Basics and Extensions

Magrin GO, Marengo JA, Boulanger J-P, et al (2014) Central and South America. In: Field CB, Barros VR, Dokken DJ, et al. (eds) Climate Change 2014: Impacts, Adaptation, and Vulnerability. Part B: Regional Aspects. Contribution of Working Group II to the Fifth Assessment Report of the Intergovernmental Panel on Climate Change. Cambridge University Press, Cambridge, United Kingdom and New York, NY, USA, pp 1499–1566

Manvailer V, Hamann A (2024) Validation of global precipitation time series products against tree ring records and remotely sensed vegetation greenness. PLoS One 19:1–13.

https://doi.org/10.1371/journal.pone.0299111

Marchi M, Castellanos-Acuña D, Hamann A, et al (2020) ClimateEU: Scale-free climate normals, historical time series, and future projections for Europe. figshare

Marini L, Økland B, Jönsson AM, et al (2017) Climate drivers of bark beetle outbreak dynamics in Norway spruce forests. Ecography (Cop) 40:1426–1435. https://doi.org/10.1111/ecog.02769

Martin J, Looker N, Hoylman Z, et al (2018) Differential use of winter precipitation by upper and lower elevation Douglas fir in the Northern Rockies. Glob Chang Biol 24:5607–5621. https://doi.org/10.1111/gcb.14435

Martinez del Castillo E, Zang CS, Buras A, et al (2022) Climate-change-driven growth decline of European beech forests. Commun Biol 5:1–9. https://doi.org/10.1038/s42003-022-03107-3

Matsuura K, Willmott CJ (2018) Terrestrial Precipitation: 1900-2017 Gridded Monthly Time Series. Arch. (Version 5.01)

Matusick G, Ruthrof KX, Kala J, et al (2018) Chronic historical drought legacy exacerbates tree mortality and crown dieback during acute heatwave-compounded drought. Environ Res Lett 13:. https://doi.org/10.1088/1748-9326/aad8cb

McDowell N, Pockman WT, Allen CD, et al (2008) Mechanisms of plant survival and mortality during drought: Why do some plants survive while others succumb to drought? New Phytol 178:719–739. https://doi.org/10.1111/j.1469-8137.2008.02436.x

Meinzer FC, McCulloh KA (2013) Xylem recovery from drought-induced embolism: Where is the hydraulic point of no return? Tree Physiol 33:331–334. https://doi.org/10.1093/treephys/tpt022

Melvin TM, Briffa KR (2008) A “signal-free” approach to dendroclimatic standardisation. Dendrochronologia 26:71–86. https://doi.org/10.1016/j.dendro.2007.12.001

Mina M, Martin-Benito D, Bugmann H, Cailleret M (2016) Forward modeling of tree-ring width improves simulation of forest growth responses to drought. Agric For Meteorol 221:13–33. https://doi.org/10.1016/j.agrformet.2016.02.005

Montwé D, Isaac-Renton M, Hamann A, Spiecker H (2016) Drought tolerance and growth in populations of a wide-ranging tree species indicate climate change risks for the boreal north. Glob Chang Biol 22:806–815. https://doi.org/10.1111/gcb.13123

Morales MS, Cook ER, Barichivich J, et al (2020) Six hundred years of South American tree rings reveal an increase in severe hydroclimatic events since mid-20th century. Proc Natl Acad Sci U S A 117:16816–16823. https://doi.org/10.1073/pnas.2002411117

Mosteller F, Tukey JW (1977) Data Analysis and Regression: a second course in statistics. Addison-Wesley

Myneni RB, Hoffman S, Knyazikhin Y, et al (2002) Global products of vegetation leaf area and fraction absorbed PAR from year one of MODIS data. Remote Sens Environ 83:214–231. https://doi.org/10.1016/S0034-4257(02)00074-3

Nardini A, Battistuzzo M, Savi T (2013) Shoot desiccation and hydraulic failure in temperate woody angiosperms during an extreme summer drought. New Phytol 200:322–329. https://doi.org/10.1111/nph.12288

Nardini A, Casolo V, Dal Borgo A, et al (2016) Rooting depth, water relations and non-structural carbohydrate dynamics in three woody angiosperms differentially affected by an extreme summer drought. Plant Cell Environ 39:618–627. https://doi.org/10.1111/pce.12646

Nehrbass-Ahles C, Babst F, Klesse S, et al (2014a) The influence of sampling design on tree-ring-based quantification of forest growth. Glob Chang Biol 20:2867–2885. https://doi.org/10.1111/GCB.12599

Nehrbass-Ahles C, Babst F, Klesse S, et al (2014b) The influence of sampling design on tree-ring-based quantification of forest growth. Glob Chang Biol 20:2867–2885. https://doi.org/10.1111/GCB.12599

New M, Lister D, Hulme M, Makin I (2002) A high-resolution data set of surface climate over global land areas. Clim Res 21:1–25. https://doi.org/10.3354/CR021001

Nguyen P, Shearer EJ, Tran H, et al (2019) The CHRS Data Portal, an easily accessible public repository for PERSIANN global satellite precipitation data. Sci Data 6:180296. https://doi.org/10.1038/sdata.2018.296

NOAA (2023) International Tree-Ring Data Bank. https://www.ncei.noaa.gov/access/paleo-search/?dataTypeId=18. Accessed 31 Mar 2023

Ogaya R, Barbeta A, Başnou C, Peñuelas J (2015) Satellite data as indicators of tree biomass growth and forest dieback in a Mediterranean holm oak forest. Ann For Sci 72:135–144. https://doi.org/10.1007/S13595-014-0408-Y/FIGURES/9

Oggioni S, Rossi L, Avanzi C, et al (2024) Drought responses of Italian silver fir provenances in

a climate change perspective. Dendrochronologia 85:126184. https://doi.org/10.1016/j.dendro.2024.126184

Olson DM, Dinerstein E, Wikramanayake ED, et al (2001) Terrestrial ecoregions of the world: a new map of life on Earth. Bioscience 51:933–938

Pasho E, Alla AQ (2015) Climate impacts on radial growth and vegetation activity of two co-existing Mediterranean pine species. Can J For Res 45:1748–1756. https://doi.org/10.1139/cjfr-2015-0146

Paz-Kagan T, Brodrick PG, Vaughn NR, et al (2017) What mediates tree mortality during drought in the southern Sierra Nevada. Ecol Appl 27:2443–2457. https://doi.org/10.1002/eap.1620

Pearl JK, Keck JR, Tintor W, et al (2020) New frontiers in tree-ring research. Holocene 30:923–941. https://doi.org/10.1177/0959683620902230

Pederson N, Hessl AE, Baatarbileg N, et al (2014) Pluvials, droughts, the Mongol Empire, and modern Mongolia. Proc Natl Acad Sci U S A 111:4375–4379. https://doi.org/10.1073/pnas.1318677111

Peters JMR, López R, Nolf M, et al (2021) Living on the edge: A continental-scale assessment of forest vulnerability to drought. Glob Chang Biol 27:3620–3641. https://doi.org/10.1111/gcb.15641

Pirtskhalava-Karpova N, Trubin A, Karpov A, Jakuš R (2024) Drought initialised bark beetle outbreak in Central Europe: Meteorological factors and infestation dynamic. For Ecol Manage 554:. https://doi.org/10.1016/j.foreco.2023.121666

Prats KA, Fanton AC, Brodersen CR, Furze ME (2023) Starch depletion in the xylem and phloem ray parenchyma of grapevine stems under drought. AoB Plants 15:1–12. https://doi.org/10.1093/aobpla/plad062

R Core Team (2021) R: A language and environment for statistical computing. Vienna, Austria

R Core Team (2022) R: A language and environment for statistical computing. Vienna, Austria

R Core Team (2024) R: A language and environment for statistical computing. Vienna, Austria

Roberts DR, Hamann A (2012) Predicting potential climate change impacts with bioclimate envelope models: A palaeoecological perspective. Glob Ecol Biogeogr 21:121–133. https://doi.org/10.1111/j.1466-8238.2011.00657.x

Ronco Jr. FP (1990) *Pinus edulis* Engelm. Pinyon. In: Burns RM, Honkala BH (eds) Silvics of

North America Volume 1. Conifers. United States Department of Agriculture, Washington, D.C., pp 327–337

Sáenz-Ceja JE, Pérez-Salicrup DR (2019) Dendrochronological reconstruction of fire history in coniferous forests in the Monarch Butterfly Biosphere Reserve, Mexico. Fire Ecol 15:. https://doi.org/10.1186/s42408-019-0034-z

Salas-Eljatib C (2021) An approach to quantify climate–productivity relationships: an example from a widespread *Nothofagus* forest. Ecol Appl 31:1–14. https://doi.org/10.1002/eap.2285

Sánchez-Salguero R, Colangelo M, Matías L, et al (2020) Shifts in growth responses to climate and exceeded drought-vulnerability thresholds characterize dieback in two Mediterranean deciduous oaks. Forests 11:. https://doi.org/10.3390/F11070714

Sang Z, Hamann A (2022) Climatic limiting factors of North American ecosystems: a remote-sensing based vulnerability analysis. Environ Res Lett 17:094011. https://doi.org/10.1088/1748-9326/AC8608

Sang Z, Sebastian-Azcona J, Hamann A, et al (2019) Adaptive limitations of white spruce populations to drought imply vulnerability to climate change in its western range. Evol Appl 12:1850–1860. https://doi.org/10.1111/eva.12845

Schneider U, Becker A, Finger P, et al (2018) GPCC full data monthly product version 2018 at 0.25°: Monthly land-surface precipitation from rain-gauges built on GTS-based and historical data. ftp://ftp.dwd.de/pub/data/gpcc/html/fulldata-monthly_v2018_doi_download.html. Accessed 1 Aug 2021

Schöngart J, Gribel R, Ferreira da Fonseca-Junior S, Haugaasen T (2015) Age and growth patterns of Brazil nut trees (*Bertholletia excelsa* Bonpl.) in Amazonia, Brazil. Biotropica 47:550–558. https://doi.org/10.1111/btp.12243

Schwarz J, Skiadaresis G, Kohler M, et al (2020) Quantifying growth responses of trees to drought—a critique of commonly used resilience indices and recommendations for future studies. Curr For Reports 6:185–200. https://doi.org/10.1007/s40725-020-00119-2

Sebastian-Azcona J, Hacke U, Hamann A (2020) Xylem anomalies as indicators of maladaptation to climate in forest trees: implications for assisted migration. Front Plant Sci 11:1–8. https://doi.org/10.3389/fpls.2020.00208

Seidl R, Thom D, Kautz M, et al (2017) Forest disturbances under climate change. Nat Clim Chang 7:395–402. https://doi.org/10.1038/nclimate3303

Senf C, Buras A, Zang CS, et al (2020) Excess forest mortality is consistently linked to drought across Europe. Nat Commun 11:1–8. https://doi.org/10.1038/s41467-020-19924-1

Serrano-Notivoli R, Tejedor E, Roberto Serrano-Notivoli C (2021) From rain to data: A review of the creation of monthly and daily station-based gridded precipitation datasets. Wiley Interdiscip Rev Water 8:e1555. https://doi.org/10.1002/WAT2.1555

Sevcikova H, Silverman B, Raftery A (2022) vote: Election Vote Counting

Shepard D (1968) A two-dimensional interpolation for irregularly-spaced data function. In: Proc 23rd Assoc Computing Machinery (ACM) Natl Conf ACM New York. New York, NY, pp 517–524

Shepard DS (1984) Computer Mapping: The SYMAP Interpolation Algorithm. In: Gaile GL, Willmott CJ (eds) Spatial Statistics and Models. Springer Netherlands, Dordrecht, pp 133–145

Shrestha UB, Gautam S, Bawa KS (2012) Widespread climate change in the Himalayas and associated changes in local ecosystems. PLoS One 7:. https://doi.org/10.1371/JOURNAL.PONE.0036741

Silvestro R, Mura C, Alano Bonacini D, et al (2023) Local adaptation shapes functional traits and resource allocation in black spruce. Sci Rep 13:1–11. https://doi.org/10.1038/s41598-023-48530-6

Simmons A, Hersbach H, Muñoz-Sabater J, et al (2021) Low frequency variability and trends in surface air temperature and humidity from ERA5 and other datasets. ECMWF Tech Memo 811:. https://doi.org/10.21957/ly5vbtbfd

Sniderhan AE, McNickle GG, Baltzer JL (2018) Assessing local adaptation vs. plasticity under different resource conditions in seedlings of a dominant boreal tree species. AoB Plants 10:1–13. https://doi.org/10.1093/aobpla/ply004

Sohn JA, Hartig F, Kohler M, et al (2016a) Heavy and frequent thinning promotes drought adaptation in Pinus sylvestris forests. Ecol Appl 26:2190–2205. https://doi.org/10.1002/eap.1373

Sohn JA, Saha S, Bauhus J (2016b) Potential of forest thinning to mitigate drought stress: A meta-analysis. For Ecol Manage 380:261–273. https://doi.org/10.1016/j.foreco.2016.07.046

Spangenberg G, Zimmermann R, Küppers M, et al (2024) Interannual radial growth response of Douglas-fir (Pseudotsuga menziesii (Mirb.) Franco) to severe droughts: an analysis along a

gradient of soil properties and rooting characteristics. Ann For Sci 81:. https://doi.org/10.1186/s13595-024-01240-z

Speer JH (2010) Fundamentals of tree-ring research. The University of Arizona Press, Tucson, Arizona

Spînu AP, Niklasson M, Zin E (2020) Mesophication in temperate Europe: A dendrochronological reconstruction of tree succession and fires in a mixed deciduous stand in Białowieża Forest. Ecol Evol 10:1029–1041. https://doi.org/10.1002/ece3.5966

St. George S, Ault TR (2014) The imprint of climate within Northern Hemisphere trees. Quat Sci Rev 89:1–4. https://doi.org/10.1016/j.quascirev.2014.01.007

Struyf A, Hubert M, Rousseeuw PJ (1997) Clustering in an object-oriented environment J Stat Softw 1:1–30

Sullivan PF, Csank AZ (2016) Contrasting sampling designs among archived datasets: implications for synthesis efforts. Tree Physiol 36:1057–1059. https://doi.org/10.1093/treephys/tpw067

Sun C, Liu Y (2016) Climate response of tree radial growth at different timescales in the Qinling mountains. PLoS One 11:e0160938. https://doi.org/10.1371/JOURNAL.PONE.0160938

Sun Q, Miao C, Duan Q, et al (2018) A review of global precipitation data sets: Data sources, estimation, and intercomparisons. Rev Geophys 56:79–107. https://doi.org/10.1002/2017RG000574

Tonelli E, Vitali A, Malandra F, et al (2023) Tree-ring and remote sensing analyses uncover the role played by elevation on European beech sensitivity to late spring frost. Sci Total Environ 857:. https://doi.org/10.1016/j.scitotenv.2022.159239

Trugman AT, Anderegg LDL, Anderegg WRL, et al (2021) Why is tree drought mortality so hard to predict? Trends Ecol Evol 36:520–532. https://doi.org/10.1016/j.tree.2021.02.001

USGS (1997) USGS 30 ARC-second Global Elevation Data, GTOPO30. Research Data Archive at the National Center for Atmospheric Research, Computational and Information Systems Laboratory

Vasconcellos TJ de, Tomazello-Filho M, Callado CH (2019) Dendrochronology and dendroclimatology of *Ceiba speciosa* (A. St.-Hil.) Ravenna (Malvaceae) exposed to urban pollution in Rio de Janeiro city, Brazil. Dendrochronologia 53:104–113. https://doi.org/10.1016/j.dendro.2018.12.004

Vicente-Serrano SM, Gouveia C, Camarero JJ, et al (2013) Response of vegetation to drought time-scales across global land biomes. Proc Natl Acad Sci U S A 110:52–57. https://doi.org/10.1073/pnas.1207068110

Villalba R, Veblen TT (1998) Influences of large-scale climatic variability on episodic tree mortality in northern Patagonia. Ecology 79:2624–2640. https://doi.org/10.1890/0012-9658(1998)079[2624:IOLSCV]2.0.CO;2

Vizcaíno-Palomar N, González-Muñoz N, González-Martínez SC, et al (2019) Most southern scots pine populations are locally adapted to drought for tree height growth. Forests 10:. https://doi.org/10.3390/f10070555

von Keyserlingk J, de Hoop M, Mayor AG, et al (2021) Resilience of vegetation to drought: Studying the effect of grazing in a Mediterranean rangeland using satellite time series. Remote Sens Environ 255:112270. https://doi.org/10.1016/j.rse.2020.112270

Wagner Y, Volkov M, Nadal-Sala D, et al (2023) Relationships between xylem embolism and tree functioning during drought, recovery, and recurring drought in Aleppo pine. Physiol Plant 175:1–11. https://doi.org/10.1111/ppl.13995

Wang S, Jia L, Cai L, et al (2022) Assessment of grassland degradation on the Tibetan Plateau based on multi-source data. Remote Sens 14:. https://doi.org/10.3390/rs14236011

Wang T, Hamann A, Spittlehouse D, Carroll C (2016) Locally downscaled and spatially customizable climate data for historical and future periods for North America. PLoS One 11:. https://doi.org/10.1371/journal.pone.0156720

Wickham H (2016) ggplot2: Elegant graphics for data analysis. Springer-Verlag New York

Wigley TML, Briffa KR, Jones PD (1984) On the average value of correlated time series, with applications in dendroclimatology and hydrometeorology. Am Meteorol Soc 201–213

Williams AP, Allen CD, Macalady AK, et al (2013) Temperature as a potent driver of regional forest drought stress and tree mortality. Nat Clim Chang 3:292–297. https://doi.org/10.1038/nclimate1693

Willmott CJ, Rowe CM, Philpot WD (1985) Small-scale climate maps: A sensitivity analysis of some common assumptions associated with grid-point interpolation and contouring. Am Cartogr 12:5–16. https://doi.org/10.1559/152304085783914686

WMO (2021) State of the climate in Latin America and the Caribbean. World Meteorological Organization (WMO), Geneva 2, Switzerland

Xiong Q, Xiao Y, Liang P, et al (2021) Trends in climate change and human interventions indicate grassland productivity on the Qinghai–Tibetan Plateau from 1980 to 2015. Ecol Indic 129:108010. https://doi.org/10.1016/j.ecolind.2021.108010

Xu K, Wang X, Liang P, et al (2017) Tree-ring widths are good proxies of annual variation in forest productivity in temperate forests. Sci Rep 7:1–8. https://doi.org/10.1038/s41598-017-02022-6

Xu X, Zhang X, Li X (2023) Evaluation of the applicability of three methods for climatic spatial interpolation in the Hengduan mountains region. J Hydrometeorol 24:35–51. https://doi.org/10.1175/JHM-D-22-0039.1

Xue J, Su B (2017) Significant remote sensing vegetation indices: A review of developments and applications. J Sensors 2017:. https://doi.org/10.1155/2017/1353691

Zald HSJ, Callahan CC, Hurteau MD, et al (2022) Tree growth responses to extreme drought after mechanical thinning and prescribed fire in a Sierra Nevada mixed-conifer forest, USA. For Ecol Manage 510:120107. https://doi.org/10.1016/j.foreco.2022.120107

Zandler H, Haag I, Samimi C (2019) Evaluation needs and temporal performance differences of gridded precipitation products in peripheral mountain regions. Sci Reports 2019 91 9:1–15. https://doi.org/10.1038/s41598-019-51666-z

Zhao S, Pederson N, Orangeville LD, et al (2018) The International Tree-Ring Data Bank (ITRDB) revisited: Data availability and global ecological representativity. J Biogeogr 46:355–368. https://doi.org/https://doi.org/10.1111/jbi.13488

Ziaco E, Truettner C, Biondi F, Bullock S (2018) Moisture-driven xylogenesis in Pinus ponderosa from a Mojave Desert mountain reveals high phenological plasticity. Plant Cell Environ 41:823–836. https://doi.org/10.1111/pce.13152

(2013) The Plant List. Version 1.1.

Appendix 1. Code for bulk import of ITRDB meta data, available from NOAA https://www1.ncdc.noaa.gov/pub/data/metadata/published/paleo/json/. Download these files to a local folder and then execute the code below for the R programming environment. Note that you have to specify the local subdirectory on page 2 below.

```
library(tidyverse)
library(rjson)
library(plyr)

# Creating blank data frame with variables of interest
meta_ITRDB_json <- tibble(fileUrl= character(),
                          urlDescription= character(),
                          linkText= character(),
                          xmlId= character(),
                          NOAAStudyId= character(),
                          studyName= character(),
                          doi= character(),
                          investigators= character(),
                          studyNotes= character(),
                          onlineResourceLink= character(),
                          studyCode= character(),
                          contributionDate= character(),
                          entryId= character(),
                          NOAASiteId= character(),
                          siteName= character(),
                          locationName= character(),
                          lat= character(),
                          long= character(),
                          minElevationMeters= character(),
                          maxElevationMeters= character(),
                          earliestYearCE= character(),
                          mostRecentYearCE= character(),
                          speciesCode= character(),
                          scientificName= character(),
                          commonName= character(),
                          dataType= character(),
                          dataTableName= character(),
                          pubCitation= character(),
                          pubUrl= character())

# Create blank objects for subsetting variables of interest within the loop.
vars_a <-  c("xmlId", "NOAAStudyId", "studyName", "doi", "dataType",
"investigators", "studyNotes", "onlineResourceLink","studyCode",
"contributionDate", "entryId")
vars_b <- c("NOAASiteId", "siteName", "locationName", "coordinates",
"minElevationMeters", "maxElevationMeters")
vars_c <- c("NOAASiteId", "paleoData")
```

```
# Retrieving all tree ring metadata file names (specify your directory!).
subdirectory <- "json_files_subdirectory/"
meta_files <- list.files(subdirectory)

# Loop extracting all metadata of interesting and compiling into a dataframe.
# Each line represent a single data file stored in the ITRDB database.
# The metadata is extracted according to hierarchy structure of json files.
# The general structure is study metadata > site metadata > file metadata.
# One 'study' can contain multiple 'sites' each of which can contain multiple
'files'.
# Each part is extracted separately and them merged at the end of each loop.

for (i in meta_files){

  start <- Sys.time()
  jsonfile <- fromJSON(file = paste0(subdirectory,i))

  # Extracting general study information
  a1 <- jsonfile %>% keep(names(jsonfile) %in% vars_a)
  a2 <- do.call(cbind, a1) %>% as_tibble()

  # Site information
  b1 <- jsonfile[["site"]]
  b2 <- map(b1, flatten)
  b3 <- map(b2, function(x) {
    subset <- discard(x, names(x) == "paleoData")
    subset_flat <- flatten(subset)})
  b4 <- map(b3, function(x) keep(x, names(x) %in% vars_b))
  b5 <- map(b4, function(x) c(x, lat = x[["coordinates"]][1],
                              long = x[["coordinates"]][2]))
  b6 <- map(b5, function(x) discard(x, names(x) == "coordinates"))
  b7 <- map(b6, function(x) do.call(cbind, x) %>% as_tibble)
  b8 <- bind_rows(b7)

  # Timespan and data table ID
  c1 <- map(b1, function(x) keep(x, names(x) %in% vars_c) %>% flatten)
  c2 <- map(c1, function(x) {
    list(NOAASiteId = list(c(rep(x$NOAASiteId, sum(names(x) !=
"NOAASiteId")))),
         paleoData = transpose(keep(x, names(x) != "NOAASiteId"))) %>%
flatten
  })
  c3 <- map(c2, function(x){
    do.call(cbind,x[c("NOAASiteId", "dataTableName",
                      "earliestYearCE", "mostRecentYearCE")]) %>% as_tibble()
  })
  c4 <- map(c3, mutate_if, is.list, ~as.character(.))
  c5 <- c4 %>% bind_rows()

  # Species info
```

```
  d1 <- map(c2, function(x){
    list(NOAASiteId = x[c("NOAASiteId")],
         species = x[c("species")] %>% flatten %>% flatten %>% transpose) %>%
      flatten() })
  d2 <- map(d1, function(x) {
    map_at(x, "commonName", function(y) {
      map(y, function (z) {

        if (is.null(names(z))) {
          names(z) = c(seq(1:length(z)))
          bind_rows(z) %>% unite(col = "commonName", 1:length(z), sep = "; ")
%>% as_tibble
        } else {
          bind_rows(z) %>% unite(col = "commonName",  1:length(z), sep = ";
") %>% as_tibble
        }
      }) %>% flatten
    })
  })
  d3 <- map(d2, function(x) do.call(cbind, x) %>% as_tibble(.name_repair =
c("universal")))
  d4 <- map(d3, function(x) x %>% mutate_if(is.list, ~as.character(.)))
  d5 <- bind_rows(d4)
  names(d5) <- if (length(d1[[1]]) > 1) {
    d1[[1]] %>% names
  } else if (length(d1) > 1) {d1[[2]] %>% names} else {
    names(d5)}

  # File URL and type
  e1 <- map(c2, function(x) {
    list(NOAASiteId = x[c("NOAASiteId")],
         dataFile = x[c("dataFile")] %>% flatten %>% flatten %>% transpose)
%>%
      flatten() })
  e2 <- map(e1, function(x) {
    do.call(cbind, x[c("NOAASiteId", "fileUrl", "urlDescription",
"linkText")]) %>% as_tibble})
  e3 <- map(e2, mutate_if, is.list, ~as.character(.))
  e4 <- bind_rows(e3)

  # Citation and URL
  f1 <- jsonfile %>% keep(names(jsonfile) %in% c("publication"))
  if(length(jsonfile[["publication"]]) == 0){
  } else {
    f2 <- map_depth(f1, 2, flatten) %>% flatten
    f3 <- map(f2, function (x) keep(x, names(x) %in% c("citation", "url")))

    f4 <- list(NOAAStudyId = list(rep(jsonfile$NOAAStudyId, length(f2))),
               publication = transpose(f3)) %>% flatten
    f5 <- do.call(cbind, f4) %>% as_tibble
```

```
    f6 <- mutate_if(f5, is.list, ~as.character(.))
    names(f6)[2:3] <- c("pubCitation", "pubUrl")
  }

  # Merging all the information of a single file together
  if (nrow(c5) == nrow(d5) &
      nrow(d5) == nrow(e4)) {
    full_extract_c <- reduce(list(c5, d5, e4), cbind)
  } else if (nrow(d5) == nrow(e4)) {
    de_bind <- cbind(d5, e4[,-c(1)])
    full_extract_c <- merge(c5, de_bind)} else {
      cd_bind <- cbind(c5, d5[-c(1)])
      full_extract_c <- merge(cd_bind, e4)
    }
  full_extract_c <- full_extract_c[, !duplicated(colnames(full_extract_c))]
  full_extract_b <- merge(b8, full_extract_c)
  full_extract_a <- merge(a2, full_extract_b)
  if(length(jsonfile[["publication"]]) == 0){
  } else { full_extract_a <- merge(full_extract_a, f6)
  }
  full_extract_a <- lapply(full_extract_a, as.character) %>% as_tibble

  # Adding the file information to the master data frame
  meta_ITRDB_json <- bind_rows(meta_ITRDB_json, full_extract_a)

  # A simple way to keep track of progress
  end <- Sys.time()
  print(paste0( i, " - ", end-start))

}

# End of import loop. You can view or export the data table.
# View(meta_ITRDB_json)
# write.csv(meta_ITRDB_json, "^ meta_ITRDB_json.csv", row.names = FALSE)
```

Appendix 2. Corrections to file type codes that were included in this snapshot of the ITRDB database. Raw ring width files and chronology files in this database submission use these converted file type code as the last letter of the filename (w, l, e, x, n, t, i, p).

Measurement type	Converted to:	File codes extracted from file names																							Grand Total
		blank	l	e	x	n	t	i	w	p	d	b	c	ba	bm	ed	ew	ld	lw	mxd	mnd	rew	rlw	rd	rw	
Ring Width	blank	4766							243																2	5011
Latewood Width	l	10	613																2							625
Earlywood Width	e	9		610													2									621
Maximum Density	x	2			574																					576
Minimum Density	n					517																				517
Latewood Density	t						311																			311
Earlywood Density	i							311																		311
Latewood Percent	p									49																49
Ring Density											9															9
Blue Intensity												7														7
Cell Wall Thickness													3													3
Basal Area														2												2
Basal Area Mass															2											2
Earlywood Mean Basic Density																2										2
Latewood Mean Basic Density																		2								2
Maximum Latewood Basic Density																				2						2
Minimum Earlywood Basic Density																					2					2
Relative Earlywood Width																						2				2
Relative Latewood Width																							2			2
Ring Mean Density																								2		2
Grand Total		4787	613	610	574	517	311	311	243	49	9	7	3	2	2	2	2	2	2	2	2	2	2	2	2	8058

Appendix 3. Code for read error detection when importing ITRDB raw data files in *.rwl* format. The code comes in three section. The first and second block represent functions that are called by the third block, which reads the .rwl data files and calls the functions from Block 1 and 2. This code is a custom modification of the original *read.tucson()* function of the *dplR* package for the R programming environment.

Block 1: Function that tests for general file formatting for errors:

```
input.ok <- function(series, decade.yr, x) {
  if (length(series) == 0) {
    return(FALSE)
  }

  ## Number of values allowed per row depends on first year modulo 10
  n.per.row <-
    apply(x, 1,
          function(x) {
            notna <- which(!is.na(x))
            n.notna <- length(notna)
            if (n.notna == 0) {
              0
            } else {
              notna[n.notna]
            }
          })
  full.per.row <- 10 - decade.yr %% 10
  ## One extra column per row is allowed:
  ## a. enough space will be allocated (max.year is larger than
  ## last year of any series)
  ## b. the extra col may contain a stop marker (non-standard location)
  idx.bad <- which(n.per.row > full.per.row + 1)
  n.bad <- length(idx.bad)
  if (n.bad > 0) {

    return(FALSE)
  }
  series.ids <- unique(series)
  nseries <- length(series.ids)
  series.index <- match(series, series.ids)
  last.row.of.series <- logical(length(series))
  for (i in seq_len(nseries)) {
    idx.these <- which(series.index == i)
    last.row.of.series[idx.these[which.max(decade.yr[idx.these])]] <-
      TRUE
  }
```

```
  flag.bad2 <- n.per.row < full.per.row
  if (!all(last.row.of.series) && all(flag.bad2[!last.row.of.series])) {
    return(FALSE)
  }
  min.year <- min(decade.yr)
  max.year <- ((max(decade.yr)+10) %/% 10) * 10
  if (max.year > as.numeric(format(Sys.Date(), "%Y")) + 100) {
    ## Must do something to stop R from trying to build huge
    ## data structures if the maximum year is not detected
    ## correctly.  Not too strict (allow about 100 years past
    ## today).
    return(FALSE)
  }
  span <- max.year - min.year + 1
  val.count <- matrix(0, span, nseries)
  for (i in seq_along(series)) {
    this.col <- series.index[i]
    these.rows <- seq(from = decade.yr[i] - min.year + 1, by = 1,
                      length.out = n.per.row[i])
    val.count[these.rows, this.col] <-
      val.count[these.rows, this.col] + 1
  }
  extra.vals <- which(val.count > 1, arr.ind=TRUE)
  n.extra <- nrow(extra.vals)
  if (n.extra > 0) {
    FALSE
  } else {
    TRUE
  }
}
# END OF CODE
```

Block 2: Function that checks for and records specific read errors:

```
#
error.collect <- function (x, decade.yr, series) {
  n.per.row <-
    apply(x, 1,
          function(x) {
            notna <- which(!is.na(x[]))
            n.notna <- length(notna)
            if (n.notna == 0) {
              0
            } else {
              notna[n.notna]
            }
          })
  full.per.row <- 10 - decade.yr %% 10
```

```
## One extra column per row is allowed:
## a. enough space will be allocated (max.year is larger than
## last year of any series)
## b. the extra col may contain a stop marker (non-standard location)
idx.bad <- which(n.per.row > full.per.row + 1)
n.bad <- length(idx.bad)
if (n.bad > 0) {
  ids.decades <- data.frame(R_COREID = series[idx.bad],
                            R_DECADE = decade.yr[idx.bad])
  warning("Rows with to many values")
} else {ids.decades <- NULL}
series.ids <- unique(series)
nseries <- length(series.ids)
series.index <- match(series, series.ids)
last.row.of.series <- logical(length(series))
for (i in seq_len(nseries)) {
  idx.these <- which(series.index == i)
  last.row.of.series[idx.these[which.max(decade.yr[idx.these])]] <-
    TRUE
}
flag.bad2 <- n.per.row < full.per.row
if (!all(last.row.of.series) && all(flag.bad2[!last.row.of.series])) {
  few.values <- "all rows (last rows excluded) have too few values"
} else {few.values <-  NULL}
min.year <- min(decade.yr)
max.year <- ((max(decade.yr)+10) %/% 10) * 10
if (max.year > as.numeric(format(Sys.Date(), "%Y")) + 100) {
  ## Must do something to stop R from trying to build huge
  ## data structures if the maximum year is not detected
  ## correctly.  Not too strict (allow about 100 years past
  ## today).
  future.years <- "file format problems (or data from the future)"
} else {future.years <- NULL}
span <- max.year - min.year + 1
val.count <- matrix(0, span, nseries)
tryCatch(
for (i in seq_along(series)) {
  this.col <- series.index[i]
  these.rows <- seq(from = decade.yr[i] - min.year + 1, by = 1,
                    length.out = n.per.row[i])
  val.count[these.rows, this.col] <-
    val.count[these.rows, this.col] + 1
},
error = function(cond){
  message(paste("failed the check for duplicates on series "), series[i])
  message(cond)
  return(errors <- NULL)
  },
warning = function(cond){
  message("Likely the file contain negative years lower than -1000.
```

```
            Argument 'long' must be set to TRUE.)
    },
  finally = {errors <- NULL}
)
  extra.vals <- which(val.count > 1, arr.ind=TRUE)
  n.extra <- nrow(extra.vals)
  if (n.extra > 0) {
    warning("Duplicated cores present")
    ids.years <- data.frame(D_COREID = series.ids[extra.vals[, 2]],
                            YEAR = min.year - 1 + extra.vals[, 1])
    ids.years <- ids.years %>% group_by(D_COREID) %>%
      summarise(D_OVERLAP_START = min(YEAR),
                D_OVERLAP_END = max(YEAR),
                D_SEQ_LENGTH = length(YEAR),
                D_YEAR_SPAN = max(YEAR) - min(YEAR) + 1)
  } else {
    ids.years <- NULL
  }

  if (any(!is.null(ids.decades) ||
          !is.null(few.values) ||
          !is.null(future.years) ||
          !is.null(ids.years))) {
    errors <- list(extra_rows = ids.decades,
                   few_values = few.values,
                   future_years = future.years,
                   duplicated_cores = ids.years)
  } else {
    errors <- NULL}
}
# END OF CODE
```

Block 3. This section reads in *.rwl* data files and calls the functions from Block 1 & 2 above.

```
#
error.identification <- function(fpath, id, header = NULL, long = FALSE,
edge.zeros = TRUE){
if(exists("input.ok") &  exists("error.collect")){
  require(tidyverse)
  ## Read data file into memory
con <- file(paste0(fpath, id, ".rwl"), encoding = "UTF-8")
on.exit(close(con))
goodLines <- readLines(con)
close(con)
on.exit()
```

```
## Strip empty lines (caused by CR CR LF endings etc.)
goodLines <- goodLines[nzchar(goodLines)]
## Remove comment lines (print them?)
foo <- regexpr("#", goodLines, fixed=TRUE)
commentFlag <- foo >= 1 & foo <= 78
goodLines <- goodLines[!commentFlag]
## Temporary file for 'goodLines'. Reading from this file is
## faster than making a textConnection to 'goodLines'.
tf <- tempfile()
tfcon <- file(tf, encoding="UTF-8")
on.exit(close(tfcon))
on.exit(unlink(tf), add=TRUE)
writeLines(goodLines, tf)
## New connection for reading from the temp file
close(tfcon)
tfcon <- file(tf, encoding="UTF-8")
if (is.null(header)) {
  ## Try to determine if the file has a header. This is failable.
  ## 3 lines in file
  hdr1 <- readLines(tfcon, n=1)
  if (length(hdr1) == 0) {
    message("file is empty")
  }
  if (nchar(hdr1) < 12) {
    stop("first line in rwl file ends before col 12")
  }
  is.head <- FALSE
  yrcheck <- suppressWarnings(as.numeric(substr(hdr1, 9, 12)))
  if (is.null(yrcheck) || length(yrcheck) != 1 || is.na(yrcheck) ||
      yrcheck < -1e04 || yrcheck > 1e04 ||
      round(yrcheck) != yrcheck) {
    is.head <- TRUE
  }
  if (!is.head) {
    datacheck <- substring(hdr1,
                           seq(from=13, by=6, length=10),
                           seq(from=18, by=6, length=10))
    datacheck <- sub("^[[:blank:]]+", "", datacheck)
    idx.good <- which(nzchar(datacheck))
    n.good <- length(idx.good)
    if (n.good == 0) {
      is.head <- TRUE
    } else {
      datacheck <- datacheck[seq_len(idx.good[n.good])]
      if (any(grepl("[[:alpha:]]", datacheck))) {
        is.head <- TRUE
      } else {
        datacheck <- suppressWarnings(as.numeric(datacheck))
        if (is.null(datacheck) ||
            any(!is.na(datacheck) &
```

```
                round(datacheck) != datacheck)) {
          is.head <- TRUE
        }
      }
    }
  }
  if (is.head) {
    hdr1.split <- strsplit(str_trim(hdr1, side="both"),
                           split="[[:space:]]+")[[1]]
    n.parts <- length(hdr1.split)
    if (n.parts >= 3 && n.parts <= 13) {
      hdr1.split <- hdr1.split[2:n.parts]
      if (!any(grepl("[[:alpha:]]", hdr1.split))) {
        yrdatacheck <- suppressWarnings(as.numeric(hdr1.split))
        if (!(is.null(yrdatacheck) ||
              any(!is.na(yrdatacheck) &
                  round(yrdatacheck) != yrdatacheck))) {
          is.head <- FALSE
        }
      }
    }
  }
  if (is.head) {
    cat(gettext("There appears to be a header in the rwl file\n",
                domain="R-dplR"))
  } else {
    cat(gettext("There does not appear to be a header in the rwl file\n",
                domain="R-dplR"))
  }
} else if (!is.logical(header) || length(header) != 1 || is.na(header)) {
  stop("'header' must be NULL, TRUE or FALSE")
} else {
  is.head <- header
}

skip.lines <- if (is.head) 3 else 0
data1 <- readLines(tfcon, n=skip.lines + 1)
if (length(data1) < skip.lines + 1) {
  stop("file has no data")
}
on.exit(unlink(tf))
## Test for presence of tabs
if (!grepl("\t", data1[length(data1)])) {
  ## Using a connection instead of a file name in read.fwf and
  ## read.table allows the function to support different encodings.
  if (isTRUE(long)) {
    ## Reading 11 years per decade allows nonstandard use of stop
    ## marker at the end of a line that already has 10
    ## measurements.  Such files exist in ITRDB.
    fields <- c(7, 5, rep(6, 11))
```

```
  } else {
    fields <- c(8, 4, rep(6, 11))
  }
  ## First, try fixed width columns as in Tucson "standard"
  dat <-
    tryCatch(read.fwf(tfcon, widths=fields, skip=skip.lines,
                      comment.char="", strip.white=TRUE,
                      blank.lines.skip=FALSE,
                      colClasses=c("character", rep("integer", 11),
                                   "character")),
             error = function(...) {
               ## If predefined column classes fail
               ## (e.g. missing values marked with "."), convert
               ## types manually
               tfcon <- file(tf, encoding="UTF-8")
               tmp <-
                 read.fwf(tfcon, widths=fields, skip=skip.lines,
                          strip.white=TRUE, blank.lines.skip=FALSE,
                          colClasses="character", comment.char="")
               for (idx in 2:12) {
                 asnum <- as.numeric(tmp[[idx]])
                 if (!identical(round(asnum), asnum)) {
                   stop("non-integral numbers found")
                 }
                 tmp[[idx]] <- as.integer(asnum)
               }
               tmp
             })
  dat <- dat[!is.na(dat[[2]]), , drop=FALSE] # requires non-NA year
  series <- dat[[1]]
  decade.yr <- dat[[2]]
  series.fixed <- series
  decade.fixed <- decade.yr
  x <- as.matrix(dat[3:12])
  ## Convert values <= 0 or < 0 (not -9999) to NA
  if (isTRUE(edge.zeros)) {
    x[x < 0 & x != -9999] <- NA
  } else {
    x[x <= 0 & x != -9999] <- NA
  }
  x.fixed <- x
  fixed.ok <- input.ok(series, decade.yr, x)
} else {
  warning("tabs used, assuming non-standard, tab-delimited file")
  fixed.ok <- FALSE
}
## If that fails, try columns separated by white space (non-standard)
if (!fixed.ok) {
  warning("fixed width failed, trying variable width columns")
  tfcon <- file(tf, encoding="UTF-8")
```

```
  ## Number of columns is decided by length(col.names)
  dat <-
    tryCatch(read.table(tfcon, skip=skip.lines, blank.lines.skip=FALSE,
                        comment.char="", col.names=letters[1:13],
                        colClasses=c("character", rep("integer", 11),
                                     "character"), fill=TRUE, quote=""),
             error = function(...) {
               ## In case predefined column classes fail
               tfcon <- file(tf, encoding="UTF-8")
               tmp <- read.table(tfcon, skip=skip.lines,
                                 blank.lines.skip=FALSE, quote="",
                                 comment.char="", fill=TRUE,
                                 col.names=letters[1:13],
                                 colClasses="character")
               tmp[[1]] <- as.character(tmp[[1]])
               for (idx in 2:12) {
                 asnum <- as.numeric(tmp[[idx]])
                 if (!identical(round(asnum), asnum)) {
                   stop("non-integral numbers found")
                 }
                 tmp[[idx]] <- as.integer(asnum)
               }
               tmp
             })
  dat <- dat[!is.na(dat[[2]]), , drop=FALSE] # requires non-NA year
  series <- dat[[1]]
  decade.yr <- dat[[2]]
  x <- as.matrix(dat[3:12])
  if (isTRUE(edge.zeros)) {
    x[x < 0 & x != -9999] <- NA
  } else {
    x[x <= 0 & x != -9999] <- NA
  }
  if (!input.ok(series, decade.yr, x)) {
    if (exists("series.fixed", inherits=FALSE) &&
        exists("decade.fixed", inherits=FALSE) &&
        exists("x.fixed", inherits=FALSE) &&
        (any(is.na(x) != is.na(x.fixed)) ||
         any(x != x.fixed, na.rm=TRUE))) {
      series <- series.fixed
      decade.yr <- decade.fixed
      warning("trying fixed width names, years, variable width data")
      if (!input.ok(series, decade.yr, x)) {
        # This is the original stop function. If the input.ok function fails
again then it stops.
        # But here we want to collect the error
        warning("Fail to read rwl file - collecting errors [1]")
        error.collect(x, decade.yr, series)

      }
```

```
    } else {
        # This is the original stop function. If the input.ok function fails
again then it stops.
        # But here we want to collect the error
        warning("Fail to read rwl file - collecting errors [2]")
        error.collect(x, decade.yr, series)

    }
  } else {
    # This is the original stop function. If the input.ok function fails
again then it stops.
    # But here we want to collect the error
    warning("Fail to read rwl file - collecting errors [3]")
    error.collect(x, decade.fixed, series.fixed)
  }
} else {NULL}
} else {warning("Please load function 'input.ok' and 'error.collect' on the
global environment before proceeding")}
}
# END OF CODE
```

Appendix 4. Code for bulk detrending of ITRDB raw data files in Tucson format (*.rwl*), and subsequently averaging them into a site chronology format (*.crn*). The code also generates a table with statistics that describe the quality of the chronology (EPS, rbar). We use three detrending methods, preserving low-frequency (modified negative exponential) medium-frequency (Spline) and high-frequency variability (Friedman) for different research objectives. Both the input (*.rwl*) files and the output (*.crn*) files are available in this database submission, but the code below can be used to modify the detrending parameters and create a new set of chronologies in one run of the code below.

```
library(tidyverse)
library(dplR)

# Change this relative file path to the subdirectory where .rwl files reside
fpath <- "rwl_files_subdirectory/"

# Lists all files to be detrended
rwl_flist <- list.files(path = fpath, pattern = ".rwl") %>%
str_replace_all(".rwl", "")
rwl_flist <- rwl_flist[!str_detect(rwl_flist, pattern = "track")]

# Stops output from read.rwl from being printed
quiet <- function(x) {
  sink(tempfile())
  on.exit(sink())
  invisible(force(x)) }

# Creates empty data tables required to run loop
chr_stats <- tibble() # Statistics about the detrending
chr_all <- list() # List to store detrended rwls

for (i in rwl_flist){
  start <- Sys.time()
  rwl <- read.rwl(paste0(fpath,i,".rwl"))

  if (!any(class(rwl) %in% c("warning"))){

# Here is where you can select and parameterize the detrending method
# For this database submission we used three methods preserving low-frequency
# (modified negative exponential) medium-frequency (Spline) and high-
# frequency variability (Friedman):
# method = "ModNegExp", pos.slope = FALSE
# method = "Spline", nyrs = NULL, f = 0.5
# method = "Friedman", span = "cv", bass = 0
```

```
    rwl_d_mod <- tryCatch(suppressWarnings(
      detrend(rwl, method = "Spline", nyrs = NULL, f = 0.5)),
                    error = function (e) {
                         return(e)
                         message("Failed to detrend")
                         },
                    warning = function (w) warn <<- as.character(w))
    if(!any(class(rwl_d_mod) == "simpleError")){
      rwl_c_mod <- rwl_d_mod %>% chron()
      chr_all[[i]] <- rwl_c_mod

      # Calculating average sample depth
      SDEPTH <- rwl_c_mod %>% select(samp.depth) %>% as.matrix
      SDEPTH_AVG <- rwl_c_mod %>% select(samp.depth) %>% as.matrix %>% mean
%>% round(3)
      rwi_runn <- tryCatch(expr = rwi.stats.running(rwl_d_mod, prewhiten =
TRUE),
                           error = function (e) return(e))
      if(SDEPTH_AVG >= 1 & !any(class(rwi_runn) == "simpleError") &
length(rwi_runn) > 2){
        rwi_stat <- rwi.stats(rwl_d_mod)

        # Calculating Estimated Population Signal (EPS)
        EPS_AVG <- rwi_stat$eps
        EPS_85_MIN_YR <- rwi_runn[min(which(rwi_runn$eps > 0.85)),
"start.year"]
        EPS_85_MAX_YR <- rwi_runn[max(which(rwi_runn$eps > 0.85)),
"end.year"]

        # RBAR
        rbar_stat <- cor(rwl_d_mod, use = "pairwise.complete.obs")

        RBAR_AVG <- rwi_stat$rbar.tot
        # RBAR_AVG <- rbar_stat %>% mean(na.rm=TRUE)
        RBAR_SD <- rbar_stat %>% sd(na.rm = TRUE) %>% round(4)
        RBAR_MIN <- rwi_runn %>% select(rbar.tot) %>% min
        RBAR_MAX <- rwi_runn %>% select(rbar.tot) %>% max
        chr_stats2 <- cbind(
          EPS_AVG, EPS_85_MIN_YR, EPS_85_MAX_YR,
          RBAR_AVG, RBAR_SD, RBAR_MIN, RBAR_MAX, SDEPTH_AVG)

      } else {message("Can't calculate statistics")

        chr_stats2 <- cbind(
          SDEPTH_AVG,
          tibble(ERROR_DET = "Failed to run rwi.stats and rwi.stats.running",
                 MSG_DET = if(!length(rwi_runn) > 2){
                   x <- "Not enough years to calculate rwi.stats.running"
                   } else {
```

```
                    x <- as.character(rwi_runn)
                    }
                )
            )
        }

    } else {
      chr_stats2 <- cbind(
        tibble(
          ERROR_DET = "Failed to detrend",
          MSG_DET = as.character(rwl_d_mod)))
    }
  } else {
    chr_stats2 <- tibble(
      ERROR_RWL = "Failed to read rwl",
      MSG_RWL = as.character(rwl))
  }


  chr_stats2 <- chr_stats2 %>% as_tibble %>% mutate(JSN_fileCode = i)
  chr_stats <- bind_rows(chr_stats, chr_stats2)

  end <- Sys.time()
  cat(paste0("-----   ", i,"   -----\n",
             "Run time:  ", round(end-start, 2), "s\n",
             "Number of cores: ", rwi_stat$n.cores, "\n\n"))
}

# Writing out the chronology files, note that this code does not generate
# headers, but headers were added to chronology files of thus database

for (i in rwl_flist){ write.crn(chr_all[[i]], paste0(i, ".crn")) }
write.csv(chr_stats, "Chronology statistics.csv", row.names = FALSE)
```

Appendix 5. Schematic of drought detection cases exemplifying all possible cases of immediate and lagged tree responses combined with sharp or slower decline (over 2 years) in moisture conditions. Red line represents standardized SPEI (Standardized Precipitation and Evapotranspiration Index) while green line represents standardized RWI (Ring Widths Index).

Appendix 6. Supplementary details on ecological drought detection and RED50 methodology.

Data sources

Tree-ring records. Total ring-width measurements from the ITRDB (available from https://www.ncei.noaa.gov/pub/data/paleo/treering/). Inclusion required ≥10 trees per site and ≥30 years of observations within 1971–2005.

Climate. Monthly temperature and precipitation from the University of Delaware global gridded product (available from https://downloads.psl.noaa.gov/Datasets/udel.airt.precip/v401/), extracted at site coordinates.

Mortality validation dataset. Global drought-induced tree mortality database is available from https://www.tree-mortality.net/globaltreemortalitydatabase/. Used for external validation of flagged droughts.

Tree-ring processing

Raw widths were detrended with the Friedman Super-Smoother ("spline") to emphasize interannual variation relevant to drought impacts. Individual series were combined with a robust mean; autocorrelation was reduced via autoregressive modeling to enhance the climate signal. The working chronology variable is the ring-width index (RWI). Missing terminal years (≤5 years at series end) were imputed where needed using a Random Forest approach.

Site-level inclusion. Sites used in the drought-response analysis satisfied: (i) ≥30 record years in 1971–2005; (ii) ≥3 ecological drought events detected; (iii) membership in a PAM cluster with ≥6 sites; (iv) removal of ≤5% outliers (spatially disjunct cluster members or metric outliers).

Climate data, growth year alignment, and SPEI

To align climate with ring formation, we defined the growth (drought) year as the 12 months ending in August for the Northern Hemisphere and February for the Southern Hemisphere. For each month we computed Thornthwaite PET, water balance (P − PET), and then SPEI. We then calculated a rolling accumulation over the user-selected growth window (default 12 months) to obtain annual MeanSPEI per site and growth year. For drought detection, SPEI was z-scored within site over 1971–2005 to yield MeanSPEIScaled.

Site-level drought detection

We focused on acute droughts (≈1–2 years). A site-year was flagged as an ecological drought when anomalous drying and growth decline were synchronized:

Immediate response (same year): SPEI < 0 and ΔSPEI ≤ −1 SD and ΔRWI (scaled) ≤ −1 SD (year-to-year).
Two-year/deferred response: SPEI < 0 and ΔSPEI over two years ≤ −1.5 SD and (ΔRWI ≤ −1 SD or two-year ΔRWI ≤ −2 SD).

Regional (group) drought years and coherence checks

We summarized site drought flags within bio-climatic groups (see S6) and declared a group drought year when ≥30% of sites flagged a drought. Mixed immediate vs. delayed responses were handled as follows: when one response type exceeded 65% of responding sites, we adopted that year; otherwise, adjacent years were averaged as a single multi-year event. Years lacking a post-event recovery window (≥2 years) were excluded. Spatial and temporal consistency was verified by reviewing neighboring sites and by removing group years with average SPEI > −0.25.

External validation. For locations within 150 km of documented drought-induced mortality, 82% of mortality events were preceded (≤3 years) by our ecological droughts, supporting construct validity.

Clustering by bio-geoclimatic similarity

Sites were clustered within continental regions using Partition Around Medoids (PAM) on full time-series matrices of annual SPEI and raw ring width (1971–2005). k per region was chosen by maximizing the average silhouette statistic. Clustering was constrained within continental/ecoregional boundaries.

Drought response indices and the RED50 metric

We computed Resistance = Drought/PreDrought, Recovery = PostDrought/Drought, and Resilience = PostDrought/PreDrought using two-year means for pre- and post-drought windows. Following Schwarz et al. (2020), we fit a negative-exponential model (Recovery = a · Resistance^{b}) and compared it to the full-resilience line (1/Resistance). RED50 is the deviation from the full-resilience line at Resistance = 0.5.

Model specification, fitting, and uncertainty

Fitted via non-linear least squares (NLS) with high iteration limits. Uncertainty was quantified by bootstrapping and propagating to RED50. Minimum 3 events per group required.

Filtering rules and exclusions

- Excluded group years with SPEI > −0.25.
- Removed years failing spatial/temporal coherence.
- Excluded end-of-series events without ≥2 post years.
- Clusters with <6 sites or sites with <3 droughts removed.
- ≤5% of sites removed as outliers.

Reproducibility notes and code availability

Implemented in R as std_drought_impact() with modular helpers.

Default parameters:
clim_growth_end = c(NH = 8, SH = 2),
clim_growth_period = 12,
clim_spei_scale = 1,
clim_rescale_spei = TRUE,
thr_pointer_year_prop_sites = 0.3,
thr_multi_drought_tiebreak = 0.65,
n_years_baseline = 2,
n_years_recovery = 2,
model_min_n_drought_events = 3,
model_resistance_val = 0.5

Outputs: intermediate objects + final RED50 table (mean, SE).

Code archived on GitHub (https://github.com/vmanvailer/treedrought).

Note: The pipeline contains temporary QA steps used during refactoring with minimal effect on results.

Appendix 7. Continental region delineations used for clustering tree ring chronologies on RED50 drought response analysis. Clustering was applied on each continental delineation independently for developing coherent clustering.

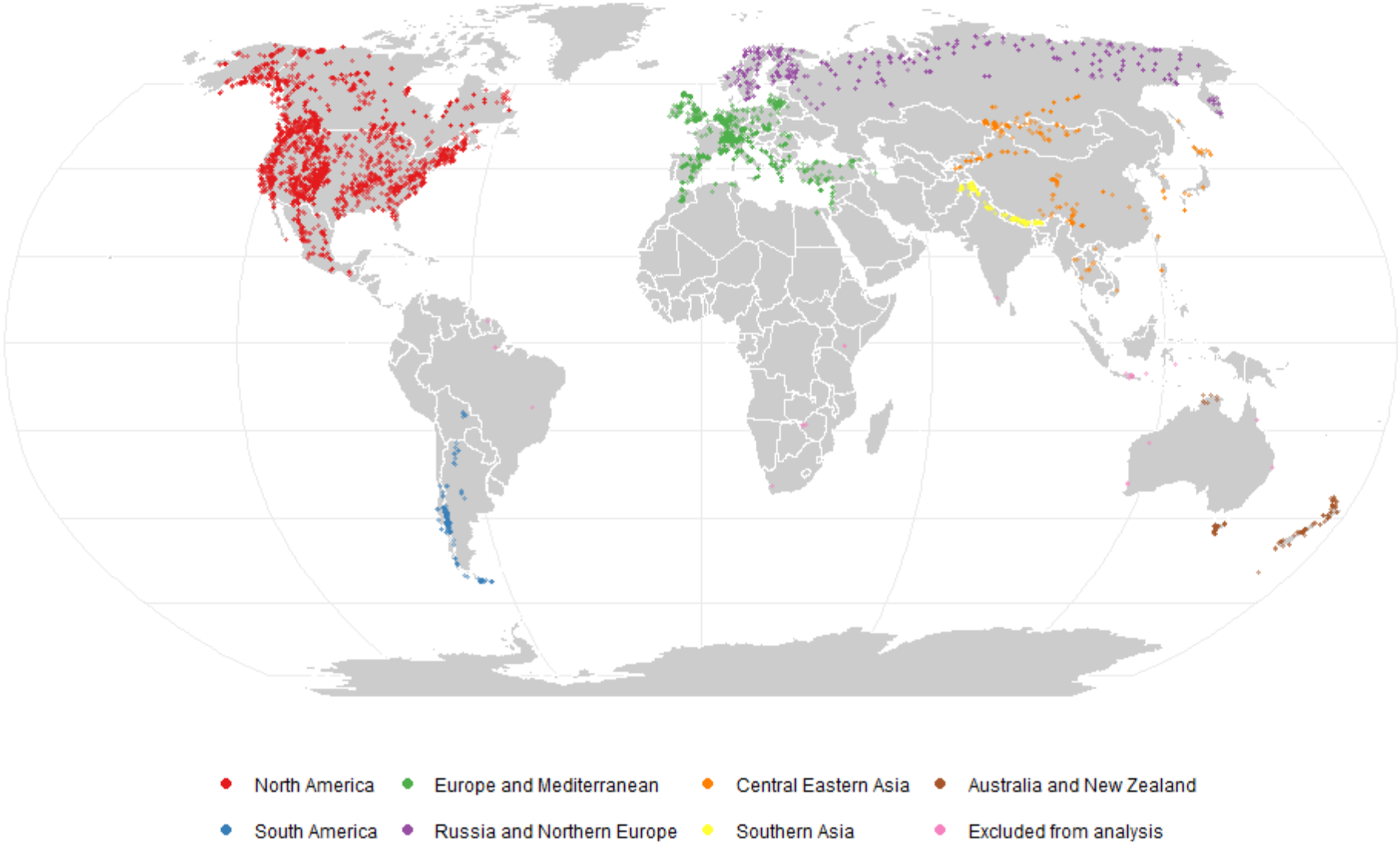

Appendix 8. Data availability over time and filtering overview. Darker shades are the cumulative number of trees available after applying each filter on top of the previous one.

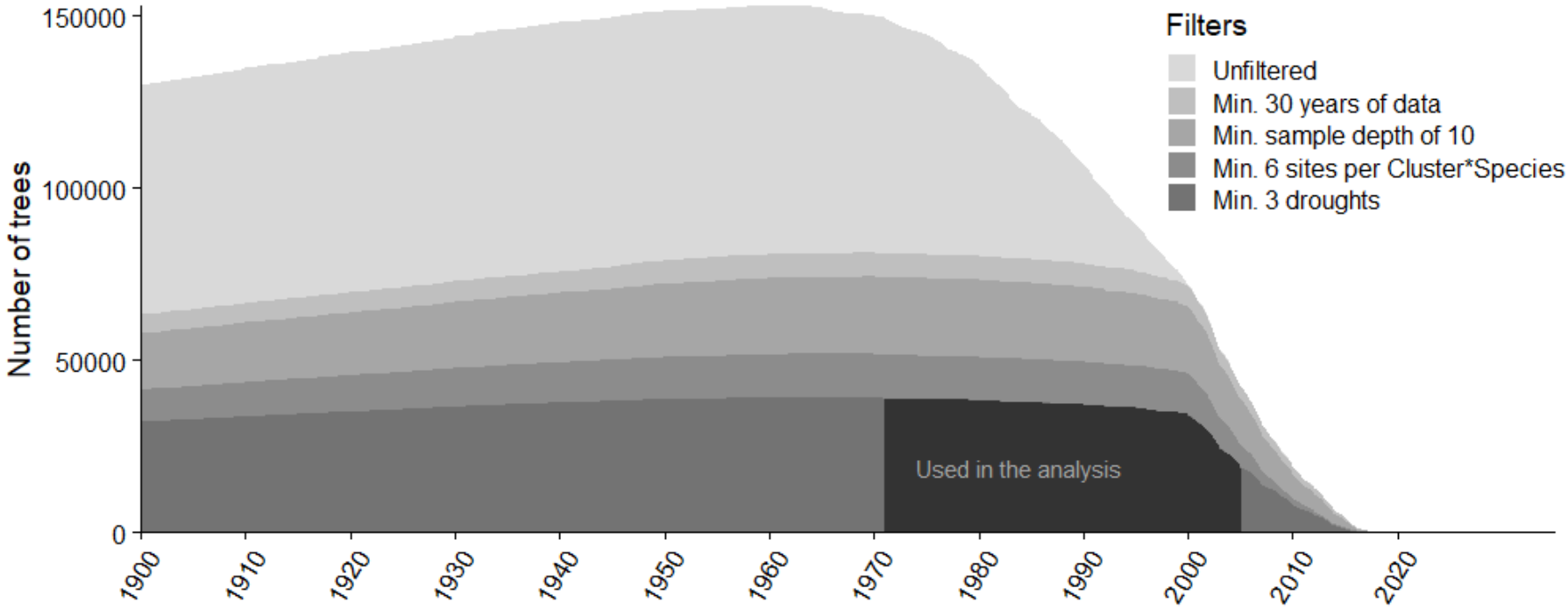

END